

The role of mitochondria in the renal Fanconi syndrome

Andrew Hall

A thesis submitted to UCL for the degree of Doctor of Philosophy

July 2009

**Department of Cell and Developmental Biology
& Centre for Nephrology
UCL
Gower Street
London WC1E 6BT**

I, Andrew Hall confirm that the work presented in this thesis is my own. Where information has been derived from other sources, I confirm that this has been indicated in the thesis.

Abstract

Clinically, the renal proximal tubule (PT) seems to be vulnerable to mitochondrial dysfunction (MD), which can affect normal transport processes (including reabsorption of low molecular weight proteins [LMWPs]), resulting in the renal Fanconi syndrome. I wanted to explore why the PT is vulnerable to MD, and how this leads to impaired LMWP transport:

(1) Using the OK cell line, to model uptake of LMWPs in the PT, I found respiratory chain (RC) inhibitors had minimal effect on the uptake of fluorescent-labelled albumin, and also had a relatively small impact on [ATP], which was maintained largely by glycolysis. Uptake of albumin was inhibited to a much greater extent by blockade of glycolysis, implying an important role for ATP. The RC inhibitor rotenone had a profound toxic effect on the structure of OK cells, due to extra-mitochondrial inhibition of microtubule polymerisation.

(2) Multi-photon imaging of live rat kidney slices showed that mitochondrial membrane potential was lower in the PT relative to distal tubule, and was better maintained in the latter following RC inhibition. The basal rate of ROS production (per cell) and glutathione levels were both higher in the PT, and RC substrates were in a more oxidised state in this segment.

(3) Urinary screening of adult patients with either (a) mitochondrial cytopathy, or (b) HIV and taking anti-retroviral therapy (ART) toxic to mitochondria, revealed high rates of tubular proteinuria (including LMWPs) in both groups. Patients taking ART had higher excretion of tubular proteins than those who were treatment naïve.

In conclusion, inhibition of ATP generation impaired protein uptake in a model of the PT, and this was mirrored by increased tubular proteinuria in patients with either genetic or toxic MD. Furthermore, differences in mitochondrial function were demonstrated along the rodent nephron, which may render the PT vulnerable to MD.

Contents

Abstract	3
List of Figures	9
List of Tables.....	11
Acknowledgements	12
Publications arising from this thesis	13
Chapter 1 - General introduction.....	14
1.1 The renal proximal tubule.....	14
1.1.1 Structure of the proximal tubule	14
1.1.2 Function of the proximal tubule – solute transport.....	14
1.1.3 Metabolism in the proximal tubule is coupled to transport.....	16
1.2 The renal Fanconi syndrome.....	18
1.2.1 Background	18
1.2.2 Aetiology.....	19
1.2.3 Pathogenesis.....	20
1.2.4 Clinical Features.....	22
1.2.5 Diagnosis of Fanconi syndrome.....	22
1.2.6 Screening for subclinical proximal tubular disease	23
1.2.7 Treatment	24
1.3 Functions of mitochondria	25
1.3.1 Origins of mitochondria	25
1.3.2 Mitochondrial ATP production.....	25
1.3.3 Reactive oxygen species production	28
1.3.4 Glutathione.....	30
1.3.5 Calcium signalling	30
1.3.6 Regulation of mitochondrial function	32
1.4 Mitochondrial cytopathy.....	33
1.4.1 Background	33
1.4.2 Phenotypic heterogeneity in mitochondrial cytopathy.....	34
1.4.3 Patho-physiology of mitochondrial cytopathy	35
1.4.4 Renal involvement in children with mitochondrial cytopathy.....	38
1.4.5 Renal involvement in adults with mitochondrial cytopathy	40

1.4.6 Differences between adults and children	41
1.5 HIV, anti-retroviral therapy and the proximal tubule	43
1.5.1 Mitochondrial toxicity of HIV and its therapy	43
1.5.2 Nephrotoxicity of Tenofovir	44
1.6 Mitochondrial dysfunction as a cause of Fanconi syndrome	46
1.6.1 Evidence for mitochondrial dysfunction as a cause of Fanconi syndrome	46
1.6.2 Possible mechanisms via which mitochondrial dysfunction might impair solute transport in the proximal tubule	46
1.7 Fluorescence live-cell imaging	47
1.7.1 Single-photon excitation confocal imaging	47
1.7.2 Multi-photon excitation fluorescence imaging	49
1.8 Experimental models of the proximal tubule	51
1.8.1 Immortalised cell cultures derived from the proximal tubule epithelium	51
1.8.2 The Opossum Kidney (OK) cell line	52
1.8.3 The renal slice model	52
1.9 Imaging of mitochondrial function	55
1.9.1 Mitochondrial membrane potential ($\Delta\psi_m$)	55
1.9.2 Reactive oxygen species production	56
1.9.3 Glutathione	56
1.9.4 NADH and FAD^{2+} autofluorescence and redox state	57
1.9.5 Calcium signalling	58
Aims	60
Chapter 2 - Methods	61
2.1 Endocytosis of albumin and dextran by OK cells	61
2.1.1 Cell culture	61
2.1.2 Cell death assay	61
2.1.3 Endocytosis assay	61
2.1.4 Dynamic measurement of intracellular ATP	63
2.1.5 Measurement of ROS production	64
2.1.6 Electron microscopy of OK cell structure	64
2.1.7 Statistical analysis	65
2.2 Multi-photon imaging of mitochondrial function in live kidney slices	65
2.2.1 Formation of live kidney slices	65
2.2.2 Identification of tubule types	66

2.2.3 Dye loading and imaging	66
2.2.4 Chemical inhibition of the respiratory chain.....	70
2.2.5 Statistical analysis	70
2.3 Clinical study	70
2.3.1 Study groups	70
2.3.2 Exclusion criteria	71
2.3.3 Ethical approval	72
2.3.4 Sample processing.....	72
2.3.5 Statistical analysis	73
Chapter 3 – Results: The effect of mitochondrial respiratory chain inhibition on endocytosis of albumin and dextran in OK cells	74
3.1 FITC-albumin uptake is greatest at the apical membrane in OK cells and is partly megalin-mediated	74
3.2 Respiratory chain inhibition causes minimal cell death in OK cells	75
3.3 Blockade of glycolysis has a much greater effect on FITC-albumin uptake than respiratory chain inhibition in OK cells.....	77
3.4 Rotenone causes an altered pattern of FITC-albumin and FITC-dextran uptake in OK cells	78
3.5 Respiratory chain inhibition has relatively little effect on cytosolic ATP levels in OK cells	81
3.6 Rotenone increases ROS production in OK cells	83
3.7 Extra-mitochondrial effects of rotenone	86
3.8 Discussion.....	88
3.8.1 The relationship between cytosolic ATP and albumin endocytosis.....	88
3.8.2 Rotenone is highly toxic to OK cells	90
3.8.3 The effect of mitochondrial respiratory chain inhibition on ROS production	92
Chapter 4 – Results: Multi-photon imaging of mitochondrial function in live slices of rat kidney.....	94
4.1 Viability and orientation	94
4.2 Mitochondrial membrane potential is higher in distal tubules	96
4.3 TMRM signal remains higher in the distal tubule in the presence of efflux pump inhibitors.....	98

4.4 Mitochondrial membrane potential is better maintained in the distal tubule during anoxia	98
4.5 ROS production is increased to a greater extent in proximal tubules by complex I inhibition.....	100
4.6 Glutathione levels are higher in the proximal tubule than distal tubule	103
4.7 Autofluorescence measurements reveal that mitochondria in the proximal tubule are in a more oxidized state	104
4.8 Calcium signalling in the renal slice.....	107
4.9 Discussion.....	109
4.9.1 Differences in mitochondrial membrane potential between proximal and distal tubules	109
4.9.2 Differences between proximal and distal tubules in response to chemical anoxia	111
4.9.3 Reactive oxygen species production in renal tubules	111
4.9.4 Glutathione in renal tubules	113
4.9.5 Calcium dyes do not load effectively in the kidney slice model.....	114
Chapter 5 – Results: Subclinical renal tubular disease in patients with mitochondrial cytopathy	115
5.1 Demographics and clinical features.....	115
5.2 The prevalence of subclinical proteinuria is high in adult patients with mitochondrial cytopathy	117
5.3 Discussion.....	120
5.3.1 Subclinical proteinuria in adult patients with mitochondrial cytopathy .	120
5.3.2 Difficulties of performing clinical studies related to mitochondrial cytopathy	121
5.3.3 Potential confounding factors	122
Chapter 6 – Results: Subclinical renal tubular disease in HIV infected patients.....	123
6.1 Demographics, HIV and treatment history	123
6.2 eGFR and serum phosphate	123
6.3 Prevalence of sub-clinical proteinuria is high in HIV patients, especially in those exposed to Tenofovir.....	124
6.4 Neither urine albumin/creatinine nor protein/creatinine ratio is sufficiently sensitive to detect all cases of subclinical nephropathy.....	128
6.5 Discussion.....	131

6.5.1 Subclinical proteinuria in HIV patients.....	133
6.5.2 Appropriate screening tests for renal tubular disease	134
6.5.3 Serum phosphate in HIV patients	134
6.5.4 Study limitations and confounding factors	135
Chapter 7 - General discussion	136
7.1 The relationship between mitochondrial function and low molecular weight protein endocytosis in the proximal tubule.....	136
7.2 Variation in mitochondrial function along the nephron.....	138
7.3 Renal dysfunction in adult patients with mitochondrial cytopathy or HIV	144
List of abbreviations.....	147
References	150
Appendix	183
Mitochondrial study - patient information sheet.....	183
HIV study - patient information sheet	186
Ethics committee approval for clinical studies	188

List of Figures

Figure 1.1. Structure of the juxta-medullary nephron.	15
Figure 1.2. Solute transport in the proximal tubule.	17
Figure 1.3. The mitochondrial respiratory chain.	26
Figure 1.4. Confocal fluorescence microscopy.	48
Figure 1.5. Principle of multi-photon excitation.	50
Figure 2.1. Anatomy of the kidney slice.	67
Figure 2.2. On-stage perfusion system for the multi-photon microscope.	68
Figure 3.1. Endocytosis of FITC-albumin by OK cells is inhibited by receptor associated protein.	75
Figure 3.2. Polarity and of FITC-albumin uptake in OK cells.	76
Figure 3.3. The effect of respiratory chain inhibition on cell death and FITC-albumin uptake in OK cells.	78
Figure 3.4. The effect of respiratory chain inhibitors on the pattern of uptake of FITC-albumin and FITC-dextran in OK cells.	80
Figure 3.5. The effects of rotenone and colchicine on FITC-albumin uptake in OK cells.	82
Figure 3.6. The effect of respiratory chain inhibition on cytosolic ATP levels in OK cells, measured using magnesium green and TMRM.	84
Figure 3.7. The effect of respiratory chain inhibition on cytosolic ATP levels in OK cells, measured using luminometry.	85
Figure 3.8. The effect of respiratory chain inhibition on reactive oxygen species production in OK cells.	87
Figure 3.9. Electron microscopy of OK cells exposed to rotenone.	89
Figure 4.1. Structure and viability of renal slices.	95
Figure 4.2. Measurement of mitochondrial membrane potential in renal tubules.	97
Figure 4.3. The effects of efflux pump inhibitors on TMRM signal in renal tubules.	99
Figure 4.4. The effect of respiratory chain inhibition on mitochondrial membrane potential in renal tubules.	101
Figure 4.5. The rate of ROS production in renal tubules.	103

Figure 4.6. Glutathione levels in renal tubules.	105
Figure 4.7. Mitochondrial redox state in renal tubules.	106
Figure 4.8. Calcium signalling in the proximal tubule measured using Rhod2.	108
Figure 5.1. Urinary markers in patients with mitochondrial cytopathy, classified by clinical phenotype.	118
Figure 5.2. Urinary markers in patients with mitochondrial cytopathy, classified by underlying genetic mutation.	119
Figure 6.1. Serum phosphate in HIV patients.	125
Figure 6.2. Urinary RBP and NAG in HIV patients.	127
Figure 6.3. Urinary albumin and protein in HIV patients.	129
Figure 6.4. The relationship between urinary albumin and other urinary markers.	130
Figure 6.5. Sensitivity of either urinary albumin or protein in detecting subclinical renal tubular disease in HIV patients.	132

List of Tables

Table 1.1. Typical phenotypic patterns observed in mitochondrial cytopathy	34
Table 5.1. Urinary results, baseline demographics, biochemistry and medical and treatment history of adult patients with mitochondrial cytopathy.	116
Table 6.1. Baseline demographics, biochemistry, and medical and treatment history of HIV patients.	124
Table 6.2. Urinary markers in HIV patients.	126
Table 6.3. Correlation among urinary markers in HIV patients.	128
Table 6.4. Agreement among urinary markers in detecting abnormal proteinuria in HIV patients.	131

Acknowledgements

I am extremely grateful to my supervisors, Prof Michael Duchen and Prof Robert Unwin, for all their help and encouragement throughout this project. I am also grateful to Prof Janos Petit-Petardi for providing training in multi-photon imaging of the kidney, which was funded by a travel grant from Zeiss. Dr Scott Wildman and Ms Linda Churchill assisted with the cell culture and immuno-staining work, and Dr Alex Pearson kindly provided the OK cells. Experiments with the luminometer were performed with Dr Michaelangelo Campanella. Dr Andrew Loesch assisted with the electron microscopy of OK cells. I would like to thank all of the members of Prof Duchen's group for general advice and support throughout my time in the laboratory. Prof Mike Hanna, Dr Shamima Rahman, Prof Nick Wood, Mr Colm Treacy and Ms Catherine Parry recruited patients from The National Hospital for Neurology, whilst Dr Ian Williams, Dr Simon Edwards, Mr Steven O'Farrell and Mr Kreesan Chetty recruited patients from The Mortimer Market HIV Centre. Dr Marta Lapsley analysed the urine samples at The South West Thames Institute for Renal Research.

This project was funded by an Entry Level Fellowship awarded by The Royal Free and UCL Medical School, and a Clinical Research Training Fellowship from Kidney Research UK. Further funding, awarded to enable the purchase of a tissue slicer, was provided by the trustees of The Arthur and Mildred Slater award, UCL.

Publications arising from this thesis

Hall AM, Edwards SG, Lapsley M, Connolly JO, Chetty K, O'Farrell S, Unwin RJ and Williams IG. Subclinical nephropathy in HIV-infected individuals on anti-retroviral therapy: tenofovir- versus nontenofovir- containing regimens. **The American Journal of Kidney Disease** 2009 Dec;54(6):1034-42.

Hall AM, Unwin RJ and Duchon MR. Multi-photon imaging of live rat kidney slices reveals differences in mitochondrial function between proximal and distal segments of the nephron in response to anoxia. **The Journal of The American Society of Nephrology** 2009 Jun;20(6):1293-302.

Chapter 1 - General introduction

1.1 The renal proximal tubule

1.1.1 Structure of the proximal tubule

Every day the kidneys within a human being filter approximately 180 litres of fluid from the blood stream, across the glomerular filtration barrier and into the renal tubules. Only about 1% of this filtered load is excreted as urine; hence, approximately 178 litres have to be reabsorbed by the renal tubule. The bulk of this reabsorption (60-70%) is performed in the proximal tubule (PT). A concise description of the structure of the PT is given below (for a more detailed account see Shirley and Unwin (Shirley DG & Unwin RJ, 2005)). The PT extends from the glomerulus to the thin descending loop of Henle, and is sub-divided into three sections, denoted S1, S2 and S3 (Figure 1.1). The S1 section is predominantly concerned with reabsorbing solutes via mechanisms that are coupled to sodium transport. These solutes include amino acids, glucose, phosphate (HPO_4^{2-}) and bicarbonate. Whilst further solute reabsorption does occur in the S2 and S3 segments, these regions are also thought to be responsible for the secretion of organic acids and bases; an important mechanism for excreting xenobiotics from the body. The first part of the PT (S1 and partly S2) is convoluted, increasing surface area (proximal convoluted tubule – PCT). The second part, including the remainder of S2 and all of S3, is straight (proximal straight tubule – PST [also known as the pars recta]) and descends in the medullary rays through the inner cortex and outer medulla, before becoming the thin descending limb of the loop of Henle. The PST is joined in the medullary ray regions by thick ascending limbs of the loop of Henle and collecting ducts.

1.1.2 Function of the proximal tubule – solute transport

The PT is a highly specialised epithelium, designed to transport large quantities of water and solutes. The luminal surface is coated with a folded brush border that dramatically increases the surface area available for absorption. A number of transporters and channels are located in the luminal membrane to facilitate

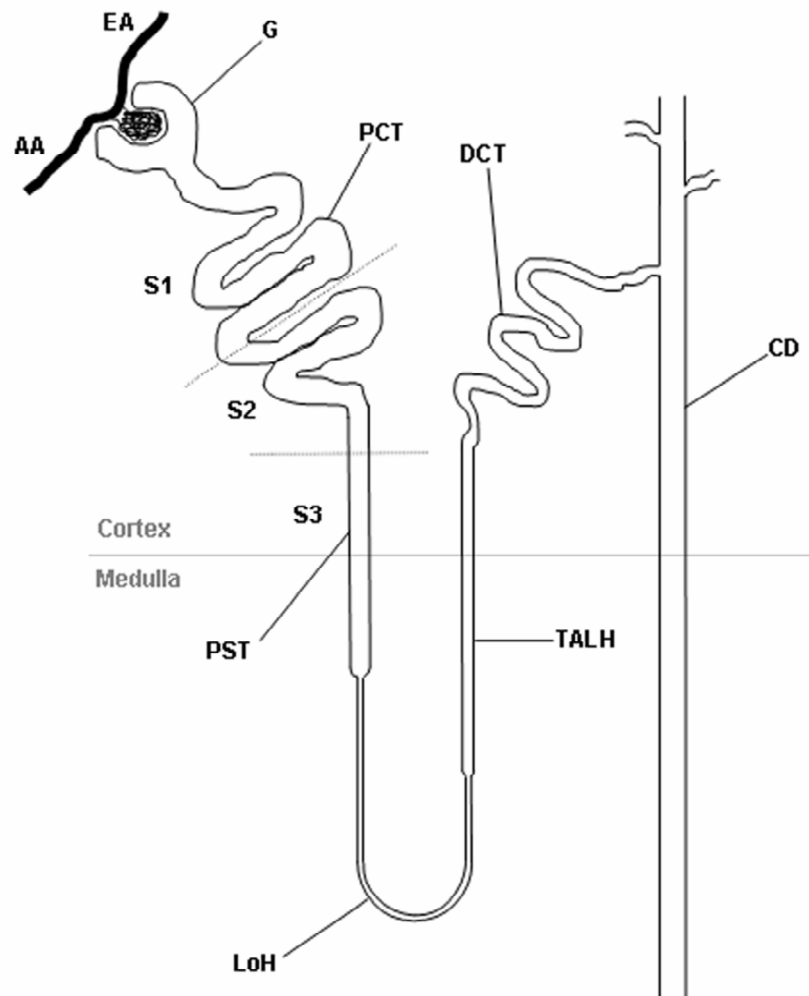


Figure 1.1. Structure of the juxta-medullary nephron.

Blood enters the glomerulus (**G**) via the afferent arteriole (**AA**) and leaves via the efferent arteriole (**EA**). Filtered fluid passes out of Bowman's capsule in the glomerulus into the proximal convoluted tubule (**PCT**), which subsequently becomes the proximal straight tubule (**PST**). The proximal tubule as a whole is sub-divided into three segments (**S1-3**). The PST descends into the medulla and becomes the thin descending limb of the loop of Henle (**LoH**). The thick ascending limb of the loop of Henle (**TALH**) ascends from the medulla into the cortex and becomes the distal convoluted tubule (**DCT**). From here, fluid drains into the collecting duct (**CD**), and passes down into the renal pelvis, to be excreted from the kidney via the ureter. The PST, TALH and CD together form the medullary rays that extend from the cortex to the medulla.

trans-cellular transport, whilst the gap junctions between cells are relatively leaky, allowing some paracellular transport to also occur. Water transport occurs via both the paracellular and transcellular routes, the latter is facilitated by water channels (aquaporin-1 – AQP-1 (Knepper *et al.*, 1996)) inserted into the cell membrane. In addition to reabsorbing a number of inorganic solutes (mainly coupled to sodium), the PT is also responsible for the uptake of low molecular proteins (LMWPs) (Christensen & Gburek, 2004), such as retinol binding protein (RBP), parathyroid hormone and insulin, which are mostly freely filtered by the glomerulus and have to be reclaimed to prevent urinary loss ('tubular proteinuria') and exposure of the distal tubule to bioactive peptides (Figure 1.2). These LMWPs are thought to be scavenged from the luminal fluid by a low-affinity high-capacity uptake system consisting of two large receptors situated in the apical membrane called megalin and cubulin (Verroust *et al.*, 2002). Megalin is a 600kDa transmembrane protein belonging to the low-density lipoprotein receptor family (Raychowdhury *et al.*, 1989), whilst cubulin is a 460kDa peripheral membrane protein identical to the intrinsic factor – vitamin B12 receptor in the small intestine (Kozyraki *et al.*, 1998). As cubulin is not a transmembrane protein, it cannot directly interact with clathryn and other mediators of the endocytotic process; instead, it is thought to bind to megalin in order to internalise ligands into the cell (Moestrup *et al.*, 1998). In addition to interacting with each other, megalin and cubulin share a number of ligands, including albumin (Zhai *et al.*, 2000). Upon binding, the receptor-ligand complexes are internalised via receptor-mediated endocytosis into endosomes. These are then acidified in an ATP dependent process, in order to promote dissociation of the proteins from the receptors (Gekle *et al.*, 1995); the latter are then recycled to the luminal membrane.

1.1.3 Metabolism in the proximal tubule is coupled to transport

Much of the transport in the PT is sodium coupled (e.g. HPO_4^{2-} , glucose, amino acids), and is driven by a low sodium concentration and relative electro-negativity within the PT cells (as compared to the lumen of the tubule). The sodium concentration within the cells of the PT is kept low by the activity of the electrogenic Na^+/K^+ -ATPase pumps located in the baso-lateral membrane. The large amounts of transport that occur in the PT therefore clearly require vast amounts of energy in the

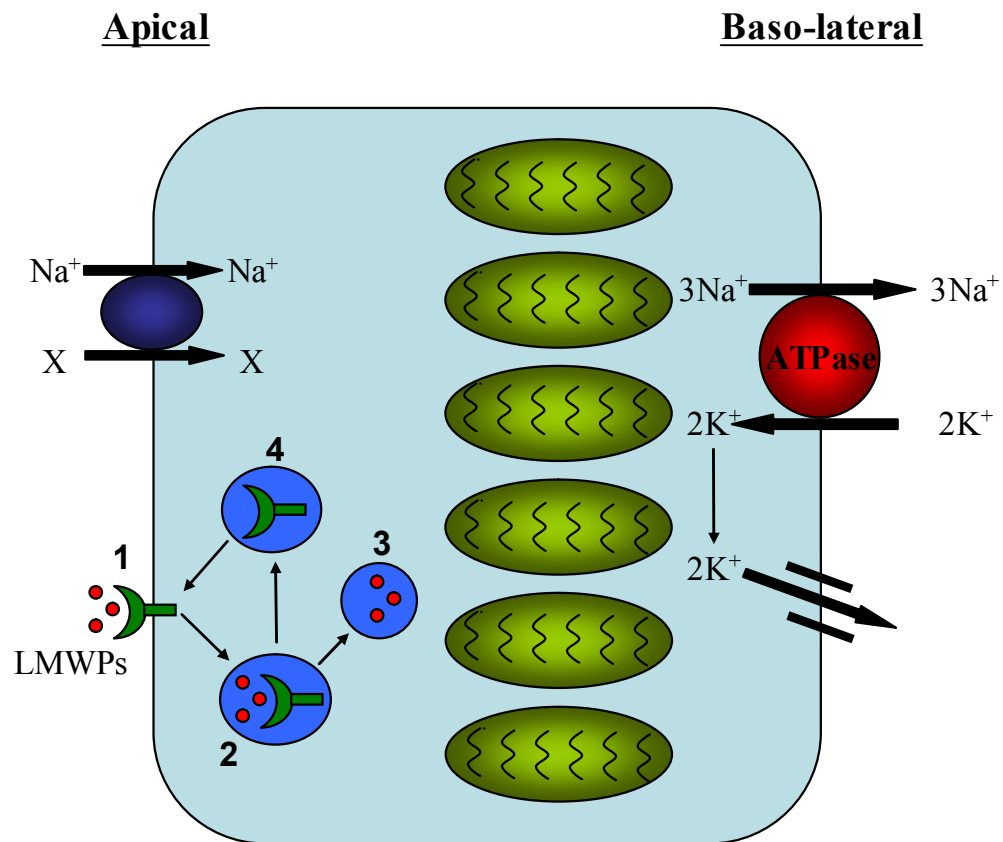


Figure 1.2. Solute transport in the proximal tubule. Substances (**X**), such as glucose, amino acids and phosphate, are co-transported at the luminal (apical) cell membrane with sodium. The gradient for sodium entry is maintained by the baso-lateral sodium pump (Na^+/K^+ -ATPase), with recycling of potassium across the baso-lateral cell membrane, via a potassium channel. Low molecular weight proteins (**LMWPs**) (<70kDa) are bound by two large non-selective receptors (megalin and an associated protein cubilin) at the luminal membrane (**1**). They bind LMWPs and the complex is internalized – via receptor-mediated endocytosis – and packaged into early endosomes (**2**). Acidification of the endosomes then dissociates the receptor-ligand complex and the protein cargo is either transferred to lysosomes, where it is degraded, or transported to the baso-lateral membrane and into the blood (**3**). The megalin receptor is recycled to the luminal membrane (**4**). Mitochondria (depicted in green) are located predominantly in the baso-lateral part of the cell.

form of ATP. The bulk of this ATP requirement is thought to be met via mitochondrial oxidative phosphorylation, which generates more ATP molecules per substrate molecule than anaerobic glycolysis (Rich, 2003). The PT contains a high density of mitochondria that are located in a baso-lateral distribution (Kaissling & Kriz, 1979). The reason for this location is not known, however, this arrangement does mean that the mitochondria are situated in close proximity to both the Na^+/K^+ -ATPase pumps (the major consumers of ATP) and the blood vessels running in between tubules (the main oxygen supply). Metabolic activity and ionic transport are thought to be tightly coupled in the kidney, in order to match ATP supply with demand (for review see (Soltoff, 1986)).

The PT is clinically vulnerable to disturbances of normal metabolism, due to mitochondrial dysfunction (MD), from insults such as genetic mitochondrial cytopathy (Niaudet & Rotig, 1996) or toxic xenobiotics (e.g., anti-retroviral therapy - ART (Izzedine *et al.*, 2005b; Izzedine *et al.*, 2005c)). The reasons for this are not properly understood; *in vivo*, the PT is thought to depend mainly on aerobic metabolism for its energy supply, with very little anaerobic capacity compared with distal tubule (DT) segments (Bagnasco *et al.*, 1985). In fact, it has been shown that a metabolic gradient exists in the tubules of the mammalian kidney, with aerobic metabolism predominant in the cortex, near the kidney surface, whilst anaerobic glycolysis predominates in the papilla; tubular cells in the outer medulla can use both forms of metabolism more or less equally (Lee & Peter, 1969). This may explain why, following significant ischaemia-reperfusion, PT cells tend to undergo necrosis, whereas apoptosis is more common in DT cells (Oberbauer *et al.*, 1999). However, there may be other aspects of mitochondrial function or its regulation that vary along the nephron, which could underlie these clinical observations.

1.2 The renal Fanconi syndrome

1.2.1 Background

The renal Fanconi syndrome (FS) (also known as Lignac-de Toni-Debré-Fanconi syndrome, and not to be confused with Fanconi's anaemia) refers to a set of clinical features resulting from a generalized failure of normal transport in the PT. FS was

originally described in the 1930s by the Swiss paediatrician Guido Fanconi. It is characterised by aminoaciduria, tubular proteinuria, phosphaturia, bicarbonate wasting and glycosuria (in the absence of diabetes and hyperglycaemia) (Brodehl, 1992). The clinical features of FS are therefore explained by deficiency of solutes normally reabsorbed in the PT, and include osteomalacia (due to hypophosphataemia) and metabolic acidosis. Tubular proteinuria is a common and early feature of FS. Tubular proteins consist of LMWPs (e.g. RBP) that are normally reabsorbed by the PT, and enzymes (e.g. N-acetyl-beta-D-glucosaminidase – NAG) that are released from damaged PT cells. RBP is relatively freely filtered by the glomerulus and almost completely reabsorbed along the PT; its presence in the urine in increased amounts usually indicates defective PT uptake and/or transport (Bernard *et al.*, 1982). NAG, which is not delivered, but is derived from PT cells, is an index of PT damage when elevated in urine (Price, 1992). The presence of excess tubular proteinuria is a sensitive and specific test for PT dysfunction (Norden *et al.*, 2000). Hypercalciuria can also occur, although the reasons for this are less clear.

1.2.2 Aetiology

FS was historically considered a rare disease, especially in adults. However, with the advent of more sensitive screening tests for tubular proteinuria, it is increasingly recognised that subclinical PT dysfunction is more common than was previously appreciated (e.g. in conditions such as diabetes (Kalansooriya *et al.*, 2007) and hypertension (Schrader *et al.*, 2006)). FS has a wide variety of causes, which include toxins (especially heavy metals like cadmium (Barbier *et al.*, 2005)), drugs (e.g. aminoglycoside antibiotics (Ghiculescu & Kubler, 2006), some anti-retroviral drugs [see later] (Izzedine *et al.*, 2003) and ifosfamide (Skinner, 2003)), myeloma (Headley *et al.*, 1972) and some auto-immune diseases (e.g. Sjögren's syndrome (Delplace, 1983)). Inherited forms of FS (which typically present in childhood) include autosomal recessive diseases like cystinosis (Schulman & Schneider, 1976), tyrosinaemia (Russo & O'Regan, 1990), fructose intolerance (Morris, Jr., 1968) and glycogen storage disease type I (Reitsma-Bierens, 1993). There is also an autosomal dominant idiopathic form of FS (Friedman *et al.*, 1978), and X-linked forms such as Dent's disease (Wrong *et al.*, 1994) and Lowe syndrome (Bockenhauer *et al.*, 2008). FS is the typical renal presentation of children with mitochondrial cytopathy

(Niaudet & Rotig, 1997) (see later – ‘Renal involvement in children with mitochondrial cytopathy’).

Some forms of FS are ‘incomplete’, that is they do not have all of the expected clinical features of PT dysfunction. For example, patients with Dent’s disease or Lowe syndrome present with most of the features of FS, but glycosuria can be absent. The prevalence of FS is unknown and difficult to estimate as there is such a wide variety of causes, many of which are relatively rare diseases. Cystinosis is thought to be the most common cause in childhood, whereas drug toxicity and myeloma are more prevalent in adulthood.

1.2.3 Pathogenesis

The underlying pathogenic mechanisms that unite these disparate causes of FS into similar identifiable clinical entities are not well understood. FS clearly involves a global breakdown of PT transport, which is quite dissimilar to monogenic transport disorders such as Bartter or Gitelman syndrome. It is, therefore, likely that the defects are occurring ‘downstream’ of the individual receptors in the transport pathways.

Tubular proteinuria is an early and sensitive sign of PT dysfunction. The importance of the megalin/cubulin system in the normal uptake of proteins by the PT has been demonstrated in animal models. Genetically modified mice lacking megalin develop significant tubular proteinuria (Leheste *et al.*, 1999), whilst inbred dogs that fail to insert cubulin into their apical PT membrane also have proteinuria, consisting of cubulin ligands (Kozyraki *et al.*, 2001; Birn *et al.*, 2000). However, a lack of cubulin does not seem to cause as severe proteinuria as megalin deficiency; perhaps because cubulin mediated uptake of ligands is also megalin dependent, but megalin is thought to be able to function in the absence of cubulin. Patients with mutations in cubulin, who have juvenile megaloblastic anaemia due to vitamin B12 malabsorption, can also develop pronounced proteinuria (Wahlstedt-Froberg *et al.*, 2003).

Dent’s disease is an X-linked hereditary form of FS, characterised by tubular proteinuria, hypercalcuria, nephrolithiasis and renal failure. It is divided into Dent 1

and Dent 2 depending on the underlying genetic mutation. Dent 1 is caused by mutations in the *CLCN5* gene (Thakker, 2000), which encodes a chloride channel required for acidification of endosomes. This promotes dissociation of megalin and cubulin receptors from their ligands, in order to allow recycling of the receptors to the apical membrane. In mouse models of Dent 1, where *CLCN5* has been knocked out, the animals develop tubular proteinuria due to impaired endosomal acidification and decreased expression of megalin and cubulin at the PT apical membrane (Christensen *et al.*, 2003; Marshansky *et al.*, 2002; Piwon *et al.*, 2000; Wang *et al.*, 2000). The animals also show decreased urinary excretion of megalin, which has been described in humans with Dent's disease, but not in another hereditary form of FS associated with tubular proteinuria (Norden *et al.*, 2002), perhaps implying that the megalin pathway is not the only mechanism of PT protein uptake that can be disturbed in FS. Dent 2 is caused by mutations in the *OCRL* gene (Hoopes, Jr. *et al.*, 2005; Utsch *et al.*, 2006), abnormalities in which can also lead to Lowe syndrome, an X-linked disease characterised by the triad of congenital cataracts, mental retardation and FS (Schurman & Scheinman, 2009). *OCRL* encodes a phosphatidylinositol 4,5-bisphosphate (PIP(2)) 5-phosphatase; the fact that mutations in either *CLCN5* or *OCRL* can both cause a similar phenotype (Dent's disease), implies overlap in the involvement of the respective gene products in endocytotic pathway in the PT. Some patients with phenotypic Dent's disease do not have identified mutations in either *CLCN5* or *ORCL*; discovery of the underlying genetic abnormalities in these patients may provide new insights into PT protein uptake mechanisms.

A defect in metabolism is an attractive hypothesis that might explain a sub-lethal functional defect in cellular transport. However, whilst there is considerable evidence implicating mitochondria in the pathogenesis of FS (see below – 'Evidence for mitochondrial dysfunction as a cause of Fanconi syndrome'), the exact mechanism by which dysfunction of these complex organelles could cause a problem with solute transport remains speculative and poorly understood. Other suggested mechanisms of a global breakdown in PT transport include back-leak of solutes and water across abnormal tight junctions between cells (Van't Hoff, 2005), an abnormality in the normal physical properties of the apical membrane (Hsu *et al.*, 1994), or a change in the membrane voltage that drives normal sodium dependent transport (Cetinkaya *et*

al., 2002). Whilst some evidence exists for all of these hypotheses, none has been conclusively proven to date, and FS remains a poorly understood condition.

1.2.4 Clinical Features

As explained above, the clinical features of FS are due to wasting of substances in the urine (HPO_4^{2-} , bicarbonate, glucose etc) that are normally retrieved from the filtrate in the PT. The typical presenting feature in adults is bone pain secondary to osteomalacia, due to hypophosphataemia. In addition, young children may experience problems due to fluid loss, causing polyuria, polydipsia and failure to thrive. This is probably due to a reduced capacity in the immature distal nephron segments to compensate for fluid losses from the PT. If large amounts of sodium are presented to the DT they may be exchanged there for potassium, under the influence of aldosterone, leading to hypokalaemia and metabolic alkalosis. Some patients may be detected via routine clinical screening (e.g. urine dipstick or serum creatinine) performed for other reasons. Patients can present with other symptoms or signs of the underlying disease; for example, renal stones or unexplained renal impairment in Dent's disease, or cardiac and neurological complications in mitochondrial disorders. A thorough family history is therefore important in all cases, especially in those without an obvious cause. A complete drug and occupational history is also crucial, particularly focusing on any exposure to heavy metals or industrial solvents, or herbal remedies obtained from unknown or unapproved sources.

1.2.5 Diagnosis of Fanconi syndrome

The diagnosis of FS is clinical and relies on identifying the cardinal features discussed above. Frequently FS will be preceded by diagnostic features of the underlying causative disease. Incomplete forms of FS can lead to clinical features that be may be more difficult to immediately attribute to a problem with PT function, and may require distinction from other non-renal diseases. For example, isolated hypophosphataemia may be due to a partial FS, but equally may be caused by malnutrition or a gastro-intestinal disease. The presence of excess tubular proteinuria is a highly sensitive marker of PT dysfunction.

Diagnosis of FS is usually achieved with the following investigations:

- Serum creatinine. This may be raised (and hence eGFR reduced), either because of impaired PT secretion of creatinine, or because of concomitant glomerular disease with reduced filtration.
- Serum HPO_4^{2-} . It needs to be ascertained that hypophosphataemia (if present) is due to renal wasting. Renal handling of HPO_4^{2-} can be assessed by calculating the capacity of the PT to reabsorb phosphate: $T_m\text{HPO}_4^{2-} / \text{GFR} = \text{Plasma } \text{HPO}_4^{2-} - (\text{Urine } \text{HPO}_4^{2-} \times [\text{Plasma Creatinine} / \text{Urine Creatinine}])$ (Walton & Bijvoet, 1975). An alternative is to calculate the fractional excretion of phosphate ($[\text{Urine } \text{HPO}_4^{2-} \times \text{Plasma Creatinine}] / [\text{Urine Creatinine} \times \text{Plasma } \text{HPO}_4^{2-}] \times 100$).
- Serum bicarbonate. Renal tubular acidosis (RTA) type II (proximal) can occur due to bicarbonate wasting, and can be distinguished from distal (type 1) RTA, because patients with proximal RTA can acidify their urine to $\text{pH} < 5.5$ following an acid load (e.g. with NH_4Cl or combined fludrocortisone and frusemide (Walsh *et al.*, 2007)), whereas patients with distal RTA cannot.
- Serum potassium. Hypokalaemia is a feature of more severe cases of FS.
- Tubular proteinuria. Typically screened for by assaying for RBP (or other LMWPs like α_1 - or β_2 -microglobulin) and PT enzymes such as NAG.
- Aminoaciduria is frequently screened for in children.

1.2.6 Screening for subclinical proximal tubular disease

The classical clinical features of FS represent the severe end of the spectrum of PT disease (analogous to stages IV-V of CKD). It is likely that many more patients have undiagnosed subclinical PT dysfunction, which can be screened for by testing for tubular proteins, such as RBP and NAG. These can be compared with urinary albumin to identify co-incident glomerular proteinuria. The glomerular filtration barrier is relatively impermeable to albumin; hence, its appearance in the urine in elevated amounts is widely accepted as a marker of glomerular disease (Norden *et al.*, 2000). Values of urinary proteins are usually expressed as a ratio to urine creatinine (i.e. $U_{\text{RBP/C}}$, $U_{\text{NAG/C}}$ and $U_{\text{A/C}}$, respectively), in order to account for differences in urine concentration between samples.

Urine protein:creatinine ($U_{P/C}$) is a test for total urinary protein excretion; it is a standard clinical screening tool for the presence of kidney disease and correlates well to the 24-hour urinary protein excretion (Ginsberg *et al.*, 1983). However, its sensitivity for detecting renal tubular disease is unclear. Recently, The National Institute for Clinical Excellence (NICE) in the UK (www.nice.org.uk/Guidance/CG73) has advocated $U_{A/C}$ as a screening tool for chronic kidney disease (CKD), as it is relatively cheap and results appear to be consistent between different reporting laboratories. However, again it is unclear to what extent $U_{A/C}$ is an effective screen for tubular disease. Although albuminuria is thought to predominantly reflect glomerular pathology, some albumin uptake is believed to occur in the PT (Thakkar *et al.*, 1998); hence, small rises in $U_{A/C}$ might be expected in patients with tubular disease.

1.2.7 Treatment

In cases of FS due to a multi-system disease (e.g. cystinosis), addressing the underlying cause is clearly of paramount importance. General treatment approaches for all forms of FS involves replacing solutes lost in the urine to prevent deficiencies:

- Vitamin D (calcitriol) and HPO_4^{2-} supplements for hypophosphataemia.
- Oral bicarbonate supplements for metabolic acidosis.
- Oral potassium for hypokalaemia.
- Fluid replacement therapy may be required in children. If chronic excess fluid losses are occurring, indomethacin can be given to pharmacologically reduce GFR.

In cases of FS that subsequently develop chronic kidney disease, general measures to slow progression are important, including blood pressure control, anti-proteinuric therapy if there is significant proteinuria, and treatment of any cardiovascular risk factors that are present (e.g. use of statins).

1.3 Functions of mitochondria

1.3.1 Origins of mitochondria

Mitochondria are intracellular organelles present in almost all eukaryotic cells. They probably evolved from a primitive aerobic prokaryotic structure that fused with a larger anaerobic cell to form a new organism with a significant metabolic advantage (Dyall *et al.*, 2004). Over time, a complex symbiotic relationship has developed between the mitochondrion and its host cell, going much further than the simple provision of ATP. Mitochondria play a central role in the regulation of a range of important cellular functions, including the generation of reactive oxygen species (ROS), intracellular Ca^{2+} homeostasis, biosynthesis and apoptosis (Duchen, 2004). Thus, MD can be deleterious to the host cell in a variety of ways. Diseases associated with MD include diabetes (Wiederkehr & Wollheim, 2006), septic shock (Singer *et al.*, 2004) and neuro-degenerative conditions such as Parkinson's disease (Mandemakers *et al.*, 2007).

1.3.2 Mitochondrial ATP production

A major function of mitochondria is to provide chemical energy for the host cell in the form of ATP, which is generated from ADP and HPO_4^{2-} via oxidative phosphorylation (Figure 1.3). ATP is the universal energy 'currency' of life; significant amounts of energy are released when ATP is converted to ADP and HPO_4^{2-} .

In living cells the ATP/ADP ratio is maintained at a high level in the cytosol; creating in effect an energy store, which can be rapidly mobilised (via ATP breakdown to ADP) and coupled to the work done in normal cellular function; for example, in powering cell membrane pumps like the Na^+/K^+ -ATPase.

The process of oxidative phosphorylation essentially converts the chemical energy stored in the bonds of carbon and hydrogen based organic fuels (such as glucose, fatty acids and amino acids) to chemical energy stored in the bonds of ATP. This is achieved by oxidising these fuel molecules and transferring the electrons along the respiratory chain (RC) complexes, ultimately to oxygen molecules to form water.

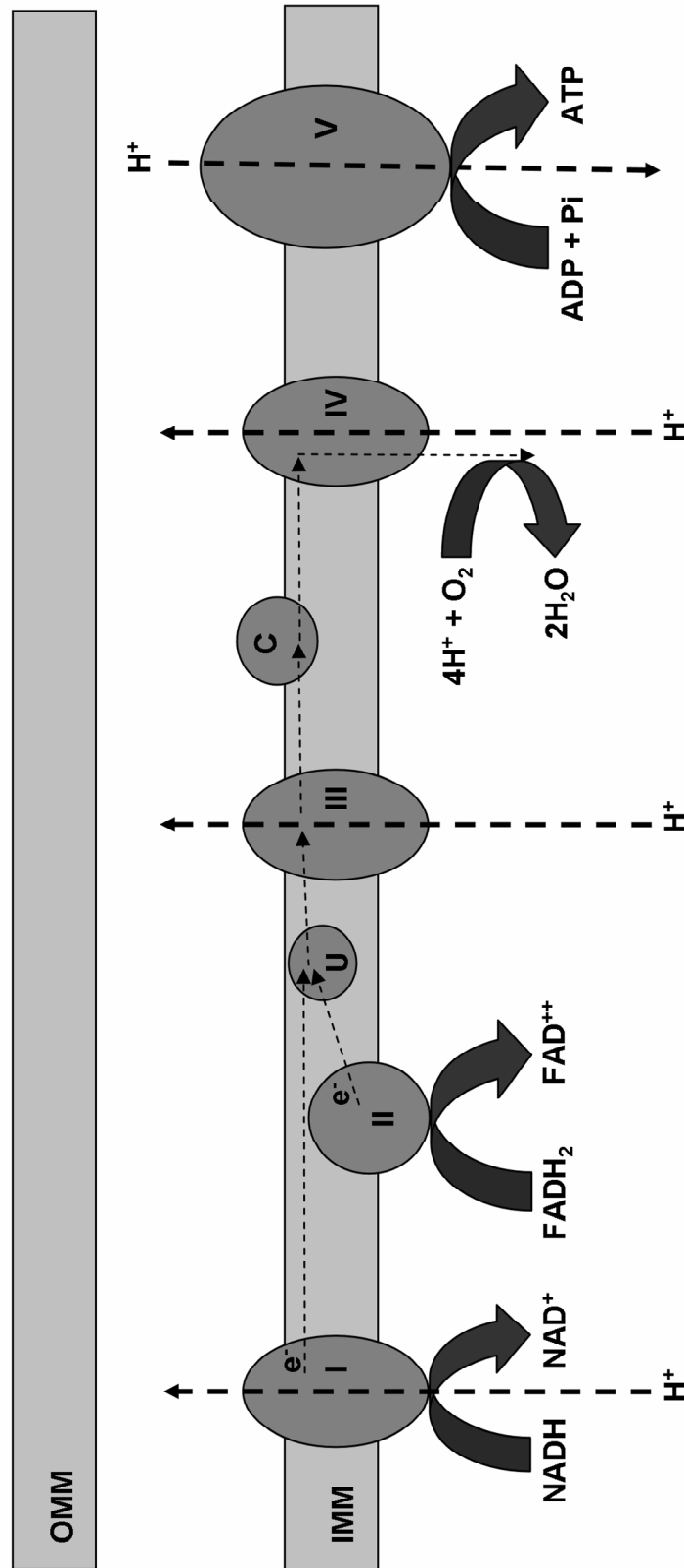


Figure 1.3. The mitochondrial respiratory chain. Electrons enter the mitochondrial respiratory chain via the oxidation of substrates NADH (complex I) and FADH_2 (complex II). They are then shuttled to complex III by ubiquinone (U), and then onto complex IV by cytochrome c (C). The energy released from the transfer of electrons is utilized to pump protons out of the mitochondrial matrix and into the inter-membrane space, which lies between the inner (IMM) and outer (OMM) mitochondrial membranes. Protons then pass back through complex V, down the electro-chemical gradient, powering the energetically unfavourable generation of ATP from ADP and inorganic phosphate (P_i). MtDNA encodes for subunits of complexes I, III, IV and V. Complex II is formed entirely of nuclear encoded sub-units.

The energy released by this process is then used to form ATP and is thus stored for future usage.

The first step of oxidative phosphorylation is the breakdown of fuel molecules to acetyl CoA. This molecule then enters the Krebs cycle within the mitochondria. Here, it is converted to a variety of intermediates. Along the way, the substrates for the mitochondrial RC are reduced; NAD^+ to NADH and FAD^{2+} to FADH_2 . These substrates are then, in turn, oxidised by complexes I and II of the RC, respectively. Having entered the RC, electrons are passed along the complexes until they reach complex IV (cytochrome c oxidase – COX), at which point they reduce oxygen to form (along with protons) water. The complexes of the RC are large clusters of proteins that are situated in close proximity in the inner mitochondrial membrane (IMM). Electrons are shuttled from complexes I and II to complex III by the cofactor ubiquinone (coenzyme Q10). From here they are passed onto complex IV by another cofactor called cytochrome c. As the electrons pass through the RC complexes energy is released, which is harnessed by complexes I, III and IV to pump protons out of the mitochondrial matrix, across the IMM and into the inter-membrane space. This then creates an electrochemical proton gradient across the IMM, sometimes called the proton motive force (PMF), which is expressed in part as a potential difference ($\Delta\Psi_m$ - typically $\sim 150\text{mV}$ (Duchen *et al.*, 2003)), and in part as a pH gradient (ΔpH). Protons then pass down this electro-chemical gradient through the ATP synthase, and this movement is used to drive the energetically unfavourable formation of ATP from ADP and PO_4^{2-} . The usage of PMF as an intermediate to harness the energy released by the oxidation of organic fuel molecules, and convert and store it as ATP molecules, is termed ‘chemiosmotic coupling’, and was first proposed by the Nobel prize winner for Chemistry Peter Mitchell (Mitchell, 1961).

The degree to which the PMF is coupled to ATP synthesis depends on the amount of proton leak back through the IMM that does not pass through the ATP synthase. This can occur physiologically, for example to generate heat in brown fat (mainly found in neonates), due to the actions of specialised uncoupling proteins (UCPs). More recently, a number of related proteins have been identified which have been labelled as belonging to a family of UCPs. The UCP of Brown fat is now known as UCP1 (Nicholls & Rial, 1999), but there are a number of related proteins, of which UCP2

and UCP3 have been most studied (for reviews see (Krauss *et al.*, 2005; Nicholls, 2006)). There seems to be an emerging consensus that these ‘uncoupling proteins’ may be activated by ROS, and that they could serve to reduce ROS generation by lowering PMF (Affourtit & Brand, 2008); this remains highly controversial and is still very much a developing field. Certain pharmacological agents can also act as uncouplers (e.g. aspirin (Petrescu & Tarba, 1997)).

In order to continually produce ATP, mitochondria require a steady supply of ADP, which enters the organelles via an adenine nucleoside translocase (ANT) that exchanges ATP for ADP (Winkler *et al.*, 1968). $\Delta\Psi_m$ is also important for mitochondrial functions other than ATP production, such as Ca^{2+} uptake into the mitochondria from the cytosol (see later – ‘Calcium signalling’) and protein import.

1.3.3 Reactive oxygen species production

ROS are unstable molecules with an excess of electrons that have wide-ranging roles in renal physiology and patho-physiology (Sachse & Wolf, 2007). Sources of intracellular ROS include the RC, NADPH oxidase and xanthine oxidase. Within the mitochondria, ROS are thought to be produced predominantly at RC complexes I and III, and the rate of production of ROS from the RC is dependent on electron flux, redox state and oxygen availability (for review see (Murphy, 2009)). The major ROS molecule generated by the RC is superoxide (O_2^-). This is then normally rapidly converted to the less toxic species hydrogen peroxide (H_2O_2) by the enzyme superoxide dismutase (SOD), of which an isoform is situated within mitochondria. The total rate of ROS production within mitochondria will therefore reflect a balance between generation by the RC and scavenging by protective enzymes.

The rate of production of ROS at complex I is favoured by the complex being in a reduced state (Kushnareva *et al.*, 2002); in other words by an excess of electrons being present to form O_2^- . This scenario typically occurs when the flux of electrons along the RC is slow or completely halted. For this reason, agents that block electron flow at complex I (such as rotenone) typically increase the production of ROS at this site (Reinecke *et al.*, 2006). When the activity of the ATP synthase is low, the potential will tend to increase and electron flow will also be slower; hence, increased

ROS production is often associated with an increased $\Delta\Psi_m$. Conversely, a lower $\Delta\Psi_m$, which tends to promote faster electron flow, is thought to decrease ROS production by the RC; a paradigm that has fuelled interest in UCPs that can potentially lower $\Delta\Psi_m$.

Another major source of O_2^- in the kidney is the NADPH oxidase, and regional differences in expression levels of the enzyme have been reported in the tubule (Gill & Wilcox, 2006). Furthermore, there is evidence that the NADPH oxidase is activated by angiotensin II, providing a putative link between systemic hypertension and oxidative stress in the kidney (Wilcox, 2002), which may be important in the pathogenesis of chronic kidney disease.

ROS are believed to have a number of toxic effects, including damage of DNA, lipid peroxidation and involvement in cell death pathways (Trachootham *et al.*, 2008). Unsurprisingly, therefore, they have been implicated in the pathogenesis of a variety of common disease processes (e.g. neurodegeneration (Fatokun *et al.*, 2008)) and are also suggested to be responsible for the ageing process (Gruber *et al.*, 2008) (although this remains controversial). Anti-oxidants have generally proved to be of limited therapeutic value, although this may be due to difficulties in targeting them to the mitochondria. As ROS species, like O_2^- , are unstable they generally react with structures in the near vicinity; a particular concern is therefore ROS induced mtDNA damage. This has been suggested as a possible mechanism of progression of disease in patients with mitochondrial cytopathy (Jacobson *et al.*, 2005) (see later - 'Pathophysiology of mitochondrial cytopathy'). The hypothesis is that mutations in mtDNA, which encode for proteins and RNA involved in the structure and maintenance of the RC, will lead to abnormal RC function, leading to increased ROS production. This in turn will damage the mtDNA further, leading to replication errors and increasing the mutation rate, thus creating a positive feedback loop that over time will cause increasing MD, which may explain the slow progression of many mitochondrial diseases (and indeed perhaps the 'normal' process of ageing). Although yet to be conclusively proven, this theory could explain why anti-oxidants may only be efficacious in clinical disease if adequately targeted to mitochondria.

1.3.4 Glutathione

Due to the potentially toxic actions of ROS, cells have acquired a range of anti-oxidant defences, including enzymes such as SOD (as mentioned above) and catalase (which catalyses the decomposition of H_2O_2 to H_2O and O_2 (Chelikani *et al.*, 2004)). Another important intracellular anti-oxidant is glutathione (GSH), which also has other key roles in the kidney, including acting as a substrate or cofactor for drug metabolism reactions (Lash, 2005). Conjugation reactions involving GSH are catalysed by the enzyme glutathione-s-transferase (GST). GSH can donate reducing equivalents to unstable molecules (i.e. ROS) and enter an oxidised state (glutathione disulphide – GSSG); it can then be converted back to the reduced form by glutathione reductase. The GSH/GSSG ratio is kept high in most cells (i.e. the GSH pool is predominantly in a reduced state), in order to provide an effective anti-oxidant system. A lowering of the GSH/GSSG ratio is, therefore, often taken as a sign of oxidant stress within a cell.

Whilst the liver is the main source of circulating GSH, the kidney is responsible for the uptake and clearance of GSH from the plasma (Griffith & Meister, 1979). Uptake of GSH by the kidney occurs predominantly in the PT, via both the apical and basolateral membranes, and utilises both sodium dependent and independent mechanisms (Lash, 2005). In addition, the PT is also capable of synthesising GSH from precursor amino acids. Experimentally, uptake of exogenous GSH by the PT appears to be protective against oxidative stress (Lash *et al.*, 1986).

1.3.5 Calcium signalling

Ca^{2+} is an important intracellular second messenger, with multiple roles in cell signalling, affecting diverse functions such as muscle contraction, neurotransmitter secretion, gene transcription and egg fertilisation (for reviews see (Bootman *et al.*, 2001; Petersen *et al.*, 2005)). Ca^{2+} signals are compartmentalised within the cell and are frequency and amplitude coded, which allows them to convey a diverse range of information. An increase in intracellular $[\text{Ca}^{2+}]$, in response to an extracellular signalling stimulus, usually occurs either due to influx of Ca^{2+} from the extracellular fluid (via transient opening of either voltage or ligand gated cation channels), or from release of Ca^{2+} from intracellular stores. The majority of Ca^{2+} within the cell is stored

in the endoplasmic reticulum (ER), and can be released in response to activation of 1,4,5-trisphosphate (IP₃) (Spat *et al.*, 1986) or ryanodine (Franzini-Armstrong & Protasi, 1997) receptors in the ER membrane. IP₃ itself is an important second messenger, generated following the action of neurotransmitters or hormones acting on receptors in the cell membrane (Streb *et al.*, 1983), while ryanodine receptors are activated by ADP ribose (Bastide *et al.*, 2002). Nicotinic acid adenine dinucleotide phosphate (NAADP) is a more recently discovered second messenger that is thought to cause intracellular Ca²⁺ release from acidic organelles (such as lysosomes) (Calcraft *et al.*, 2009).

Following an increase in intracellular [Ca²⁺], rapid uptake of Ca²⁺ then usually occurs, partly back into the ER, but also into the mitochondria, which act as a major reservoir for Ca²⁺ uptake. This movement of Ca²⁺ into mitochondria is driven by the electrochemical potential for Ca²⁺ across the mitochondrial membrane – a low intramitochondrial [Ca²⁺] and a negative membrane potential, and is carried through a Ca²⁺ uniporter (Kirichok *et al.*, 2004). Depending on their intracellular localisation, mitochondria can therefore act as a ‘firewall’ against Ca²⁺ signals propagating across the cell, and this can be extremely important in spatially localising a Ca²⁺ signal within a polarised cell (Camello-Almaraz *et al.*, 2002). Ca²⁺ taken up by mitochondria can be extruded via a Na⁺/Ca²⁺ exchanger, in order to restore the resting state. Intracellular [Ca²⁺] is kept relatively low under quiescent conditions by the activity of plasma membrane (PMCA) and sarco/endoplasmic reticulum (SERCA) Ca²⁺ ATPase pumps.

Ca²⁺ signals in the PT have been observed in response to the physiological agonist ATP, and these signals might have a role in regulating solute transport (Lee *et al.*, 2005) and cell proliferation (Lee & Han, 2006). Furthermore, elevations in intracellular [Ca²⁺] have been implicated in the pathogenesis of ischaemic renal failure (Edelstein *et al.*, 1997). It therefore follows that a disturbance in normal mitochondrial function is likely to cause alterations in normal Ca²⁺ signalling within the PT, which may in turn have a functional effect on solute transport.

1.3.6 Regulation of mitochondrial function

As discussed above, much has been learnt about mitochondrial function. In contrast, relatively little is known to date about *regulation* of function, particularly *in vivo*. In the kidney, metabolism is thought to be tightly coupled to membrane transport (Soltoff, 1986). For example, an increase in solute transport will be reflected in an increase in Na^+/K^+ -ATPase activity, which will decrease cytosolic [ATP]. This, in turn, will increase the ADP/ATP ratio in the mitochondria and favour the generation of ATP by the mitochondrial ATP synthase. Conversely, a decrease in transport activity, and increase in cytosolic [ATP], can lead to a lowering of $\Delta\Psi_m$ and ATP production, via an inhibitory feedback mechanism on the RC (Kadenbach & Arnold, 1999).

Ca^{2+} is recognized to have an important regulatory role with regards to mitochondrial function; an increase in mitochondrial Ca^{2+} can increase the activity of key enzymes involved in the supply of substrates to the RC (McCormack *et al.*, 1990), and is also thought to directly increase the activity of the ATP synthase (Territo *et al.*, 2000). Mitochondrial mass can be altered in muscle in response to challenges such as exercise, cold and starvation. This process is thought to be mediated, at least in part, by changes in the activity of AMP-activated protein kinase (AMPK); an evolutionarily conserved fuel sensor, which is activated by decreases in intracellular ATP/AMP ratio (Zong *et al.*, 2002). Activated AMPK is believed to lead to an increase in mitochondrial biogenesis via the effects of the transcription factor PGC-1 α (Jager *et al.*, 2007). Interestingly, the drug metformin (a widely used treatment for type II diabetes in patients with the ‘metabolic syndrome’) has been shown to activate AMPK (Zhou *et al.*, 2001).

At the level of an individual mitochondrion, ATP production is dependent on F_1F_0 -ATP synthase activity, which in turn is determined by both $\Delta\Psi_m$ and the ADP/ATP ratio. $\Delta\Psi_m$ is dependent on substrate supply and RC complex activity, the degree of proton leak across the inner mitochondrial membrane and the activity of the ATP synthase. The nuclear-encoded mitochondrial protein IF1 has recently been shown to have effects on ATP synthase activity and $\Delta\Psi_m$ in cultured cells (Campanella *et al.*, 2008), and also on mitochondrial mass and structure (Campanella *et al.*, 2009). In

terms of overall ATP production in a given mitochondrion, the total number of RC complexes and ATPase pumps is also clearly important. Therefore, it is apparent that a number of different factors can affect mitochondrial ATP production, with the final common pathway being the ATP synthase.

1.4 Mitochondrial cytopathy

1.4.1 Background

Mitochondria contain their own DNA (mtDNA) about 16.6 Kb long, which is primarily maternally inherited and encodes for 13 proteins involved in the RC and two rRNA subunits and 22 tRNA molecules necessary for protein synthesis (Taanman, 1999). The majority of a mitochondrion's approximately 1000 proteins are encoded by nuclear (nDNA), rather than mtDNA. Unlike nDNA, mtDNA exists as many copies in each cell and is thought to have a mutation rate as much as ten times higher than nDNA (Brown *et al.*, 1979). This is thought to be secondary to the combination of a higher replication rate, closer proximity to the ROS-producing RC and a lack of the protection that is afforded to nDNA by histones. This may cause variation between cells in their mutant load, a phenomenon known as heteroplasmy; cells in which all copies of mtDNA are affected are said to be homoplasmic. It therefore follows that in order for clinical disease to develop, a threshold level of mutant load has to occur within the cells of a particular tissue. This threshold may itself in turn depend on the relevant dependence of a particular tissue on aerobic or anaerobic metabolism.

Mutations in mtDNA can take the form of deletions or point substitutions. Multiple mtDNA deletions can be due to a defect in nDNA, causing a secondary abnormality in mtDNA replication or repair. Diseases that are thought to be primarily due to a defect in mitochondrial function are referred to as mitochondrial cytopathy, in order to distinguish them from conditions in which mitochondrial involvement is a secondary phenomenon, e.g., in cell death following ischaemia-reperfusion injury (Plotnikov *et al.*, 2007). Clearly, organs with a high rate of aerobic metabolism (e.g., the heart, skeletal muscle, brain and kidney) are more susceptible to mitochondrial disease than cells or tissues with a higher anaerobic glycolytic capacity. Even within

a tissue, variations exist among cell types in their relative dependence on aerobic metabolism. Cells that are terminally differentiated (like podocytes) are especially prone to the effects of mtDNA mutations, as rapidly dividing cells may segregate mutant mtDNA unevenly, leading to daughter cells with differing mutant load. Over time, due to a selective survival advantage, the daughter cells with a lower mutant load may predominate, explaining why mutant loads are often lower in rapidly dividing cells (such as leukocytes) than in other tissues in the body.

1.4.2 Phenotypic heterogeneity in mitochondrial cytopathy

Although certain patterns of disease are observed in mitochondrial cytopathy (Table 1.1), generally affecting the major aerobic organs, there is much phenotypic heterogeneity.

Syndrome	Features
Kearns-Sayre	Cardiac conduction defects, ophthalmoplegia, retinitis pigmentosa, deafness, cerebellar ataxia
Leber's optic atrophy	Blindness (predominantly in males)
Leigh	Seizures, dementia, brain stem dysfunction
MELAS	Encephalo-myopathy, lactic acidemia and stroke like episodes
MERRF	Myoclonic seizures, myopathy, short stature
MIDD	Maternally inherited diabetes and deafness
NARP	Neuropathy, ataxia, retinitis pigmentosa, and ptosis
Pearson	Anaemia, pancreatic dysfunction
PEO	Progressive external ophthalmoplegia
SANDO	Sensory ataxic neuropathy, dysarthria and ophthalmoplegia

Table 1.1. Typical phenotypic patterns observed in mitochondrial cytopathy.

The same point mutation can produce a range of very different phenotypes; for example, the A3243G mtDNA point mutation in the TL1 gene is associated with MELAS (mitochondrial encephalo-myopathy lactic acidosis and stroke like episodes) (Sproule & Kaufmann, 2008), renal glomerular disease (focal segmental

glomerulosclerosis – FSGS) (Guery *et al.*, 2003) and MIDD (maternally inherited deafness and diabetes) (Guillausseau *et al.*, 2001). Conversely, identical phenotypes can be produced by different mutations. The reasons for this heterogeneity in phenotype are not well understood. Possible explanations include interaction between nDNA and mtDNA encoded proteins, unrecognised nDNA mutations and the effects of environmental toxins.

The importance of the interaction between nuclear and mitochondrial genomes cannot be overstated. MtDNA only encodes for a small proportion of mitochondrial proteins and replication; transcription and translation are dependent on nuclear encoded proteins that must be imported into mitochondria. It is thought that many of the nuclear-encoded mitochondrial genes currently residing in the nucleus were originally located in the mitochondrial genome, and have moved over time to the nucleus for greater protection and a reduced mutation rate. It may be that in patients with an identified pathogenic mtDNA mutation another, as yet unidentified, mutation in nDNA is necessary to co-exist or develop for disease to occur. Environmental toxins acting on a background of mutations in nuclear or mtDNA genes encoding mitochondrial proteins could affect the timing, severity and organ specificity of mitochondrial disease. For example, several toxins have been identified that may cause diseases such as renal FS by disturbing mitochondrial function: aminoglycosides (Simmons, Jr. *et al.*, 1980), ifosfamide (DiCataldo A. *et al.*, 1999), and heavy metals (such as cadmium (Takebayashi *et al.*, 2003)) are all examples. The PT is particularly vulnerable to mitochondrial toxins, perhaps because it is a major site for the excretion of xenobiotics.

1.4.3 Patho-physiology of mitochondrial cytopathy

How exactly a single point mutation in mtDNA can lead to clinical disease is not well understood. Some insights into the cellular consequences of mtDNA mutation have been gained from studies of transmitochondrial cybrids. These are immortalized human cells depleted of mtDNA by exposure to a nucleoside analogue such as 2',3'dideoxycytidine (ddC) (Nelson *et al.*, 1997), which inhibits mtDNA replication. Donor mitochondria are then introduced by fusion with platelets or enucleated skin

fibroblasts, derived from patients with a known mtDNA mutation. This model has the advantage that the effects of mtDNA mutations on cell metabolism can be investigated without the confounding effects of unknown variations in nuclear genes encoding mitochondrial proteins.

In cybrids derived from patients with MELAS due to the A3243G mutation, significant reductions in mitochondrial translation products and impaired RC function occur (Chomyn *et al.*, 1992). The A3243G mutation has also been associated with a number of cellular biochemical defects in addition to reduced RC function, including increased oxidative stress (Rusanen *et al.*, 2000), impaired Ca^{2+} homeostasis (Moudy *et al.*, 1995), lower $\Delta\psi_m$ (James *et al.*, 1996), abnormal post-transcriptional tRNA modification (Helm *et al.*, 1999), and increased sensitivity to signals for apoptosis (Mirabella *et al.*, 2000). Yet significant protection was conferred by only a 6% level of wildtype mtDNA in A3243G cybrids, indicating that a mutant load of ~95% is required to produce abnormalities in cultured cells, and perhaps also in disease. In patients with MELAS the mutant load varies widely among different cell types and individuals, and clinical disease can occur with much less than a 95% mutant load, which suggests that other factors are necessary *in vivo* for disease to manifest itself, and/or that cybrid cells are relatively resistant to the effects of mtDNA mutation, perhaps due to significant anaerobic metabolic capacity.

Some information has been obtained from studies in animal models with regards to the mechanism(s) via which MD may cause disease in the kidneys. Puromycin aminonucleoside nephrosis (PAN) is a rat model of human FSGS (Hagiwara *et al.*, 2006). In this model injections of puromycin aminonucleoside produced an early nephrotic phase (analogous to minimal change disease in humans), followed by the histological changes seen in FSGS. The development of FSGS was associated with a reduction in whole kidney mtDNA and in mtDNA-encoded proteins in glomeruli. Abnormalities in mitochondrial morphology in podocytes were also noted on microscopy. How PAN causes these changes in mtDNA is unknown. In this model, nitric oxide (NO) levels rose and fell in phase with the changes in mtDNA, which might be important as NO can affect mitochondrial biogenesis through the generation of cGMP (Nisoli *et al.*, 2004).

In the 'mito-mouse' (a mouse model of mitochondrial cytopathy), although multi-organ disease did occur, the cause of death was renal failure at about 6 months of age (Nakada *et al.*, 2001). Histology of the kidneys showed dilated proximal and distal tubules, as well as glomerular segmental sclerosis. RC function tests from affected kidneys indicated that COX activity was reduced to ~28% of normal. This model provides direct evidence for a link between mutation of mtDNA, a reduction in RC function in the kidney and renal failure. Interestingly, the authors reported that the tubular disease was largely cortical, perhaps reflecting the gradient in anaerobic glycolytic capacity that exists in the kidney, increasing from cortex to medulla (Lee & Peter, 1969). In general, producing useful animal models of mitochondrial cytopathy has proved difficult for a variety of reasons, including the lack of a simple method to transfer mtDNA alone, phenotypic variability observed with the same mtDNA mutation and the fact that apparently pathogenic mutations in humans can be neutral polymorphisms in other species (for review see (Khan *et al.*, 2006)). The 'mito-mouse' was generated by injecting mitochondria containing a 4696 base-pair mtDNA deletion into mouse embryos. Other approaches have involved altering nuclear genes to affect mtDNA replication and induce mutations (e.g. mutated pol- γ (Trifunovic *et al.*, 2004; Kujoth *et al.*, 2005)), or expression of restriction enzymes targeted to mitochondria to induce mutations of mtDNA (Bayona-Bafaluy *et al.*, 2005). Although these techniques can produce animals with organ dysfunction and shortened life-spans, the phenotypes vary due to the random nature of mtDNA mutations that are induced. Substantial improvements, especially with regards to mtDNA transfer techniques, will be required in order to model human mitochondrial cytopathy more accurately, and in particular the effects of common pathogenic single mtDNA mutations.

In spite of a major research effort, how mitochondrial cytopathy can lead to disease at a cellular level is still unclear. As previously mentioned (see earlier – 'Reactive oxygen species production'), one attractive theory is that mtDNA mutations may increase oxidative stress, which in turn causes oxidative damage to the RC, acting as a positive feedback mechanism that amplifies mitochondrial dysfunction (Jacobson *et al.*, 2005). Such a process could account for the slow progression of disease in many patients, despite the expression of the mutation from birth, but this is speculative.

It is well recognised that patients with end stage renal failure, even if on haemodialysis, can develop a uraemic myopathy. This may be related to a range of factors, including alterations in vitamin D metabolism and erythropoietin deficiency. However, there is some evidence for abnormal mitochondrial function in skeletal muscle in these patients too, suggesting that they may have any acquired form of mitochondrial cytopathy, and that the relationship between renal disease and mitochondrial dysfunction may be a two-way process. Skeletal muscle biopsies from haemodialysis patients have shown abnormalities in mitochondrial morphology on electron microscopy (Diesel *et al.*, 1993; Shah *et al.*, 1983) and revealed limited aerobic capacity (Moore *et al.*, 1993); however, others have reported preserved mitochondrial function (Miro *et al.*, 2002; Barany *et al.*, 1991). Excess lactate production during exercise has been described in haemodialysis patients (Parrish, 1981; Lundin *et al.*, 1987), but this may be related to abnormalities in oxygen delivery rather than intrinsic mitochondrial defects (Sala *et al.*, 2001). Finally, carnitine deficiency has been implicated in uraemic myopathy. Carnitine is located on the inner side of the mitochondrial membrane, and plays a key role in transporting fatty acids from the cytosol into the mitochondria so they may be broken down, via beta-oxidation, to be used as substrates for oxidative phosphorylation. Haemodialysis patients can become carnitine deficient due to losses across the dialytic membranes (Guarnieri *et al.*, 2001), which might explain the development of myopathy. However, some studies have disputed that dialysis patients are actually carnitine deficient in muscle (Mingardi *et al.*, 1980; Wanner & Horl, 1988), and carnitine supplementation has not been conclusively proven to objectively improve uraemic myopathy (Davenport, 2004; Vaux *et al.*, 2004).

1.4.4 Renal involvement in children with mitochondrial cytopathy

Much of the current literature on mitochondrial cytopathy and renal disease comes from paediatrics and has been presented in several published reviews (Niaudet & Rotig, 1997; Niaudet, 1998; Rotig, 2003). The commonest renal manifestation seems to be FS (Martin-Hernandez *et al.*, 2005; Neiberger *et al.*, 2002); although the nephrotic syndrome, tubulo-interstitial disease, a Bartter's-like syndrome and renal tubular acidosis have all been described (Niaudet & Rotig, 1996). So far, no clear

pattern has emerged linking particular gene mutations with specific RC defects or a particular renal phenotype. However, it has been noted that most of the children described present at an early age (generally under 2 years old) and renal dysfunction was diagnosed after developing a severe and generalized multi-system disorder. A range of underlying gene defects has been described, including point mutations and deletions of mtDNA. Children with FS often have mtDNA deletions and have syndromes known to be caused by mtDNA deletion, such as Pearson (refractory sideroblastic anaemia, diabetes and lactic acidosis) or Kearns-Sayre (external ophthalmoplegia, retinopathy, myopathy and ataxia).

A variety of mutations in nuclear genes encoding mitochondrial proteins have been reported in the last few years that cause renal disease in children. Both tubulopathy (Rahman *et al.*, 2001) and nephrotic syndrome (Salviati *et al.*, 2005; Rotig *et al.*, 2000) have been associated with co-enzyme Q10 (ubiquinone) deficiency, and, more recently, mutations in two nuclear genes (*COQ2* (Quinzii *et al.*, 2006) and *PDSS2* (Lopez *et al.*, 2006)) encoding components of the co-enzyme Q10 biosynthetic pathway have been described in patients with renal disease. Mutation of *BCS1L* can lead to impaired complex III assembly (Lonlay *et al.*, 2001), while mutation of *COX10* can lead to impaired complex IV activity (Valnot *et al.*, 2000); both have been described in patients with PT disease. Recently, a mtDNA depletion syndrome causing tubular disease (due to a defect in the nuclear gene *RRM2B* (Bourdon *et al.*, 2007)) has been described.

A screening study in children with mitochondrial cytopathy showed that almost half had either FS or sub-clinical proximal tubulopathy (Martin-Hernandez *et al.*, 2005), suggesting that the burden of PT disease in these patients is significantly underestimated, whatever the underlying mutation. Measuring serum lactate has often been used as a screening test for mitochondrial cytopathy, though in the presence of renal disease (FS) it may be normal owing to increased urinary loss of lactate, which is normally reabsorbed by the PT (Thirumurugan *et al.*, 2004). In children with multi-system mitochondrial cytopathy the prognosis is often poor; the reason for the high prevalence of PT disease in children is not known.

1.4.5 Renal involvement in adults with mitochondrial cytopathy

The situation to date in the literature concerning adults with mitochondrial cytopathy seems to be somewhat different from children. Although a range of renal pathologies have been reported, including tubulo-interstitial disease and multi-cystic disease, the most common histological finding has been glomerular sclerosis (FSGS) (Guery *et al.*, 2003; Li *et al.*, 2007; Lowik *et al.*, 2005). For reasons that are not yet clear, there appears to be a female preponderance in the literature, which has not been observed in children, and there is wide variation in age at presentation. FSGS has been described in children with mitochondrial cytopathy (Gucer *et al.*, 2005; Scaglia *et al.*, 2003), but does not appear to be as frequent as tubular disease. Involvement of other organs is common, but the severe multi-system disease seen in children is rare. Hearing loss seems to be particularly common and has led to some confusion with Alport's disease (which can be differentiated by the presence of haematuria and non-progressive hearing loss). Diabetes is also common and can be aggravated by steroids given to treat FSGS, although renal histology suggests that diabetes is not responsible for the nephropathy (Guery *et al.*, 2003).

In contrast to mitochondrial cytopathy-related renal involvement in children, a significant number of adult patients seem to present with renal disease before a mitochondrial diagnosis. Various clues can suggest the underlying diagnosis, including the presence of subclinical disease in other tissues, a positive family history (though not necessarily of renal disease) with maternal inheritance, a lack of response to conventional therapy, and the presence of abnormal looking mitochondria on electron microscopy (EM) of renal biopsy tissue.

In contrast to the heterogeneity of underlying mtDNA mutations in paediatric patients, only a single point mutation (A3243G) appears to predominate in adult patients with renal disease. In addition to causing a variety of renal disorders, this mutation is associated with >80% of cases of MELAS syndrome (Schmiedel *et al.*, 2003) and MIDD (Reardon *et al.*, 1992). It is also been associated with cardiomyopathy (Nan *et al.*, 2002) and external ophthalmoplegia (Hansrote *et al.*, 2002). In renal patients, the prevalence of this mutation might be far higher than currently recognised: one study of diabetic patients on haemodialysis reported a

prevalence of 5.9% (Iwasaki *et al.*, 2001), compared with an estimated prevalence of 0.24% in the general population (Manwaring *et al.*, 2007). Moreover, in a screening study of patients with MIDD, 28% were found to have renal involvement ranging from asymptomatic proteinuria to end stage renal disease (Guillausseau *et al.*, 2001). The A3243G mutation is thought to account for ~0.06% of cases of diabetes mellitus in the UK (Gerbitz *et al.*, 1995). Mutations of mtDNA, including A3243G (Sangkhathat *et al.*, 2005), have also been described in patients with kidney tumours (Hervouet & Godinot, 2006; Wada *et al.*, 2006).

1.4.6 Differences between adults and children

Interesting differences between paediatric and adult patients with mitochondrial cytopathy-related renal disease exist in the literature to date. Children seem to present with a proximal tubulopathy at an early age, as part of an established and severe multi-organ disease due to mtDNA deletions (and/or nuclear mutations), and to have a poor prognosis. The mutations are generally sporadic and they are not usually passed on because of the early onset and severity of disease, and because survival into adulthood is rare (although in general humans don't seem to pass on mtDNA deletions to their offspring for reasons that are still unclear).

To some extent the pattern of genetic mutations described causing mitochondrial cytopathy and renal disease in children and adults reflects the general situation in mitochondrial cytopathy; whereby nuclear mutations are more likely to present in childhood, whereas mtDNA mutations tend to present later in life (for a review of mitochondrial disease in childhood see (Moslemi & Darin, 2007)). Most nuclear mutations are expressed in all tissues and would be expected to cause severe multi-system disease. However, the clinical pattern of disease does not always follow the levels of expression of mutant genes in different tissues (Papadopoulou *et al.*, 1999). The reasons for this are still unclear; although a possible explanation is that expression levels may vary during embryonic development, resulting in particular patterns of disease in the newborn (Rotig & Munnich, 2003), but this is unproven. Within the kidney, differential expression of affected proteins in different regions of the nephron (e.g., glomerulus vs. tubule) provides an attractive, though speculative, explanation for the spectrum of phenotypes seen in mitochondrial cytopathy. In

adults with point mtDNA mutations, heteroplasmy of mutant load among different tissues is an obvious explanation for the wide variation in phenotype, including severity and organ specificity.

Unlike children, adults tend to present with a milder phenotype and sometimes with only renal disease. Furthermore, renal pathology is more usually glomerular; in all cases the underlying defect is due to a single point mutation in mtDNA that can be maternally inherited. The reason why a particular pathology (FSGS) should occur in these cases is unknown. Any terminally differentiated cells with a heteroplasmic mtDNA pool will be vulnerable to mitochondrial cytopathy, since cell division provides an opportunity to segregate mutant mtDNA unevenly between daughter cells, which can result in a clone of cells with a lower mutant load and a metabolic (and selective) advantage. Daughter cells with a higher mutant load may be recognised as damaged and are deleted by apoptosis. Podocytes are terminally differentiated and unable to undergo regenerative proliferation in response to cell loss (Pavenstadt *et al.*, 2003), which might explain the relatively high prevalence of glomerular disease in adults with mitochondrial cytopathy.

Recently, interest has grown in the capacity of the renal tubule to regenerate itself following an acute toxic insult. The origin of the cells that repopulate the tubule is currently uncertain; possibilities include proliferation of existing tubular cells or migration of stem cells into the damaged kidney from the blood stream (Imai & Iwatani, 2007). If the former hypothesis is true, and the renal tubule has an inherent capacity to regenerate itself via division of epithelial cells, this would provide a potential mechanism via which mtDNA mutant load could be reduced over time. This might explain why terminally differentiated cells that cannot be regenerated, such as podocytes, might be more vulnerable to the chronic effects of mtDNA mutations.

It is surprising that one mtDNA mutation appears to predominate in adult nephrology, given the high rate of mtDNA mutation, and that >200 mtDNA mutations that have been described in other medical specialities (see MITOMAP: A Human Mitochondrial Genome Database [<http://www.mitomap.org>]). It could reflect

a lack of awareness of mitochondrial cytopathy as a cause of renal disease; eventually other unexplained cases of chronic renal disease may be linked to other mtDNA mutations. Because it seems to be a common mutation, A3243G is included in mtDNA screening by most clinical genetics laboratories and this may bias towards a high reported prevalence.

To date, the literature on renal disease in adults with mitochondrial cytopathy is small, and apparent differences between children and adults should therefore be interpreted with caution, especially as systematic screening studies of nephropathy in adults with mitochondrial disease (using sensitive renal tubular markers) have not been performed previously. In theory, given the vulnerability of the PT to MD, high rates of renal tubular disease would also be expected in adults with mitochondrial cytopathy. As more and more patients are recognised to have mitochondrial disease (due to improvements in diagnostic techniques), and increasing numbers survive to adulthood, understanding the effects of MD on the adult kidney is becoming increasingly important.

1.5 HIV, anti-retroviral therapy and the proximal tubule

1.5.1 Mitochondrial toxicity of HIV and its therapy

As survival from HIV improves, due to the development of more clinically effective anti-retroviral therapy (ART), the balance of nephropathy attributed to HIV is changing from direct pathological effects of the virus (traditional HIV associated nephropathy – ‘HIVAN’) to ART-related renal toxicity (Wyatt & Klotman, 2006; Roling *et al.*, 2006). It is therefore important that the burden and nature of ART-related kidney disease is investigated and understood.

Both HIV and some forms of ART are thought to be toxic to mitochondria. In treatment naïve patients, depletion of mtDNA has been reported in peripheral blood mononuclear cells, consistent with a toxic effect of the virus (Maagaard *et al.*, 2006), which is also thought to induce oxidative stress in some cell types (Mollace *et al.*, 2001). Nucleoside analogue reverse transcriptase inhibitors (NRTIs) are a commonly used form of ART. They are incorporated into the replicating virus by the reverse

transcriptase enzyme that recognises them as appropriate substrates. However, once incorporated they cause a cessation of transcription. They are highly effective, especially when used in combination with other forms of ART (highly active ART – HAART), and have revolutionised the expected survival from the disease. However, they are not without significant side effects, including mitochondrial toxicity. The basis of this toxicity is that NRTIs inhibit the mtDNA polymerase gamma (pol- γ) (Lewis & Dalakas, 1995), the enzyme responsible for mtDNA replication. Unlike nDNA, mtDNA does not utilise other polymerases and is therefore specifically affected, leading to a gradual decrease in mtDNA levels (often expressed as the mtDNA/nDNA ratio). Patients taking ART may develop hyperlipidaemia, central obesity and insulin resistance; features of the ‘metabolic syndrome’, in which mitochondrial toxicity is thought to play a central role in the pathogenesis (Villarroya *et al.*, 2007).

In vitro tests in cell lines derived from various different organs appear to show a consistent ‘pecking order’ of NRTI related mitochondrial toxicity as follows (in descending order of toxicity): didanosine (ddI), stavudine, zidovudine (AZT), and finally tenofovir (TDF - which is thought to have little or no *in vitro* mitochondrial toxicity at all) (Birkus *et al.*, 2002). However, *in vivo*, the situation is somewhat different, with certain agents appearing to cause toxicity in particular organs (e.g. AZT and the heart, ddI and the pancreas, TDF and the kidney (Hoschele, 2006)). The reasons for this are not clear, but potentially confounding factors include pol- γ - independent mechanisms of mitochondrial toxicity, the toxic effects of the virus itself, previously undiagnosed underlying mtDNA mutations and drug interactions. Perhaps unsurprisingly, ART thought to be toxic to mitochondria has been reported to cause FS (Miller *et al.*, 2003; Izzedine *et al.*, 2003).

1.5.2 Nephrotoxicity of Tenofovir

TDF is a widely used and effective *nucleotide* reverse transcriptase inhibitor that, unlike other NRTIs, is thought to have little or no mitochondrial toxicity *in vitro* (Biesecker *et al.*, 2003; Birkus *et al.*, 2002; Vidal *et al.*, 2006). Furthermore, randomised control studies have not shown an association between treatment with TDF and clinically significant renal toxicity (Jones *et al.*, 2004; Izzedine *et al.*,

2005a; Schooley *et al.*, 2002). Subsequently, however, numerous case reports of renal tubular toxicity in patients taking TDF have emerged in the literature (de la Prada *et al.*, 2006; Malik *et al.*, 2005; Peyriere *et al.*, 2004; Quimby & Brito, 2005; Rifkin & Perazella, 2004). In many of these cases, patients developed FS. Most of the original TDF studies that screened for renal dysfunction focused on measuring serum creatinine (and eGFR) and urine dipstick proteinuria (mainly albuminuria); both of which are predominantly markers of glomerular disease, and will not necessarily detect tubular disease, especially in milder cases.

The mechanism of TDF toxicity is not well understood. As previously mentioned, *in vitro* tests suggest that TDF is not toxic to mitochondria, however, some evidence has emerged in the literature to suggest that TDF may potentiate the mitochondrial toxicity of other forms of ART used concurrently. For example, the combination of TDF and ddI has been associated with mtDNA depletion in human kidney biopsies (Cote *et al.*, 2006) and peripheral blood mononuclear cells (Saumoy *et al.*, 2004). Recently, another study, using a mouse model of HIV (hemizygous HIV-1 TG mice (Dickie *et al.*, 1991)), has re-examined the mitochondrial toxicity of TDF (Kohler *et al.*, 2009). Although the authors of this study found that TDF caused an increase in the overall mtDNA/nDNA ratio in the whole mouse kidney, in isolated PTs of animals exposed to TDF there was a significant reduction in the mtDNA/nDNA ratio. This implies that TDF is specifically toxic to mitochondria in the PT, perhaps because of the fact that active secretion by this nephron segment into the urine is a significant excretion pathway for the drug (Barditch-Crovo *et al.*, 2001). Drug interactions that interfere with the excretion pathway of TDF may therefore play an important role in the development of tubular toxicity; in many of the reported cases of TDF induced FS patients have also been taking ritonavir boosted PIs and/or ddI as part of their HAART. TDF and ddI are both renally excreted via the PT and compete for the same baso-lateral organic anion transporter (Cihlar *et al.*, 2001). TDF exits the PT cells via luminal multi-drug resistance-associated protein-4 (MRP4) transporters (Imaoka *et al.*, 2007); Ritonovir is a substrate for MRP2 transporters (Huisman *et al.*, 2002), and it has been suggested that an interaction at MRP4 transporters between TDF and ritonavir might account for an increase in cellular TDF levels to toxic levels, although this remains to be proven.

1.6 Mitochondrial dysfunction as a cause of Fanconi syndrome

1.6.1 Evidence for mitochondrial dysfunction as a cause of Fanconi syndrome

As discussed previously, the pathogenesis of FS is poorly understood. A sub-lethal defect in PT cell metabolism has been suggested as an attractive (if speculative) unifying mechanism, which might lead to a breakdown of PT cell transport in the absence of cell death. Various strands of evidence exist to implicate mitochondrial dysfunction in the patho-physiology and support this hypothesis. Firstly, as stated earlier, the typical renal presentation of children with mitochondrial cytopathy is FS. Secondly, various drugs known to be toxic to mitochondria have been found to cause reversible FS (including ART) (Izzedine *et al.*, 2003). Thirdly, abnormalities in mitochondrial appearance have been reported in experimental and clinical types of FS, including myeloma (Morel-Maroger Striker *et al.*, 1994). Moreover, FS has been reported in primary biliary cirrhosis, a condition characterised by the presence of anti-mitochondrial antibodies (Lino *et al.*, 2005). Fourthly, several inborn errors of metabolism can cause FS, and the excess metabolites that accumulate in these disorders (such as cystinosis (Foreman *et al.*, 1995) and tyrosinaemia (Roth *et al.*, 1991)) have been found to be toxic to mitochondria. Lastly, directly applying inhibitors of the mitochondrial respiratory chain can lead to inhibition of sodium and PO_4^{2-} transport in PT cells *in vitro* (Gullans *et al.*, 1982).

1.6.2 Possible mechanisms via which mitochondrial dysfunction might impair solute transport in the proximal tubule

Although there is a wealth of clinical evidence implicating mitochondrial dysfunction in the pathogenesis of FS, the exact mechanism that links the two remains unknown. As discussed already, much remains to be learnt in general about the cellular mechanisms by which mitochondrial cytopathy causes disease in any organ.

Clearly, a reduction in cytosolic ATP, due to abnormal RC function, is one possibility. In an *in vitro* model of cystinosis-induced FS in isolated PTs, depletion of intracellular ATP and defective transport were both attenuated by incubation with exogenous ATP (Coor *et al.*, 1991). PT cells are thought to have very little anaerobic

capacity for generating ATP (Bagnasco *et al.*, 1985), so a reduction in RC activity is likely to have a significant effect on cytosolic ATP levels in this nephron segment. As endocytosis is an active process, alterations in local ATP concentration might be expected to have an inhibitory effect. However, given the varied and important cellular roles of mitochondria beyond ATP synthesis, it is quite possible that MD could affect endocytosis by other non-ATP mediated mechanisms, such as altered Ca^{2+} signalling or increased ROS production. Mitochondria have a crucial role in regulating intracellular Ca^{2+} signalling, including the spatial localisation of Ca^{2+} signals in polarised epithelia such as pancreatic acinar cells (Camello-Almaraz *et al.*, 2002). However, nothing is known to date about the effect of mitochondria on the spatial localisation of Ca^{2+} signals in the PT. Changes in Ca^{2+} concentration have been implicated as a control mechanism for endocytosis in neurons (Wu, 2004), and increasing the concentration of Ca^{2+} in a renal cell line with ionomycin was reported to affect endocytosis of the LMWP insulin (Carvou *et al.*, 2007). ROS generated from mitochondria have been reported to affect endocytosis in alveolar epithelial cells (Dada *et al.*, 2003).

1.7 Fluorescence live-cell imaging

1.7.1 Single-photon excitation confocal imaging

Fluorescence microscopy utilizes the fact that electrons orbiting certain molecules (called fluorophores) can be excited to a higher state by absorbing a photon of light at a wavelength particular to the fluorophore. After a period of time, the electrons will return to the ground state, and in doing so will emit light at lower energy, and hence at a longer wavelength. Standard confocal fluorescence microscopy involves illuminating a region of interest in a specimen with a laser at a wavelength known to excite the fluorophore being studied (Wright *et al.*, 1993). Emitted light from the fluorophore is then passed through a series of filters to remove both any reflected excitation light and also light emitted from any other fluorophores that may be partially excited. A pinhole is used to collect light only that is confocal to the plane of focus desired in the specimen, in order to produce a sharply focused image (Figure 1.4). Photonmultiplier tubes (PMTs) are then used as detectors in order to convert the light signal into a digital image that can be used for analysis with appropriate

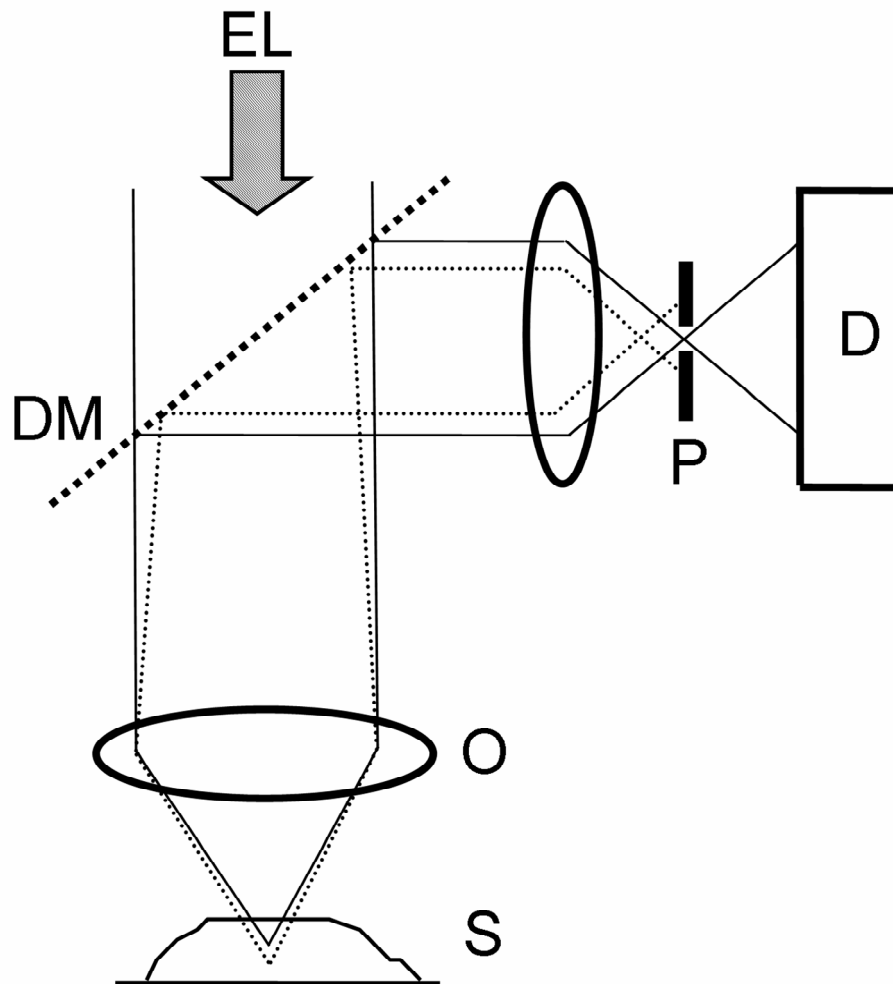


Figure 1.4. Confocal fluorescence microscopy. Excitation light (**EL**) is focused onto a specimen (**S**) with an objective (**O**). Emitted light is filtered using dichroic mirrors (**DM**) towards a detector (**D**). A pinhole (**P**) is used to collect only light emitted from the plane of focus.

imaging software. PMTs work on the principle that incoming photons are converted to electrons by a photocathode; this electron signal is then amplified by a series of electrodes (called dynodes) in order to produce an electrical signal. The fluorescent properties of some fluorophores may be altered by certain conditions, e.g. binding of other molecules, such as Ca^{2+} or ROS. This phenomenon has been exploited extensively in biological research as a means of observing physiological processes at a molecular level in real time within living cells, which would otherwise not be visible using standard light microscopy.

1.7.2 Multi-photon excitation fluorescence imaging

Whilst an appropriate and powerful technique for investigating physiological processes in isolated or monolayers of cells, standard single-photon excitation confocal microscopy has limitations with regards to imaging whole sections of tissue (such as tissue slices or whole organs). The main drawbacks are, firstly, that light in the ultraviolet to visible range (typically used for single-photon excitation of many dyes) does not penetrate solid tissue nearly as well, and undergoes more scattering, compared to longer wavelength (infrared) light. Secondly, confocal imaging results in a double cone section of tissue being illuminated, with the consequence of potential bleaching and phototoxicity outside of the plane of focus.

These disadvantages of single-photon excitation imaging led to the development of multi-photon imaging. The principles of multi-photon imaging were first described by Maria Göppert-Mayer in a PhD thesis in 1931. The technique has since been developed by Denk (Denk & Svoboda, 1997) and others, and is now more widely used in biological imaging. Essentially, multi-photon imaging relies on the principle that electrons in fluorophores can be excited not only by a single photon at the appropriate wavelength, but also, alternatively, by 2 photons arriving simultaneously, each at approximately half the wavelength (and hence half the energy), or even 3 arriving, each at approximately a third of the wavelength (Figure 1.5). In practice most multi-photon microscopy relies on two-photon excitation, hence the terms multi-photon and two-photon microscopy are often used inter-changeably.

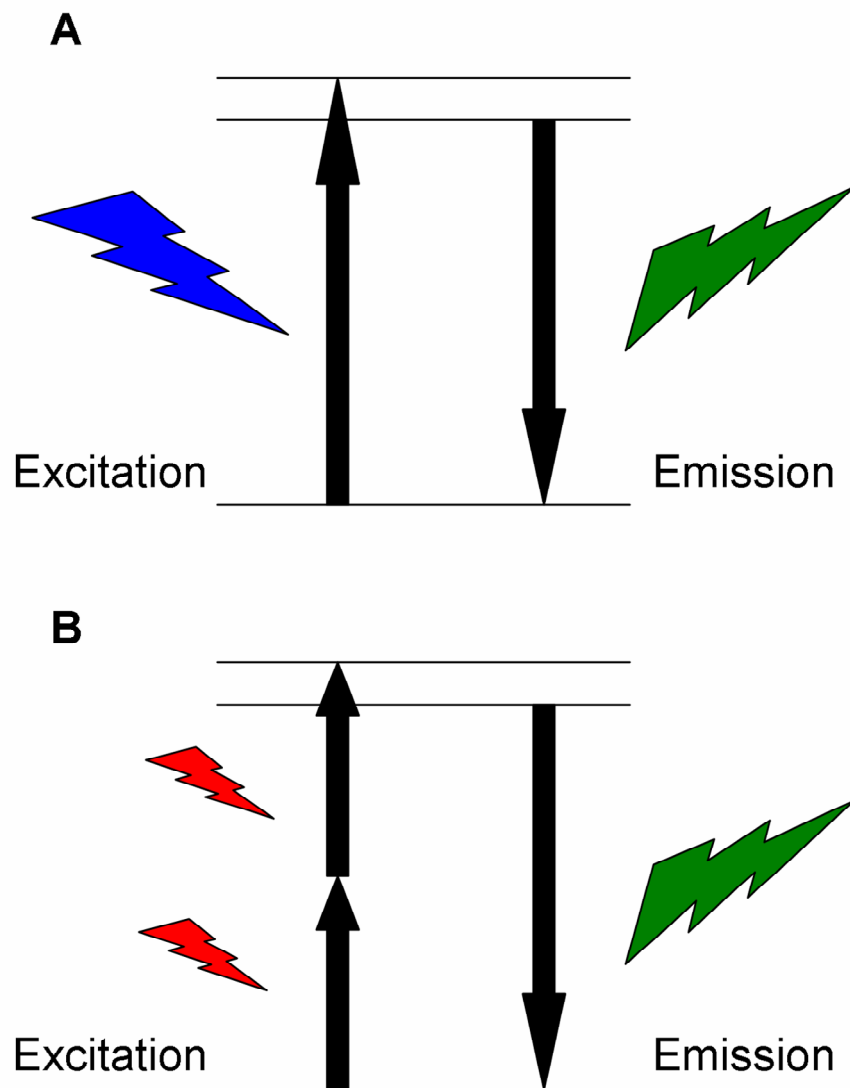


Figure 1.5. Principle of multi-photon excitation. Electrons orbiting a fluorophore can be excited by photons arriving at a specific wavelength (**A**); this is termed single-photon excitation. When the electrons return to the ground state they emit light at a longer wavelength. Alternatively, electrons can be excited by 2 or more photons arriving simultaneously at a longer wavelength (**B**); this is termed multi-photon excitation.

The fact that excitation will only occur if 2 or more photons arrive at a fluorophore simultaneously has two major implications for multi-photon microscopy. First, in order to increase the likelihood of simultaneous arrival, without having to increase laser power to toxic levels, the excitation laser needs to be pulsed at high frequency. Second, because excitation is only likely to occur in an environment of high photon density, the probability of excitation drops off steeply (as a fourth power function) anywhere in the tissue other than the narrow plane of focus. Hence, surrounding tissue is far less exposed to photo-toxicity than in standard single-photon confocal microscopy. This can be particularly advantageous when imaging a specimen repeatedly, for example during a timed series experiment. Furthermore, the image is intrinsically confocal, and a pinhole is not required.

Multi-photon microscopy is, therefore, an ideal technique for studying cellular physiology in intact tissue sections. It is an exciting tool in biological imaging with significant potential. Its use in the renal field has been relatively limited so far, although some groups have utilised it to make some interesting and novel observations of renal function *in vivo* (Molitoris & Sandoval, 2005; Sipos *et al.*, 2007); some of which have questioned our understanding of basic renal physiology (Russo *et al.*, 2007; Russo *et al.*, 2009). However, multi-photon microscopy has not been used previously to make measures of mitochondrial function in the kidney.

1.8 Experimental models of the proximal tubule

1.8.1 Immortalised cell cultures derived from the proximal tubule epithelium

Experimental models of the PT range from isolated cultured cells derived from the PT (either primary or immortalised), to more intact *in vitro* tissue preparations (such as isolated tubules or kidney slices), right up to fully intact kidneys either *in vivo* or perfused *in vitro*. All have various advantages and disadvantages.

A number of immortalised cell models of the PT exist in research, which are derived from different organisms. These include the Ilcpk (pig) (Ishibashi, 2006), HKC (human) (Niculescu-Duvaz *et al.*, 2007) and WKPT (rat) (Carvou *et al.*, 2007). They have the advantage of being relatively easy and cheap to grow, and provide an almost

limitless supply of tissue for experiments, without the need for further animal sacrifice. However, although widely used and capable of forming transporting monolayers in culture, all of these models suffer from several drawbacks. Firstly, following removal from the *in vivo* situation, PT epithelial cells tend to rapidly lose their phenotype, and this has been the major limiting factor in the usage of primary PT cultures in *in vitro* studies. Secondly, as part of the general loss of phenotype, cultured PT cells have considerably less transport capacity, with a much less well developed luminal brush border, than *in vivo*. Lastly, in common with most immortalised cultured cell lines, the metabolism of PT cells tends to change with time and passage number, with a gradual switch to a greater usage of anaerobic ATP generation, rather than aerobic oxidative phosphorylation (Gstraunthaler *et al.*, 1999). In contrast, *in vivo* the cells of the PT are thought to have very limited anaerobic capacity.

1.8.2 The Opossum Kidney (OK) cell line

OK cells are an immortalised PT cell line derived from the American opossum (*Didelphys virginiana*). They are a much used model of PT epithelium and take up LMWPs via receptor mediated endocytosis (Sidaway *et al.*, 2004); the rate of uptake is generally thought to be greater than that of other PT-derived cell lines. They form a polarised monolayer with both tight junctions and a brush border (Rabkin *et al.*, 1989). The existence of megalin and cubulin (two crucial components of the PT endocytotic apparatus) has been demonstrated in OK cells (Zhai *et al.*, 2000). Furthermore, OK cells have also been used in studies of uptake of dextrans via fluid phase endocytosis (pinocytosis) (Gekle *et al.*, 1995). Notwithstanding the general drawbacks of immortalised cells in culture, they are considered to provide a suitable model in which to investigate the effect of potential inhibitors on LMWP uptake.

1.8.3 The renal slice model

Although a useful model, cell lines are always limited by the relevance of any findings to the situation *in vivo*. This is due to the fact that, when removed from their native environment, cells can undergo significant phenotypic changes. Native tissue is therefore preferable, not only because it is more ‘physiological’, and findings are

more likely to reflect the true *in vivo* state, but also because it allows comparison between adjacent cells of different tissue types. This sort of comparative approach can be very revealing in understanding the topographical patterns of disease observed within organs.

Clearly, the most physiological approach to studying the kidney is to use a whole intact functioning organ, ideally *in vivo*. The isolated perfused kidney has been used previously for pharmacological (Taft, 2004) and transport experiments (McTigue *et al.*, 1983), but not generally for imaging studies. *In vivo* imaging of the intact kidney with a standard confocal microscope has been described, however, this approach was limited by the fact that laser penetration into the tissue is very limited (50-100µm), allowing only the very superficial structures in the organ to be studied. Nevertheless, this approach did allow the visualisation of physiological processes, such as insulin endocytosis, in real time in a live rodent (Simeoni *et al.*, 2004).

The renal imaging field has subsequently been significantly enhanced by the development of multi-photon imaging, which allows visualisation of structures up to ~200µm below the surface of the organ. This has permitted the studying, in real time, of a range of physiological processes, including glomerular filtration, LMWP endocytosis, and both capillary and tubular flow rates (Molitoris & Sandoval, 2005; Sipos *et al.*, 2007). However, imaging a whole organ still presents significant practical difficulties, in spite of the advances in imaging technology. These include the challenge of keeping the organ (and the animal if imaging *in vivo*) in good health, throughout the period of experimentation. Furthermore, in spite of increased laser penetration, it is still only possible to visualise structures such as the glomeruli in certain species of rat (e.g. Munich Wistar (Hackbarth *et al.*, 1983)), and large sections of the kidney (such as the medulla) remain beyond the reach of the laser. However, the main limiting factor at present, at least in terms of imaging cellular processes, is the difficulty of achieving adequate loading into cells of standard fluorophores. When loading these dyes into isolated cells in culture, they are often incubated for some time (usually over half an hour) and may require other agents (such as pluronic, which disperses micelles of the lipophilic dye) to enhance uptake into cells. Clearly, these sorts of incubation times are not feasible in the intact organ, where dyes have to be perfused through the vasculature, and individual cells within

the organ are likely to come into contact with relatively small amounts of the dye for short periods of time. In the intact animal, where dyes are usually injected via the femoral vein, the dye will be diluted in the entire body water volume. Large volumes of dye may therefore be required, which is a problem due to the high cost of many of the dyes. Furthermore, in the case of AM-ester dyes, extracellular esterases can break down the dyes before they even reach the target organ (Jobsis *et al.*, 2007). In the particular case of the kidney, the vast array of efflux pumps that exist in the cell membrane, which are capable of extruding foreign molecules (like dyes) from the tubular cells (Launay-Vacher *et al.*, 2006), provide yet another challenge for *in vivo* imaging.

A compromise solution that allows both visualisation of all nephron segments and incubation with dyes for prolonged periods is the renal slice model. Here, slices of kidney are made with a tissue slicer at a typical thickness of 200µm. This approach preserves to some extent the architecture of the organ and thus allows comparisons to be made between different tubule types side-by-side. Interactions between adjacent cells that may be vital for normal signalling and metabolism may still occur. By slicing at the appropriate level, either the cortex or medulla can be visualised. Tissue slices have been used for a range of kidney studies (Bacic *et al.*, 2003; Hong *et al.*, 1983; Parrish *et al.*, 1995; Plotnikov *et al.*, 2007; Rosenberg *et al.*, 1961; Vickers *et al.*, 2004; Weinberger *et al.*, 1975), and important insights have been made with regards to renal metabolism using this approach (Balaban *et al.*, 1980; Lee & Peter, 1969). However, this model does have some drawbacks too. For a start, the slicing process is inherently traumatic, and results in the obliteration of natural osmotic and solute gradients that normally occur across polarised cells in the kidney, and drive transport processes. Therefore it is unclear to what extent transport will still occur in *ex vivo* kidney slices. Given that metabolism is thought to be coupled to ATP demand for transport in the cells of the nephron, it is therefore possible that the *in vivo* situation may not be accurately modelled in the slice preparation. Furthermore, the inner parts of the slice may be poorly accessible to dyes and reagents, and also to oxygen, which may lead to hypoxia and altered metabolism (Balaban *et al.*, 1980).

In spite of these drawbacks, the reality is that the tissue slice is a much used and useful model that provides a balance between the benefits of *in vivo* intact organ

work and *in vitro* cell culture. For example, multi-photon imaging of brain slices has provided important insights into physiological processes in the central nervous system, such as neurotransmitter release (Axmacher *et al.*, 2004) and Ca^{2+} signalling (Ladewig *et al.*, 2003). However, the technology has not, as yet, been applied to kidney slices.

1.9 Imaging of mitochondrial function

1.9.1 Mitochondrial membrane potential ($\Delta\psi_m$)

Various aspects of mitochondrial function can in turn be measured using suitable fluorescent probes, and imaged in real-time using confocal single or multi-photon excitation confocal microscopy. $\Delta\psi_m$ is central to mitochondrial function, affecting processes such as ATP and ROS production, and Ca^{2+} and protein import. It can be measured using positively charged lipophilic fluorescent dyes, such as tetramethyl rhodamine methyl ester (TMRM), which accumulate into the mitochondrial matrix due to the relative negativity within the organelle, compared with the cytosol (Duchen *et al.*, 2003). The degree of accumulation is proportional to $\Delta\psi_m$, when the dyes are used in the ‘linear range’. That is, at a sufficiently low concentration that they will not self-quench emitted light, due to a high concentration of dye in a relatively small area and resulting high probability of collisional quenching. To test which mode these dyes are behaving in, a RC uncoupling agent (e.g. carbonylcyanide p-trifluoromethoxyphenylhydrazone [FCCP]) can be applied that will depolarise $\Delta\psi_m$, and cause the dye to redistribute into the cytosol and surrounding extracellular fluid; if the dye is operating in the linear range (typically nM concentrations), this will cause a decrease in the mitochondrial fluorescence signal. However, the reverse will happen if the dye is in the quench/de-quench range (typically μM concentrations), as a movement of dye out of the mitochondria will reduce the level of auto-quenching, and lead to an increase in mitochondrial fluorescence signal.

$\Delta\psi_m$ is dependent on a number of factors; including RC activity, the rate of ATP synthesis and the degree of proton leak. A change in $\Delta\psi_m$ may therefore reflect a change in one or more of these factors. Very little is known about variations in $\Delta\psi_m$

between different tissue types *in vivo*. However, it has been postulated that a relatively low membrane potential may potentially be advantageous in aerobic tissues as ROS production increases with increasing potential; hence, maintaining a low potential might reduce harmful ROS production in the long-term (Kadenbach, 2003).

1.9.2 Reactive oxygen species production

Fluorescent probes such as dichlorodihydrofluorescein (DCF) (LeBel *et al.*, 1992) and dihydroethidium (also called hydroethidine - HET) (Bindokas *et al.*, 1996) can be used in intact cells to measure the rate of ROS production. HET is normally fluorescent in the blue range, but upon oxidation by O_2^- it becomes fluorescent in the red range. Over time, the red fluorescence signal in a cell loaded with HET will increase, and the rate of increase in signal is taken to be proportional to the rate of ROS production. Ethidium is freely diffusible within cells and binds DNA avidly; therefore, signal change is normally predominantly observed in the nucleus of the cell. HET has been used previously to investigate rates of ROS production in isolated segments of the nephron (Li *et al.*, 2002; Zou *et al.*, 2001). Mitosox is a fluorescent ROS-sensitive dye that is tagged with a triphenylphosphonium (TPP^+) cation to specifically target it to mitochondria (Robinson *et al.*, 2006) (in a potential dependent manner); changes in mitosox fluorescence signal are therefore thought to reflect changes in mitochondrial O_2^- production (Abramov *et al.*, 2007).

1.9.3 Glutathione

Because of the potentially damaging effects of ROS, living cells require protective anti-oxidant systems. One of the major intracellular anti-oxidants is GSH. Intracellular levels of GSH can be measured via biochemical methods (Brehe *et al.*, 1976). Alternatively, for live cell imaging the dye monochlorobimane (MCB) can be used as it forms a fluorescent adduct with GSH in a reaction catalyzed by GST (Keelan *et al.*, 2001), and emits a signal in the blue range when excited with ultraviolet light.

1.9.4 NADH and FAD^{2+} autofluorescence and redox state

The reduced forms of NAD^+ (NADH) and flavoprotein ($FADH_2$) are the substrates for complexes I and II of the RC, respectively. It has been known since the 1950s that NADH (and not NAD^+) is fluorescent in the blue range when excited with ultraviolet light (for review see (Mayevsky & Chance, 2007)). Conversely, oxidised flavoproteins (FAD^{2+}), but not the reduced form ($FADH_2$), are fluorescent in the green range when excited at about 450nm. Therefore, with appropriate excitation and optics, by measuring the relative intensity of the fluorescence signals arising from NADH and FAD^{2+} , it has been suggested that a ratiometric readout is available of the relative redox states of the two substrate pools (Duchen *et al.*, 2003).

The signals *per se* do not give any information about the total size of the substrate pools, simply the amounts that are in either a reduced (NADH) or oxidised (FAD^{2+}) state. Because of this, protocols have been developed to allow calibration of the full dynamic range (complete reduction to complete oxidation), in order to make sense of them. This calibration can be performed by manipulating RC activity. For example, RC inhibition (e.g. with cyanide [CN]) will push the substrate pools into a fully reduced state, as oxidation of the substrates at RC complexes will cease to occur, but reduction of the substrates by intermediates in the Krebs's cycle will continue, until a maximally reduced state is achieved. Under these circumstances, the NADH signal will be maximal, whilst the FAD^{2+} signal will be minimal. The advantage of using CN as a RC blocking agent is that its effects are readily reversible and it can be washed off. After a suitable period of recovery, a RC uncoupling agent, such as FCCP, can be applied that will lead to maximal RC activity (as it is no longer constrained by the rate-limiting ATP synthase). Under these conditions, substrates at RC complexes I and II will be maximally oxidised in order to support RC activity to as greater extent as is possible. The NADH signal will therefore be at its lowest, whilst the FAD^{2+} signal will be at its highest. By normalising the baseline NADH and FAD^{2+} signals to these two extreme states (typically by denoting them as a value from 1 to 0), the resting signals can be calibrated to the maximal available substrate pools.

These techniques have been used, for example, to learn more about the metabolism of eggs (Dumollard *et al.*, 2007), carotid body cells (Duchen & Biscoe, 1992) and cardiac myocytes (O'Rourke *et al.*, 1994). Once established, the resting redox state can be used, in tandem with other measurements (such as $\Delta\psi_m$) to gain insights into RC activity within intact live cells. For example, the substrates in mitochondria in a cell with a high ATP turnover rate would be expected to be in a relatively oxidised state, whereas in a cell under ischaemic conditions (and RC compromise), the substrates would be expected to be in a more reduced state. One caveat to the above is that the redox state of RC substrates is not only determined by RC activity. As the oxidised forms of the RC substrates are continuously reduced by intermediates in the Krebs's cycle, it follows that changes in Krebs's cycle activity could also affect the redox state of RC substrates. These sorts of changes could potentially occur if there was any significant alteration in the supply of acetyl-CoA (the final common pathway of carbohydrate, fatty acid and amino acid metabolism) to the Krebs's cycle, e.g. during starvation. However, in normal experimental conditions, the supply of nutrients in the media used is held constant, under these conditions changes in mitochondrial redox state will predominantly reflect changes in RC function.

1.9.5 Calcium signalling

A variety of Ca^{2+} -sensitive molecular probes are now available that can be loaded into intact cells and respond to changes in intracellular $[\text{Ca}^{2+}]$ with a change in their fluorescent properties, which in turn can be measured using confocal or digital imaging techniques (for review see (Takahashi *et al.*, 1999)). Indicators vary according to their properties, for example, some (e.g. Fluo-3 and Fluo-4) require single wavelength excitation, whilst others are ratiometric (e.g. Fura-2). Some tend to aggregate into organelles (e.g. Rhod-2 into mitochondria (Trollinger *et al.*, 1997)), which can be useful in resolving compartmentalised Ca^{2+} signals, however, the extent to which they do so can depend on the cell type and loading protocol used.

In order to permit adequate loading into intact cells, most Ca^{2+} -sensitive dyes are prepared as an AM-ester, which masks charged groups and increases their lipid solubility, and hence movement through the cell membrane. Once inside of the cell, intracellular esterases de-esterify the conjugated dyes, and the remaining charged

hydrophilic fluorescent indicator becomes trapped within the cell or organelle. Changes in intracellular $[Ca^{2+}]$, in response to a common extracellular agonist (such as ATP or histamine) can then be detected as changes in the intensity of the fluorescence signal emitted by the dye.

Aims

1. To explore the underlying cellular mechanisms whereby mitochondrial dysfunction can lead to impaired proximal tubular transport of low molecular weight proteins, via receptor mediated endocytosis, using the OK cell line as an *in vitro* model of the proximal tubule.
2. To investigate differences in mitochondrial function between the proximal tubule and more distal parts of the nephron, both at rest and in response to respiratory chain inhibition, in order to help to explain the clinical vulnerability of the proximal tubule to mitochondrial dysfunction.
3. To establish a clinical link between changes in mitochondrial function and proximal tubular transport, by determining the prevalence and nature of tubular proteinuria (raised urinary levels of low molecular weight proteins and proximal tubular enzymes) in patients with mitochondrial dysfunction; either genetic, or acquired due to HIV and/or its treatment.

Chapter 2 - Methods

2.1 Endocytosis of albumin and dextran by OK cells

2.1.1 Cell culture

OK cells were kindly provided by Dr Alex Pearson (South West Thames Institute for Renal Research). They were grown in DMEM:F12, supplemented with 5% fetal bovine serum, and passaged every 6 days. For experiments, cells were grown on 13mm sterile cover slips, coated with poly-L-lysine, in 24-well plates until confluent (usually 5-6 days).

2.1.2 Cell death assay

To establish whether or not OK cells were alive after exposure to RC inhibitors for 2 hours, cells were loaded with Hoechst 33342 5 μ M (excited at 720nm) and Propidium iodide 10 μ M (excited at 514nm). The former stains all cell nuclei, whilst the latter is normally excluded by a viable cell membrane, and thus stains only the nuclei of permeabilised, dead cells (Ciancio *et al.*, 1988). Digitonin (20 μ M), which disrupts the integrity of the cell membrane, was used as a positive control. When assessing the specific toxicity of the glycolytic inhibitors iodoacetic acid (IAA) and 2-deoxyglucose (2-DG), pyruvate 5mM was added to the solution as a substrate for oxidative phosphorylation.

2.1.3 Endocytosis assay

FITC-labelled albumin (FA) was used as a ligand for endocytosis by OK cells in order to model LMWP uptake in the PT. Cell models of the PT vary in the degree to which they endocytose different proteins. OK cells are known to endocytose albumin avidly (Gekle *et al.*, 1995); hence, this protein was chosen as a ligand. FITC-insulin has also been used previously as a ligand for *in vitro* studies of PT endocytosis (Rabkin *et al.*, 1989), however, preliminary experiments revealed very low uptake in the OK cells. FITC-dextran (FD) was used to investigate fluid-phase endocytosis (pinocytosis).

For endocytosis experiments, OK cells were washed 4 times in a HEPES-buffered solution (pH 7.4), containing (in mmol/l): NaCl 138, KCl 5.6, NaHCO₃ 4.2, NaH₂PO₄ 1.2, MgCl₂ 1.2, CaCl₂ 2.6, glucose 10 and HEPES 10. They were then incubated in HEPES-buffered solution (pH 7.4) containing FA (50µg/ml) or FD (5mg/ml) for 1 hour at 37°C. The cells were then washed with 0.2M acetic acid/0.5M NaCl to remove any FA bound to the external cell membrane, and then subsequently 6 times with ice cold HEPES-buffered solution, to remove any FA or FD in solution and prevent further endocytosis (which is temperature dependent). The cells were fixed with 4% para-formaldehyde for 15 minutes, and were then mounted on slides with Citifluor AF1 glycerol/phosphate buffered saline mountant (Citifluor Ltd, London, UK), and imaged with a Zeiss LSM 510 inverted confocal microscope (Carl Zeiss Ltd, Welwyn Garden City, Hertfordshire, UK). Random fields were selected, using the bright field setting, with a x40 oil immersion objective, and a 10µm deep image z-stack (with 1µm intervals) was imaged for each field at 488nm. The mean fluorescence signal collected for each stack was calculated using Zeiss LSM software, with identical threshold values used throughout.

The polarity of endocytosis in OK cells (i.e. apical versus baso-lateral uptake) was established by growing cells to confluence on Transwell plates (Appleton Woods, Birmingham, UK). FA was then applied to either the apical or baso-lateral membrane of the insert, using the same protocol as above. Inserts were removed and mounted using Mowiol (a mountant that sets solid - a kind gift from Dr N Carvou, UCL), and imaged according to the same protocol as above.

To investigate the effects of mitochondrial RC inhibitors on the uptake of FA or FD in OK cells, either rotenone 10µM, piericidin 10µM or CN 1mM (all supra-maximal concentrations) were added to the HEPES-buffered solution at the start of the 1 hour incubation, to inhibit either complex I (rotenone and piericidin) or IV (CN) of the RC, respectively. 2-DG 5mM was used (in the presence of pyruvate 5mM) to investigate the effect of blocking glycolysis.

2.1.4 Dynamic measurement of intracellular ATP

Two different methods were employed to measure the effects of RC inhibition on cytosolic [ATP]. The first involved the usage of the dyes Magnesium Green (Mg Green, Molecular probes, Invitrogen, Paisley, UK) and TMRM, to provide a dual readout of changes in ATP levels and $\Delta\psi_m$ (Leyssens *et al.*, 1996). The principle of this test is that cytosolic free $[Mg^{2+}]$ changes inversely in response to changes in [ATP], due to that fact that ATP has a higher affinity for Mg^{2+} than ADP, and most Mg^{2+} in the cell is bound to ATP. Mg Green fluorescence signal intensity changes in proportion to increases or decreases in $[Mg^{2+}]$; therefore, the fluorescence signal changes *inversely* in response to alterations in [ATP]. Meanwhile, changes in TMRM signal represent changes in $\Delta\psi_m$.

Mg Green was loaded at a concentration of 5 μ M with 0.01% pluronic and 2.5mM probenecid (to enhance loading) at 20°C for 20 minutes. It was then washed off and the cells were incubated for a further 20 minutes with TMRM 50nM and verapamil 100 μ M (to enhance loading). TMRM 50nM is a suitably low concentration such that the dye operates in the ‘linear range’; i.e. a reduction in $\Delta\psi_m$ leads to a decrease in the mitochondrial TMRM fluorescence signal and a corresponding increase in the cytosolic TMRM signal. The bulk of the extra-nuclear volume in OK cells is filled with mitochondria; hence, in order to obtain a ‘cytosolic’ signal for recording simultaneous changes in Mg Green and TMRM, regions of interest (ROIs) within the nuclei of cells were used for the purposes of analysis.

The second method utilized for measuring changes in ATP levels was a luciferin-luciferase assay, with changes in luminescence recorded using a custom built luminometer (with assistance from Cairn Research, Faversham, Kent). OK cells were transfected with cytoplasmically targeted luciferase (Invitrogen, Paisley, UK), according to the manufacturer’s protocol. Luciferin 50 μ M was then added and the luminescence signal emitted measured. The RC inhibitor rotenone 10 μ M and the glycolysis inhibitor IAA 1mM were sequentially added to the recording chamber, in order to investigate the effects of each on the luminescence signal (and, therefore, on cytosolic [ATP]).

2.1.5 Measurement of ROS production

In order to measure mitochondrial ROS production, OK cells were loaded with the O_2^- sensitive dye mitosox 5 μ M (Molecular probes, Invitrogen, Paisley, UK), which localizes to mitochondria. The cells were incubated with the dye for 10 minutes at room temperature before imaging. MitoSox was excited at 543nm and light was collected using a 560-615nm band-pass filter. NADH was simultaneously excited at 364 nm, and emitted signal was collected using a 435-485nm band-pass filter. Images were acquired only every 2 minutes to minimise laser-induced photo-toxicity. After a 10 minute control period, the RC inhibitors rotenone 10 μ M, piericidin 10 μ M or CN 1mM were added. For the purposes of analysis, the NADH signal was used to identify mitochondrial dense areas of the cell, around which ROIs were drawn. The rate of increase in fluorescence signal was taken to be proportional to the rate of ROS production.

2.1.6 Electron microscopy of OK cell structure

EM of OK cells was performed with the assistance of the Dr A Loesch, at The EM Unit of The Royal Free and UCL Medical School. OK cells were grown on melinex polyester film until a confluent monolayer had been formed (5-7 days). Cells were then exposed to rotenone 10 μ M in a HEPES-buffered solution (see earlier – ‘Endocytosis assay’) for 1 hour at 37°C. At the end of the experiment the drug was washed off and primary fixation was performed in 1% paraformaldehyde/1.5% glutaraldehyde in phosphate buffered solution (PBS). Following a wash with PBS, secondary fixation was performed using 1% osmium tetroxide/1.5% potassium ferricyanide in PBS. The cells were then thoroughly washed with distilled water followed by dehydration through graded ethanol (30%, 50%, 70%, 90% and 100%). They were infiltrated with a 50:50 mixture of 100% ethanol/Epoxy resin and finally an overnight infiltration was performed with 100% resin.

Pieces of the melinex were then flat embedded with the cells face up in the liquid resin. These were then polymerised at 70°C overnight. The melinex was then stripped away from the cells leaving them embedded in the resin. The resin blocks were trimmed down and a secondary embedding was carried out with the cells face up. Using a Reichert Ultracut E ultramicrotome, semi-thin sections were cut with glass

knives and stained with toluidine blue. Ultra-thin sections were cut with diamond knife picked up on copper grids and stained with uranyl acetate and Reynold's lead citrate. The grids were viewed with a Philips CM120 electron microscope and digital images collected with an AMT digital camera.

2.1.7 Statistical analysis

The results are calculated as means \pm SEM. One-way analysis of variance (ANOVA) was used to investigate statistical differences among the study groups. Where differences were found, individual groups were then compared with each other by an unpaired t-test. A p value of <0.05 was taken as significant.

2.2 Multi-photon imaging of mitochondrial function in live kidney slices

2.2.1 Formation of live kidney slices

In the second part of the laboratory study, live slices of rat kidney were used to investigate differences in mitochondrial function amongst different segments of the nephron. To make the slices, kidneys were used from adult male Sprague Dawley rats. All procedures were carried out in accordance with the Animals (Scientific Procedures) Act 1986. Animals (weighing 250-400g) were anesthetized using intra-peritoneal pentobarbitone (50-100mg/kg). After adequate anaesthesia, the left kidney was removed via a midline incision and immediately placed in ice-cold HEPES-buffered solution containing (in mM): NaCl 118, NaHCO₃ 10, KCl 4.7, MgSO₄ 1.44, KH₂PO₄ 1.2, CaCl₂ 1.8, Hepes 10, glucose 5 and pyruvate 5. One pole of the kidney was sectioned from the rest of the organ and mounted on a stage using glue, in ice cold oxygenated HEPES-buffered solution (pH 7.4) containing glucose and sodium pyruvate (both 5mM). Slices were then made at 200 μ m using a Micron 650V tissue slicer. The slices were incubated at room temperature until usage, in a chamber containing HEPES-buffered solution (pH 7.4), further supplemented with sodium butyrate (5mM), and gassed with carbogen (95% CO₂, 5%O₂).

2.2.2 Identification of tubule types

Different tubule types in kidney slices are easily distinguishable by their size and morphology (see Figure 2.1 and Results). In order to confirm the identity of tubule types, immunostaining was performed using antibodies that bind to known nephron segments. PT cells were labelled with a mouse antibody to aquaporin-1 (AQP-1) (Sabolic *et al.*, 1992), whilst DT cells were labelled with a sheep antibody to Tamm Horsfall protein (THP) (Bachmann *et al.*, 1985).

The protocol for staining of PT with anti-AQP-1 antibodies was as follows. Rat kidney slices (200µm) were fixed overnight at 4°C in 4% paraformaldehyde. They were then washed for 10 minutes in PBST (0.1M phosphate buffer solution and 0.1% triton), and incubated for 30 minutes with PBST and 10% donkey serum. A mouse antibody to AQP-1 was diluted 1/200 in PBST and incubated overnight with the slice. This was then washed 3 times in PBS. A secondary donkey anti-mouse antibody (conjugated to FITC) was diluted 1/200 in PBS and applied for 2 hours. The specimen was subsequently washed 3 times with PBS and mounted with Citifluor AF1 glycerol/phosphate buffered saline mountant (Citifluor Ltd, London, UK). The same protocol was used for staining of DT with anti-THP antibodies; however, bovine serum albumin (rather than donkey serum) was used as the blocking agent, the primary antibody was used at 1/500 and incubated for 3 hours, and streptavidin red was used instead of FITC to identify staining.

2.2.3 Dye loading and imaging

A perfusion system was devised that allowed both dyes and reagents to be applied to the slice (Figure 2.2). Gravity was used to feed solutions containing dyes into the specially designed slice chamber (Harvard Apparatus, Edenbridge, Kent, UK). A peristaltic suction pump was used to provide the outflow from the chamber. This set-up allowed rapid changes to take place between different solutions. Dyes were perfused and recirculated for at least 20 minutes before imaging to allow adequate loading. Various markers of mitochondrial function were imaged in real time, in different tubule types, using a Zeiss LSM 510 upright multi-photon NLO (non-linear optics) (Carl Zeiss Ltd, Welwyn Garden City, Hertfordshire, UK), coupled with a Coherent Chameleon tunable laser (Coherent UK Ltd, Ely, UK). Experiments were

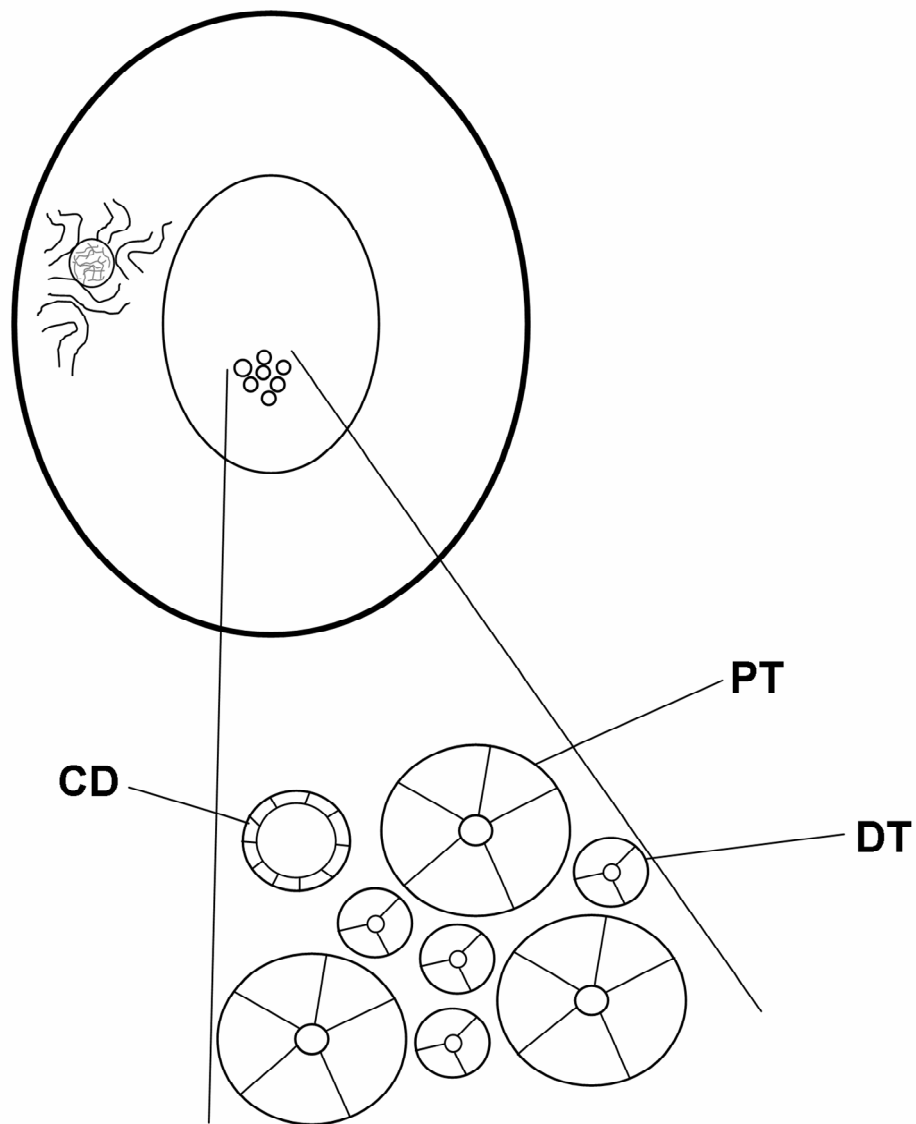


Figure 2.1. Anatomy of the kidney slice. Transverse sections through the pole of a rat kidney have an outer rim of cortex consisting mainly of proximal convoluted tubules and glomeruli. The medullary rays lie more centrally and run vertically from the cortex to the medulla; hence, they are mainly seen in cross section in this preparation. Medullary rays consist of proximal (**PT**) and distal (**DT**) tubules, along with collecting ducts (**CD**) and blood vessels. Tubules can easily be distinguished by their size and morphology.

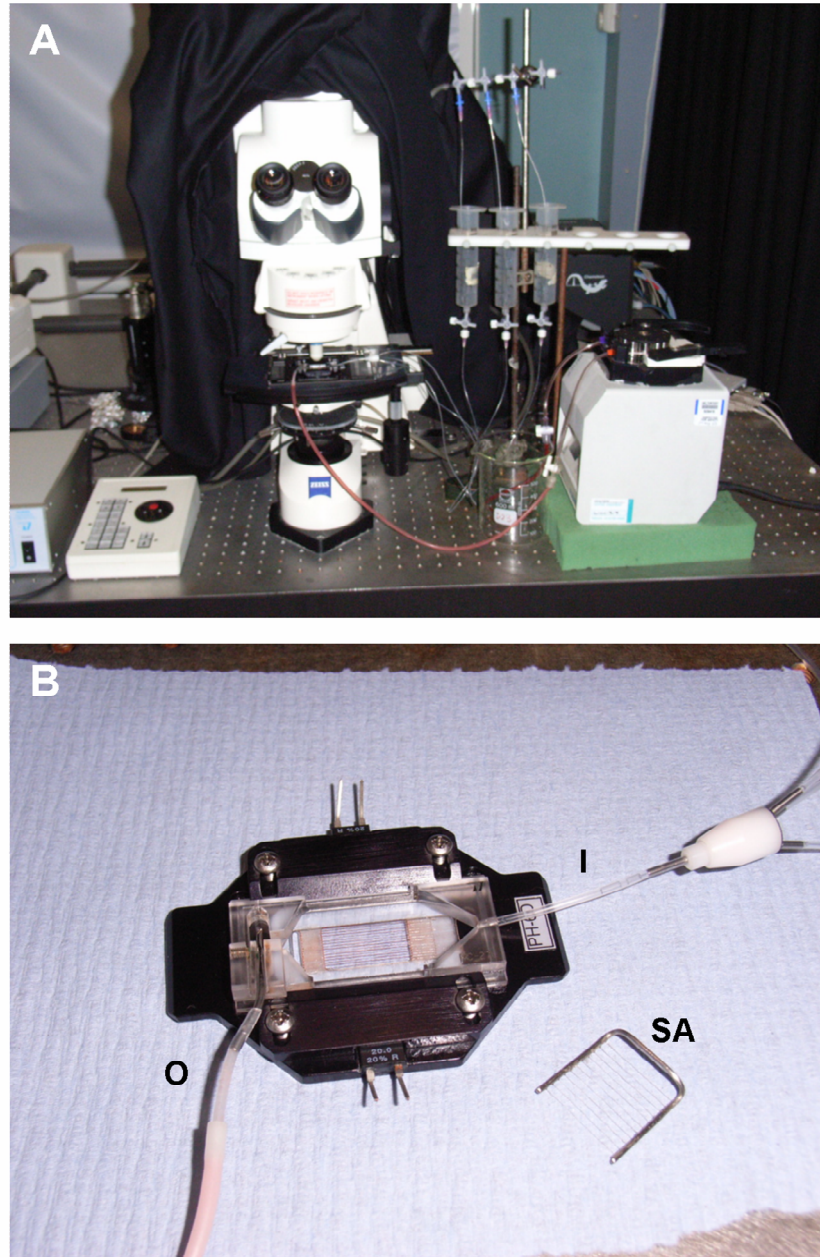


Figure 2.2. On-stage perfusion system for the multi-photon microscope. The perfusion system is depicted (A). The imaging chamber was situated below the objective of a Zeiss LSM 510 upright NLO. Oxygenated solution entered the chamber via a gravity feed system and multiple syringes allowed rapid switching between different solutions. Fluid was removed from the chamber using a suction pump. The imaging chamber is depicted in more detail (B), showing the inlet (I) and outlet (O), as well as the slice anchor (SA), which was used to hold the sample in place.

performed at room temperature, as at 37°C the slices were extremely sensitive to small fluctuations in temperature, and responded by swelling or contracting. This inevitably changed the focal plane (which is relatively narrow in multi-photon imaging), and made imaging over a period of time extremely difficult.

For single measurements of resting $\Delta\psi_m$, regions of a slice were randomly selected using the bright field setting, and the fluorescence signal at the plane of maximal overall intensity was then recorded. ROIs were drawn around individual tubules to obtain the mean fluorescence intensity per tubule. For experiments involving HET, regions of interest were drawn around the cell nuclei, where the bulk of the signal change was observed (as the dye binds to DNA). All values given are the mean signal, per image pixel, within the relevant region of interest. In timed series experiments images were taken in serial z-stacks in order to account for movement in the z axis over time. These z-stacks were then reconstructed as 2-D images using the Zeiss LSM software. Image analysis was performed using Zeiss LSM and Image J (<http://rsbweb.nih.gov/ij/>) software.

For all probes used the optimal excitation wavelength was established by generating two-photon excitation spectra. Calcein-AM was used at a concentration of 2 μ M (with 0.002% pluronic) and was excited at 800nm. TMRM was used at a concentration of 50nM; verapamil 10 μ M was used to inhibit dye export from the cells by the multi-drug resistance transporter (MDR). TMRM was optimally excited at 860nm. Rhodamine 123 was used at a concentration of 100nM and excited at 800nm. HET was loaded at a concentration of 5 μ M, while MCB was used at a concentration of 50 μ M; both were excited at 720nm. Mitochondrial NADH fluorescence was excited at 720nm; FAD²⁺ was excited at 458nm (single-photon excitation, as I found that the signal was masked by other sources of green autofluorescence when imaging with two-photon excitation). Emitted light was collected with the following filters: band-pass 435-485nm (NADH and MCB), long-pass 515nm (calcein), band-pass 500-550nm (FAD²⁺) and band-pass 575-640nm (TMRM, Rhodamine 123 and HET).

2.2.4 Chemical inhibition of the respiratory chain

In order to investigate differences between mitochondria in the PT and other nephron segments, in response to a toxic stimulus, chemical inhibition of the RC was used as a model of ischaemia. For control experiments the slices were perfused with HEPES-buffered solution (containing glucose and pyruvate as substrates), and gassed with carbogen (95% CO₂, 5% O₂), at a speed of ~5ml/min. To model ischaemia, the substrates were replaced with choline chloride (to maintain osmolarity), gassed with nitrogen or argon, and the pH was reduced to 6.9. Because the slices were imaged in an open chamber (designed for an upright microscope), oxygen could potentially diffuse into the solution from the surrounding air, resulting in 'hypoxia' rather than 'anoxia' (the *in vivo* situation). A RC inhibitor (CN 1mM) was therefore included to model anoxia, as per a method used for similar work involving ischaemia in brain slices (Karadottir *et al.*, 2005). Oxygen was still kept as low as possible, by gassing with nitrogen or argon, to minimise the likelihood of artefactual ROS production.

2.2.5 Statistical analysis

The results are calculated as means \pm SEM. The significance of differences between groups was examined using the unpaired t-test. A p value <0.05 was taken as significant.

2.3 Clinical study

2.3.1 Study groups

To further characterise the clinical effects of MD on the human kidney, I have screened two well defined populations of patients for evidence of PT dysfunction. The first consisted of adult patients (>18 years old [the effects of MD on the kidney in children have been studied previously (Martin-Hernandez *et al.*, 2005)]), with known genetic or biochemical mitochondrial disease, who attend the clinics of Prof MG Hanna, Dr S Rahman and Prof N Wood at The National Hospital for Neurology. The majority have undergone detailed mtDNA screening with identification of mutations, and some have also undergone RC function tests on muscle tissue.

The second group consisted of HIV patients attending The Mortimer Market Centre, Camden PCT, who may or may not be taking ART, some forms of which are thought to be toxic to mitochondria. HIV itself is thought to be toxic to the renal tubule (Conaldi *et al.*, 1998); hence, I recruited treatment naïve patients, as well as those taking ART. Those on ART were sub-divided into two groups, depending on whether or not they had ever been exposed to TDF; in order to address the question (given the recent concerns in the literature) about whether TDF is more toxic to the PT than other forms of ART.

Data on demographics, drug and medical history and routine laboratory tests were collected from review of clinic notes and clinic databases. The Modification of Diet in Renal Disease (MDRD) method (4-variable, IDMS-traceable) was used to calculate eGFR (Levey *et al.*, 1999).

2.3.2 Exclusion criteria

Pre-existing renal disease, which was defined as a serum creatinine $>130\mu\text{mol/l}$ and/or dipstick positive proteinuria, was the main exclusion criteria. Clearly, in the modern era of routine eGFR reporting by laboratories, a patient with a serum creatinine $<130\mu\text{mol/l}$ does not necessarily have a normal eGFR. However, in non-renal clinics, this is the sort of arbitrary cut-off below which non-renal physicians would probably be fairly reassured about renal function, and would be unlikely to investigate further. Due to the relative rarity of mitochondrial cytopathy, no further exclusion criteria were applied to these patients.

In the HIV study, patients who were co-infected with viral Hepatitis B or C, or had diabetes, were excluded, due to their potentially confounding effects on renal function. Furthermore, patients with any previous history of significant renal disease (even if it had since resolved) were also excluded. Patients in both treatment groups were stable on their current ART regimen for more than 6 months, and had an HIV RNA level <50 copies/ml for at least 3 months prior to study entry (although not necessarily <50 copies/ml at the actual time of recruitment).

2.3.3 Ethical approval

The study was approved by the National Hospital for Neurology and Neurosurgery Regional Ethics Committee. It was also formally approved by the Research and Development Departments of University College London Hospitals NHS Trust and North Central London Research Network. Patients were recruited by physicians working in the relevant clinics. All patients provided written informed consent. Copies of the patient information sheets and consent forms are included in the appendix.

2.3.4 Sample processing

Urine samples were collected and frozen at -80°C within 4 hours. They were then analysed by Dr M Lapsley (Chemical Pathology, St Helier Hospital) for RBP, NAG and albumin. $U_{P/C}$ was measured by The Clinical Biochemistry Service at University College London Hospitals NHS Trust.

Urinary RBP was measured using a sandwich micro-titre plate enzyme immunoassay, with polyclonal antibodies from Dako Ltd (Denmark); the second antibody was labelled with horseradish peroxidase. Reference ranges for the normal adult population have been established previously (Lapsley *et al.*, 1998). Urinary NAG was measured with a kit from PPR Diagnostics Ltd (London, UK), using a microtitre plate format direct assay of enzyme activity, and using 2-methoxy-4-(2-nitrovinyl) phenyl- glucosaminide as substrate; the reference range used was that given by the manufacturers. For the purposes of the study, the upper limits of normal for $U_{RBP/C}$ and $U_{NAG/C}$ were defined as 2 standard deviations above the mean value in the reference populations ($U_{RBP/C} < 18\mu\text{g}/\text{mmol}$ and $U_{NAG/C} < 28\mu\text{mol}/\text{hour}/\text{mmol}$).

Urinary albumin was measured on a Siemens Advia 2400 Chemistry System (Siemens Healthcare, Camberley, UK) by an immuno-turbidimetric (antibody reaction) method, using reagents from Olympus Ltd (Watford, UK). Urinary creatinine was also measured on a Siemens Advia 2400 using a modified Jaffe reaction. Urinary protein was measured using a Roche Integra 800 analyzer (Roche Diagnostics UK, Burgess Hill, UK).

To investigate the effectiveness of either $U_{P/C}$ or $U_{A/C}$ as screening tools for detecting renal tubular disorders, the proportions of patients in each study group with abnormal values of $U_{P/C}$ and $U_{A/C}$ were compared to the proportions with evidence of tubular disease (defined as elevated $U_{RBP/C}$ and/or $U_{NAG/C}$).

2.3.5 Statistical analysis

One-way analysis of variance (ANOVA - for parametric data) or the Kruskal-Wallis test (for non-parametric data) was used to investigate statistical differences among the study groups. Where differences were found, individual groups were then compared with each other by an unpaired t-test (for parametric data) or an unpaired Mann-Whitney test (for non-parametric data). The relationship between variables was explored using the Spearman correlation coefficient (r_s). A p value of < 0.05 was taken as significant. Agreement between different urinary tests in defining abnormal proteinuria was measured by Kappa (κ) test (0, no agreement to 1, perfect agreement).

Chapter 3 – Results: The effect of mitochondrial respiratory chain inhibition on endocytosis of albumin and dextran in OK cells

3.1 FITC-albumin uptake is greatest at the apical membrane in OK cells and is partly megalin-mediated

OK cells form a confluent monolayer when grown in normal culture conditions; they endocytose FITC-albumin (FA) when incubated at 37°C, which can be measured as a progressive increase in fluorescence signal over 1 hour (Figure 3.1A). This endocytosis is, at least in part, mediated via the megalin receptor, as it is inhibited by receptor associated protein (RAP), an inhibitor of megalin mediated endocytosis in OK cells (Zhai *et al.*, 2000) (Figure 3.1B).

To assess the polarity of FA uptake, OK cells were grown on Transwell inserts until confluent. Significantly greater uptake of FA was observed after 1 hour when FA was applied to the apical membrane than when applied to the baso-lateral membrane (Figure 3.2). This is consistent with the situation in the PT *in vivo*, where LMWP endocytosis is thought to occur mainly at the apical membrane. From here on, endocytosis experiments were performed with OK cells grown as monolayers on coverslips, where the cell membrane exposed to ligands is predominantly apical.

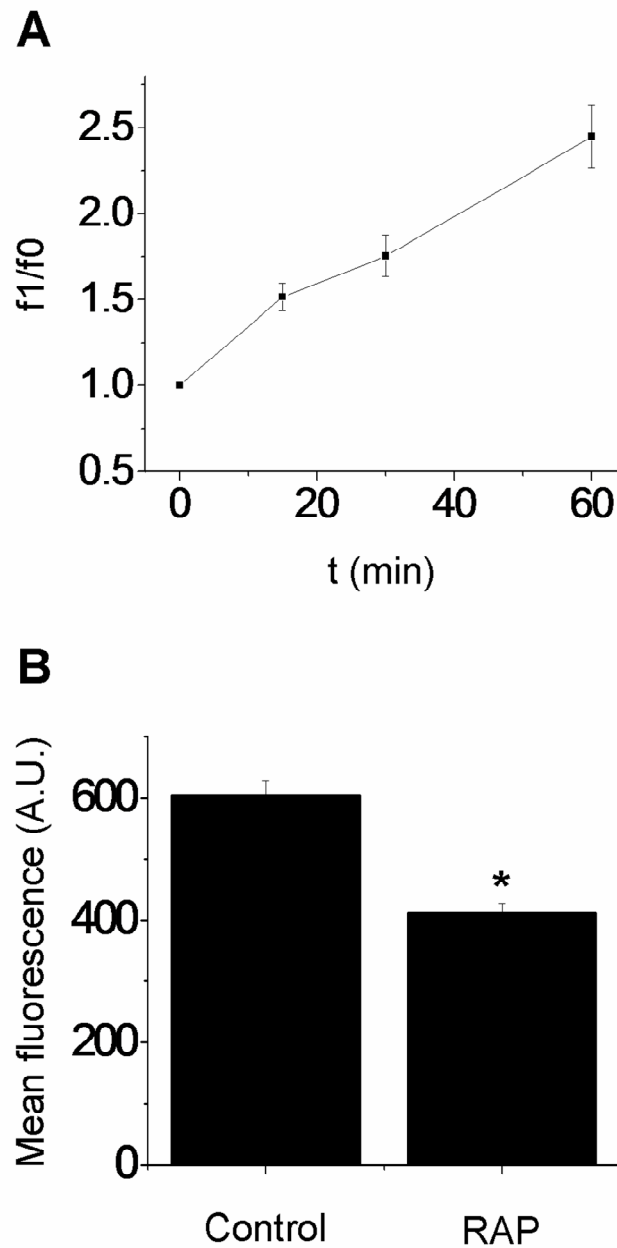


Figure 3.1. Endocytosis of FITC-albumin by OK cells is inhibited by receptor associated protein. OK cells endocytose FITC-albumin progressively over 1 hour (**A**). Uptake is partly megalin-mediated, as demonstrated by a reduced fluorescence signal after 1 hour in the presence of the megalin receptor inhibitor receptor associated protein (RAP) (**B**). Values given are mean fluorescence (\pm S.E.) per x40 objective field, from a total of 15 fields. (* $p < 0.005$).

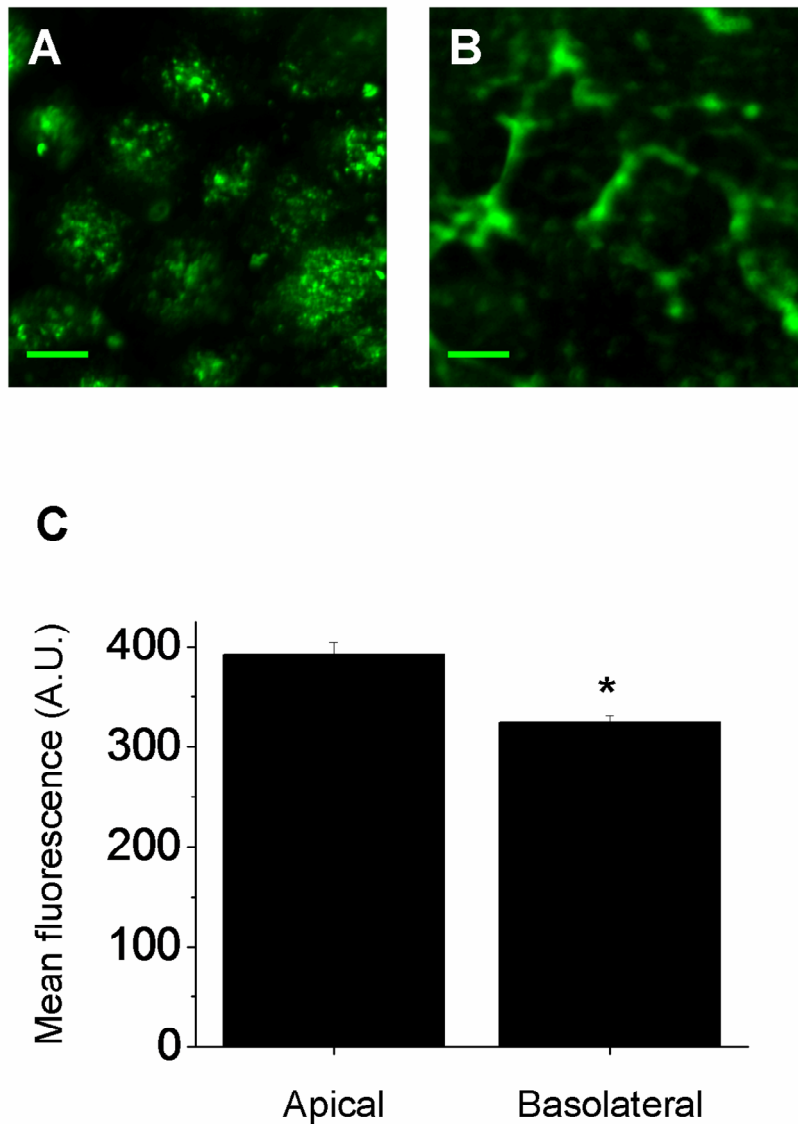


Figure 3.2. Polarity of FITC-albumin uptake in OK cells.

Experiments performed on OK cells grown on transwell inserts revealed both apical (A) and baso-lateral (B) uptake of FA (scale bar=10μm); however, the amount of apical uptake was greater (C). Values given are mean fluorescence (± S.E.) per x40 objective field (n=10). (*p<0.005).

3.2 Respiratory chain inhibition causes minimal cell death in OK cells

To ensure that exposure of OK cells to inhibitors of the mitochondrial RC does not result in rapid necrotic cell death, within the time period of the endocytosis assay, a standard hoechst/propidium iodide assay was performed. After 2 hours (twice the length of the endocytosis assay period), the proportion of dead cells observed (compared to control [$0.17\% \pm 0.17$ per x40 objective field, $n=5$]) was not significantly increased following incubation with rotenone $10\mu\text{M}$ ($2.39\% \pm 0.73$, $n=5$, $p>0.9$), CN 1mM ($0.20\% \pm 0.20$, $n=5$, $p>0.9$) or 2-DG ($1.62\% \pm 0.50$, $n=5$, $p>0.9$) (Figure 3.3A). A much higher rate of cell death was observed with IAA 1mM (in the presence of pyruvate) ($38.75\% \pm 3.72$, $n=5$), which was significantly different from all other groups ($p<0.001$). As IAA is an inhibitor of glycolysis, this result could imply a relatively greater dependence on this metabolic pathway for survival in these cells (although 2-DG did not have the same effect).

3.3 Blockade of glycolysis has a much greater effect on FITC-albumin uptake than respiratory chain inhibition in OK cells.

The control fluorescence signal emitted by OK cells per x40 objective field (assigned the value of 100%), after incubation for 1 hour at 37°C with FA, was reduced by a small amount by incubation with the RC inhibitors rotenone $10\mu\text{M}$ (92.8% of control signal ± 2.4 , $n=20$), piericidin $10\mu\text{M}$ ($89.5\% \pm 2.0$, $n=20$) or CN 1mM ($93.7\% \pm 1.8$, $n=20$) (Figure 3.3B); although only the results obtained with piericidin achieved statistical significance ($p<0.05$). This shows that inhibition of the RC in OK cells has only a small effect on receptor-mediated endocytosis at the apical membrane. However, incubation with 2-DG produced a much larger decrease in fluorescence signal (51.6% of control signal ± 1.7 , $n=15$, $p<0.001$); implying that blockade of glycolysis has a greater inhibitory effect on endocytosis than RC inhibition in this model.

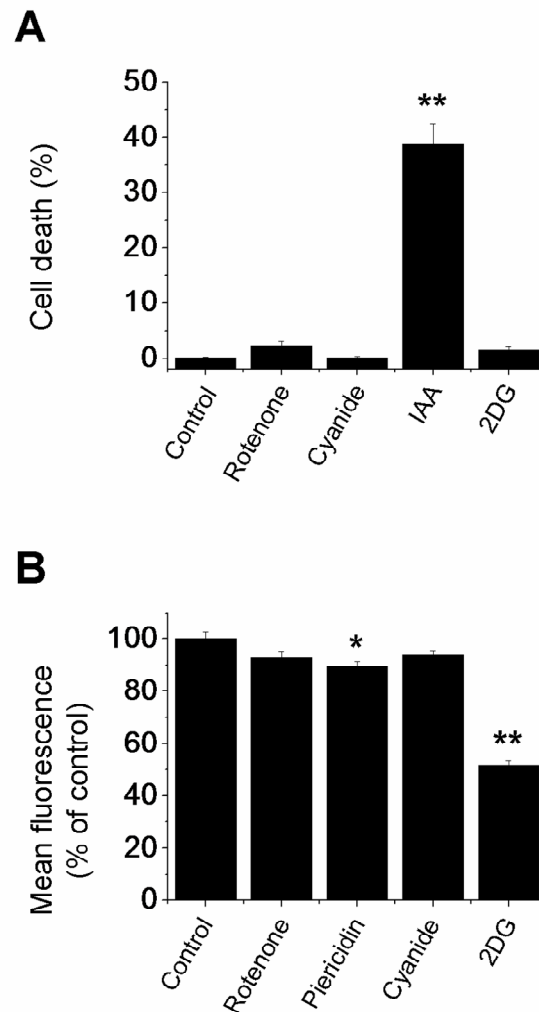


Figure 3.3. The effect of respiratory chain inhibition on cell death and FITC-albumin uptake in OK cells. Necrosis in OK cells was measured using a Hoechst/propidium iodide assay (**A**). There was no significant increase, compared to control, in the percentage of dead cells after 2 hours incubation at 37°C with rotenone, piericidin, cyanide or 2-deoxyglucose (2-DG). However, the percentage of dead cells was significantly increased by incubation with iodoacetic acid (IAA). Values given are mean percentage (\pm S.E.) of propidium iodide positive cells per x40 field, from a total of 5 fields for each experiment. Uptake of FITC-albumin in OK cells over 1 hour at 37°C was inhibited by a small but significant amount by the respiratory chain inhibitor piericidin 10 μ M. No significant decrease was observed with rotenone 10 μ M or cyanide 1mM. 2-DG caused a much larger impairment of FITC-albumin uptake (**B**). Values given are mean fluorescence (\pm S.E.) per x40 objective field, from a total of 20 fields for all experiments (except 2-DG; n=15). (**p<0.001, *p<0.05).

3.4 Rotenone causes an altered pattern of FITC-albumin and FITC-dextran uptake in OK cells

When imaging the uptake of FA in OK cells, it was noted that although there was relatively little difference between the various RC inhibitors in the effect on total uptake, there was a marked difference in the pattern of uptake that was unique to rotenone. Neither piericidin nor CN appeared to change the control pattern of FA uptake (Figure 3.4A,C-E); however, a striking difference was observed in the presence of rotenone (Figure 3.4B and F). Instead of the normal predominance of uptake at the apical brush border, the rotenone treated cells appeared flatter and uptake was more lateral in the cells.

The uptake of FA in OK cells is thought to be predominantly via receptor-mediated endocytosis; an efficient and relatively specific uptake system. However, cells are thought to be able to import substances from their surrounding environment via fluid phase endocytosis (pinocytosis), which occurs due to constant invagination and pinching off of normal cell membranes. This is a much less efficient uptake system, nevertheless it may play a role in the reabsorption of solutes in the PT. Dextran molecules are known to be taken up by the PT *in vivo* (Molitoris & Sandoval, 2005), and by OK cells *in vitro* via fluid phase endocytosis (Gekle *et al.*, 1995).

I therefore investigated the effect of rotenone on fluid phase endocytosis in OK cells. The control pattern of uptake of FD was similar to that of FA, with the majority of FD appearing in the vicinity of the apical brush border (Figure 3.4G). Rotenone 10 μ M also markedly affected the pattern of uptake of FD, in a manner analogous to its effects on FA uptake (Figure 3.4H). This suggests that the striking effects of rotenone on FA uptake are more likely to be due widespread structural changes within the cell, affecting generalized uptake machinery, rather than a specific targeted effect on megalin/cubulin receptor-mediated endocytosis (see below – ‘Extra-mitochondrial effects of rotenone’).

The effects of rotenone on the pattern of FA uptake were unlikely to be due to an impairment of substrate utilization at complex I, as piericidin did not have the same

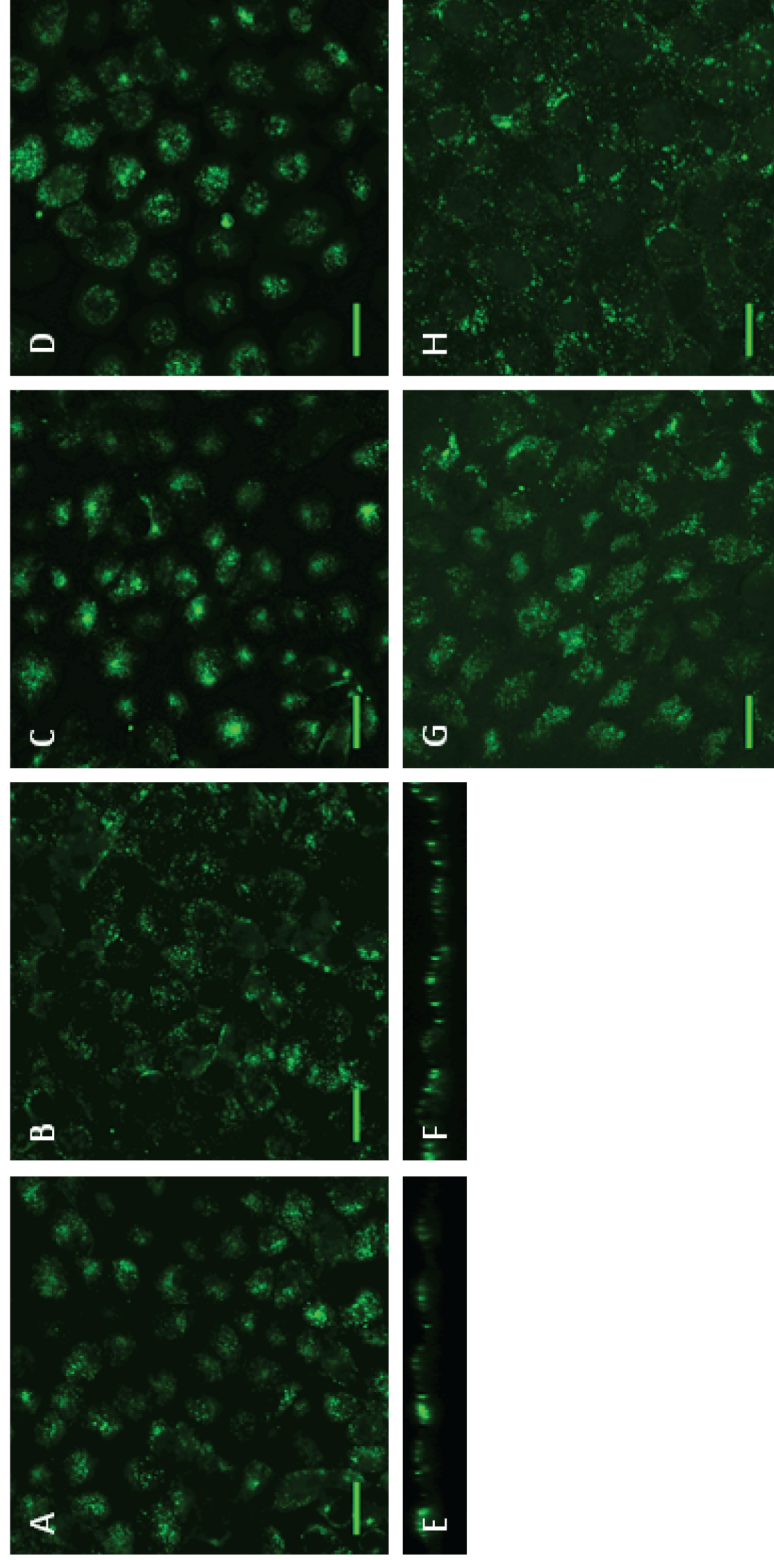


Figure 3.4. The effect of respiratory chain inhibitors on the pattern of uptake of FITC-albumin and FITC-dextran in OK cells. The control pattern of uptake of FITC-albumin in OK cells (A) was markedly altered by exposure to the respiratory chain (RC) inhibitor rotenone 10 μ M (B), but was not affected by exposure to the RC inhibitors piericidin 10 μ M (C) and cyanide 1mM (D). Images shown are representative x63 objective fields of OK cells incubated with FITC-albumin at 37°C for 1 hour. Z-projection views of x63 fields show apical brush border uptake of FA in control cells (E) and an altered uptake pattern in rotenone treated cells (F). The control pattern of uptake of FITC-dextran (G), a marker of fluid-phase endocytosis, was also affected by rotenone 10 μ M (H). Scale bar =20 μ m.

effect. Accordingly, bypassing the inhibition of electron flow at complex I with the addition of the complex II substrate methyl-succinate 5mM (which should restore normal RC function and ATP production) did not affect the uptake pattern observed with rotenone (Figure 3.5A).

I postulated that the effects of rotenone may have been due to excess ROS production (see below – ‘Rotenone increases ROS production in OK cells’), as rotenone causes inhibition of the RC at complex I, a potential site of ROS generation in mitochondria. However, the anti-oxidant MnTBAP 50 μ M had no effect on the pattern of FA uptake seen with rotenone, either alone (Figure 3.5B), or even in combination with a cocktail of other anti-oxidant agents (catalase 250U/ml [a catalyst for the decomposition of hydrogen peroxide], Trolox 750 μ M [an anti-oxidant derivative of vitamin E] and ascorbate 1mM [vitamin C – another anti-oxidant]) (Figure 3.5C).

3.5 Respiratory chain inhibition has relatively little effect on cytosolic ATP levels in OK cells

Receptor mediated endocytosis is an active process, thought to be dependent on ATP (Podbilewicz & Mellman, 1990). To measure the effect of RC inhibition on cytosolic ATP levels, OK cells were loaded with the ATP-sensitive dye Mg green and excited at 488nm. Mg green fluorescence signal changes inversely in response to changes in cytosolic ATP levels. Cells were simultaneously loaded with TMRM 50nM, a marker of mitochondrial membrane potential ($\Delta\psi_m$), which was excited at 543nm. Regions of interest (ROI) were drawn around nuclei in order to obtain a cytosolic signal for the benefit of analysis.

Inhibition of the RC with rotenone 10 μ M caused no increase in the Mg green signal, suggesting a minimal effect on the cytosolic ATP level (Figure 3.6). However, rotenone did cause an increase in the cytosolic TMRM signal, consistent with depolarization of $\Delta\psi_m$ and redistribution of the dye from the mitochondria into the cytosol. This change provided a positive control and implied that the drug was ‘working’ as expected (i.e. inhibiting RC activity). In response to subsequent

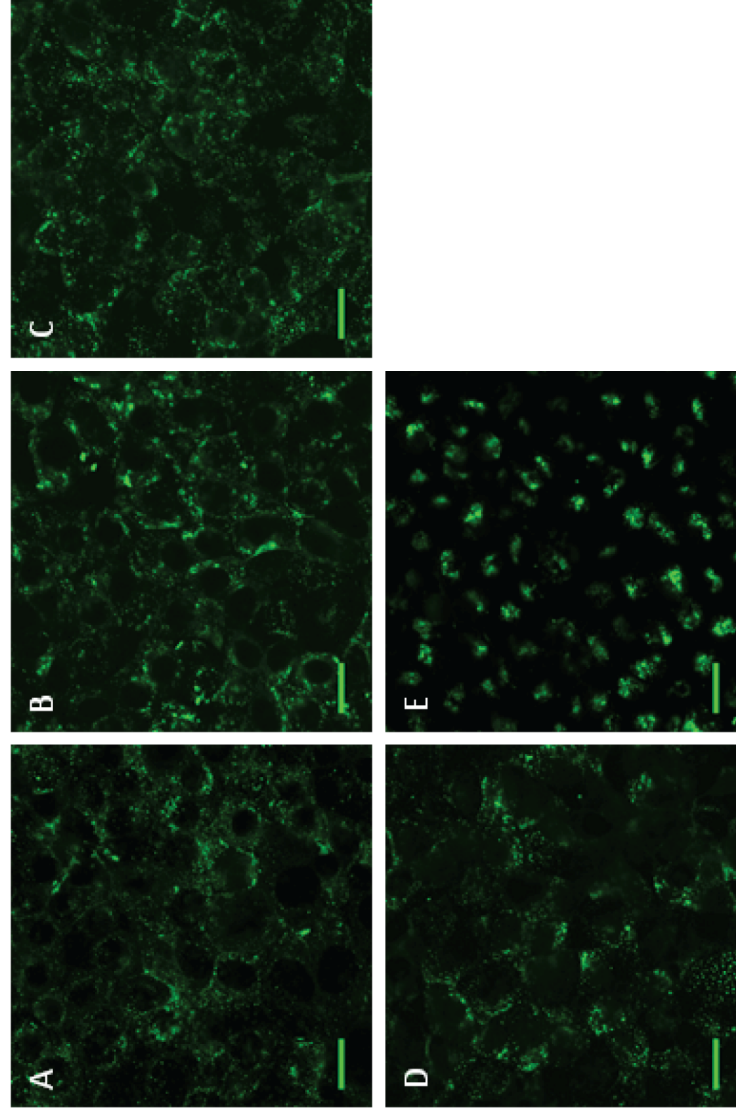


Figure 3.5. The effects of rotenone and colchicine on FITC-albumin uptake in OK cells. The pattern of FITC-albumin uptake observed in the presence of rotenone 10 μ M was not altered by incubation with either the complex II substrate methyl-succinate 5mM (**A**) or the anti-oxidant MnTBAP 50 μ M (alone [**B**], or in combination with catalase 250U/ml, Trolox 750 μ M and ascorbate 1mM [**C**]). An uptake pattern similar to that caused by rotenone was observed following exposure to colchicine, an inhibitor of microtubule assembly (**D**). The control pattern of FITC- albumin uptake was restored in the presence of rotenone by Taxol 10 μ M, a microtubule stabilizing agent (**E**). Scale bar =20 μ m.

inhibition of glycolysis with IAA (1mM), Mg green signal increased, consistent with a fall in cytoplasmic ATP concentration. IAA also caused a further rise in the TMRM signal, consistent with further depolarization of $\Delta\psi_m$, which is dependent on reverse activity of the F_1F_0 -ATPase and ATP breakdown for maintenance of potential when the RC is blocked.

The effect of RC inhibition on cytosolic ATP levels was further investigated using a luciferin-luciferase assay and a custom built luminometer. Addition of luciferin to OK cells, transfected with cytosolic luciferase, produced a large rise in luminescence, reflecting high transfection efficiency. Addition of rotenone 10 μ M caused only a small drop in luminescence signal (normalized luminescence value 0.735 ± 0.009 [where 1 = maximal signal post luciferin and 0 = zero counts]). A much greater decrease was observed in response to the addition of IAA 1mM (normalized luminescence value 0.185 ± 0.003 , n=11 experiments, $p < 0.01$); a representative luminescence trace from one of these experiments is shown along with the normalized pooled values (Figure 3.7).

Overall, these results suggest that the OK cells, like many immortalized cultured cells, are predominantly dependent on anaerobic glycolysis for ATP production, and RC inhibition has at most only a minimal effect on cytoplasmic ATP levels. This could potentially explain the relatively small effect of RC inhibition on FA uptake in my *in vitro* assay.

3.6 Rotenone increases ROS production in OK cells

Mitochondria have other important roles besides ATP production and are a major source of ROS, which have wide-ranging physiological and patho-physiological effects. I therefore investigated the effects of RC inhibition on mitochondrial ROS production in OK cells by loading them with the ROS-sensitive dye mitosox, which localizes to mitochondria and was excited at 543nm. For the purposes of analysis, ROIs were drawn around mitochondrial-rich regions of each cell, which were identified randomly using the mitochondrial NADH signal emitted when excited at 364nm. The fluorescence signal from cells loaded with mitosox increased

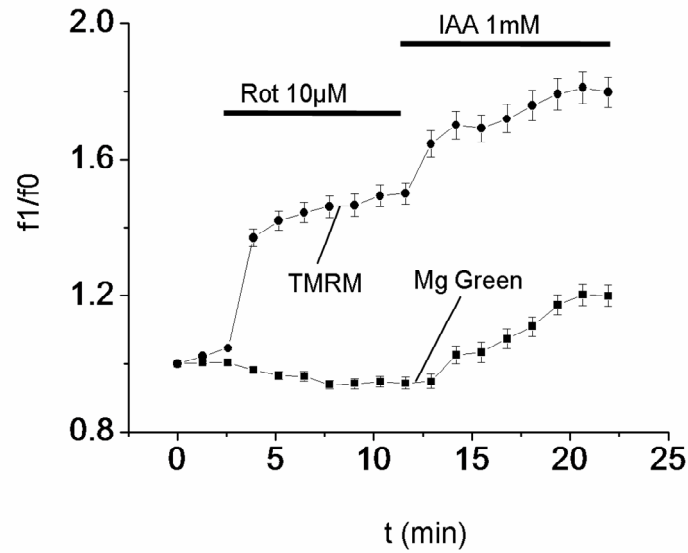


Figure 3.6. The effect of respiratory chain inhibition on cytosolic ATP levels in OK cells, measured using magnesium green and TMRM. Rotenone caused an increase in cytosolic TMRM signal consistent with depolarisation of $\Delta\psi_m$. However, iodoacetic acid (IAA) had a much greater effect on magnesium green signal than rotenone, implying that cytosolic ATP is predominantly derived from anaerobic metabolism in OK cells. Values given are mean nuclear fluorescence signal (\pm S.E.) from a total of 154 (TMRM) and 126 (magnesium green) cells.

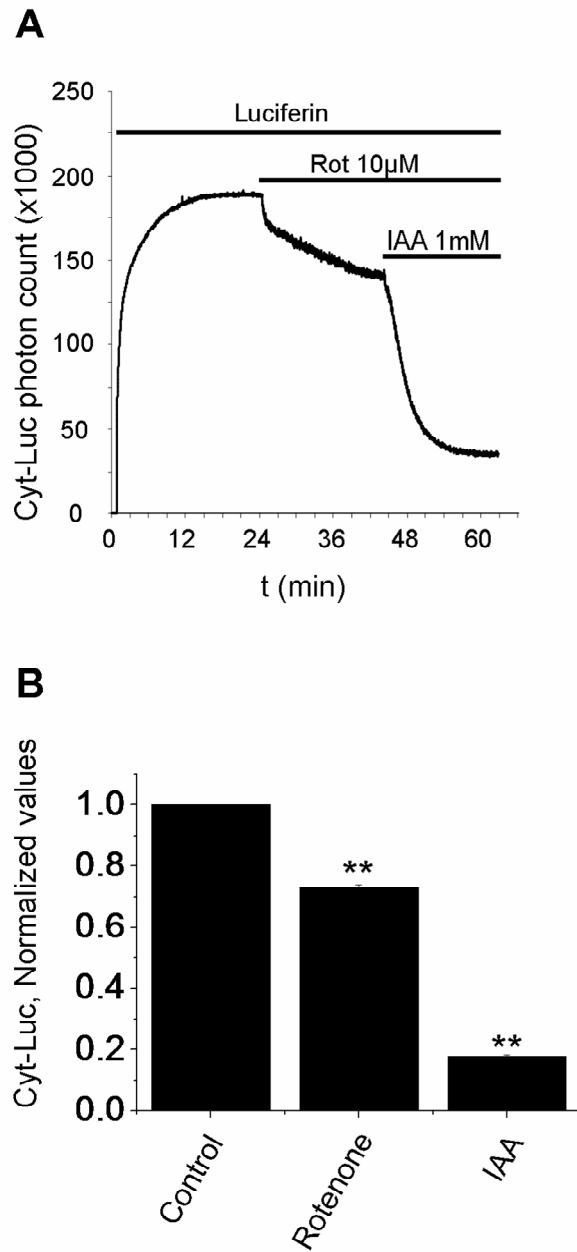


Figure 3.7. The effect of respiratory chain inhibition on cytosolic ATP levels in OK cells, measured using luminometry. OK cells transfected with a cytosolic luciferase emitted a luminescence signal in the presence of luciferin, the intensity of which was ATP-dependent. RC inhibition with rotenone produced only a small decrease in signal intensity, whilst a significantly larger decrease occurred following blockade of glycolysis with iodoacetic acid (IAA). Data depicted are a sample representative luminescence trace **(A)**, and normalised values from 11 experiments **(B)** (** $p < 0.01$).

progressively with time, and the rate of increase was taken to be proportional to the rate of ROS production.

Rotenone 10 μ M caused a significant increase in the rate of change of mitoxox signal (rate post-rotenone 282% \pm 21 of the control rate, n=163 cells, p<0.001), but this increase was obliterated in the presence of the anti-oxidant MnTBAP 50 μ M (rate post rotenone and MnTBAP 103% \pm 16 of the control rate, n=225 cells) (Figure 3.8). This implies that MnTBAP is capable of nullifying the increase in ROS production normally seen in response to rotenone, suggesting that a rise ROS was not likely to be responsible for the profound structural effects of rotenone on the OK cells, as these were not prevented by MnTBAP at the same dose.

The rate of change of mitoxox signal was not significantly increased by piericidin (99% \pm 4 of the control rate, n=218 cells, p>0.9), another RC complex I inhibitor, suggesting that the increase in ROS production observed with rotenone is specific to that drug, rather than inhibition of complex I *per se*. The rate of change of mitoxox signal was significantly decreased by CN (57% \pm 5 of control rate, n=140 cells, p<0.001), showing that blockade of the RC at complex IV reduces the rate of ROS production in OK cells.

3.7 Extra-mitochondrial effects of rotenone

Given that MnTBAP did not prevent the effects of rotenone on the pattern of FA endocytosis (in spite of the fact that it clearly prevented the rise in ROS production associated with rotenone), and that the RC inhibitors piericidin and CN did not produce the same pattern, it was considered that the effect of rotenone on endocytosis could have been extra-mitochondrial.

There is some literature suggesting that rotenone can depolymerise microtubules (Brinkley *et al.*, 1974; Marshall & Himes, 1978; Ren & Feng, 2007), in addition to its effects on the RC, and an intact cytoskeleton is required for albumin endocytosis in OK cells (Gekle *et al.*, 1997). Colchicine is an established inhibitor of microtubule

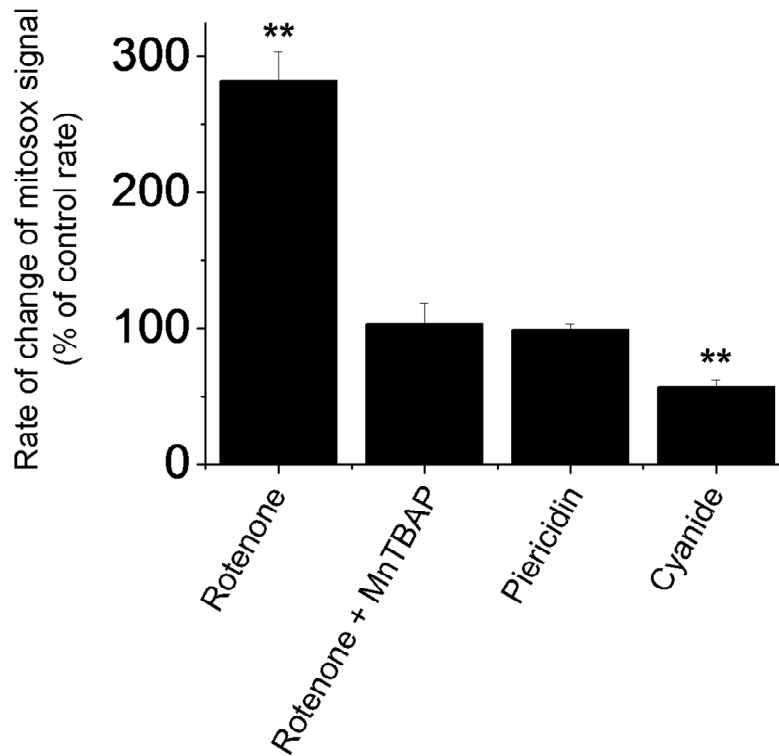


Figure 3.8. The effect of respiratory chain inhibition on reactive oxygen species production in OK cells.

Mitochondrial reactive oxygen species (ROS) production in OK cells was measured using the dye mitox. The rate of change of mitox signal was taken to be proportional to the rate of ROS production. Rotenone 10 μ M caused a significant increase in the rate of ROS production, compared to control. However, this increase was obliterated by the antioxidant MnTBAP 50 μ M. No significant difference was observed from the control rate with the addition of piericidin 10 μ M. Cyanide 1mM caused a significant decrease from the control rate. Values given are mean rate of increase in fluorescence signal per ROI, expressed as a percentage of the control rate (\pm S.E.) from 163 cells (rotenone), 225 cells (rotenone + MnTBAP), 218 cells (piericidin) and 140 cells (cyanide). (** $p < 0.001$).

polymerisation, and a pattern of FA uptake similar to that seen with rotenone was observed in response to colchicine 10 μ M (Figure 3.5D). Furthermore, co-incubation with Taxol (a microtubule stabilizing agent) and rotenone produced a pattern of FA uptake similar to control (Figure 3.5E). These results suggest that the effects of rotenone on the pattern of FA uptake in OK cells were due to inhibition of microtubule polymerization.

The structural effects of rotenone on OK cells were further investigated using EM. Control images demonstrated that OK cells form a confluent polarized monolayer in culture with an apical brush border (Figure 3.9A-C). Addition of rotenone 10 μ M caused widespread structural damage, including the loss of the brush border, and the appearance of numerous large vacuoles and abnormally shaped swollen mitochondria (Figure 3.9D-F).

3.8 Discussion

3.8.1 *The relationship between cytosolic ATP and albumin endocytosis*

Inhibition of the mitochondrial RC *in vitro* in OK cells produced only a small effect on the uptake of FA, which was surprising given the apparent vulnerability of the PT to MD *in vivo*. In patients with mitochondrial cytopathy, RC function may be impaired (though not necessarily), but complete cessation of RC activity within cells is unlikely. It was therefore also surprising that OK cells showed very little necrosis after 2 hours of complete RC blockade, given that they are derived from the PT, which has very little anaerobic ATP-generating capacity *in vivo*, and is the prominent site of necrosis following experimental ischaemia-reperfusion injury (Shanley *et al.*, 1986c). However, in contrast to the native PT, I have demonstrated that OK cells do indeed have significant capacity to generate ATP anaerobically, which probably explains their resistance to RC blockade. This may well also explain why only a small decrease in FA endocytosis was observed following RC inhibition; the magnitude of decrease of endocytosis was of the same order as the reduction in cytosolic [ATP] after RC inhibition. This is suggestive (though not conclusive) that ATP may play an important role in endocytosis, as found in other studies (see later – ‘General discussion - The relationship between mitochondrial function and

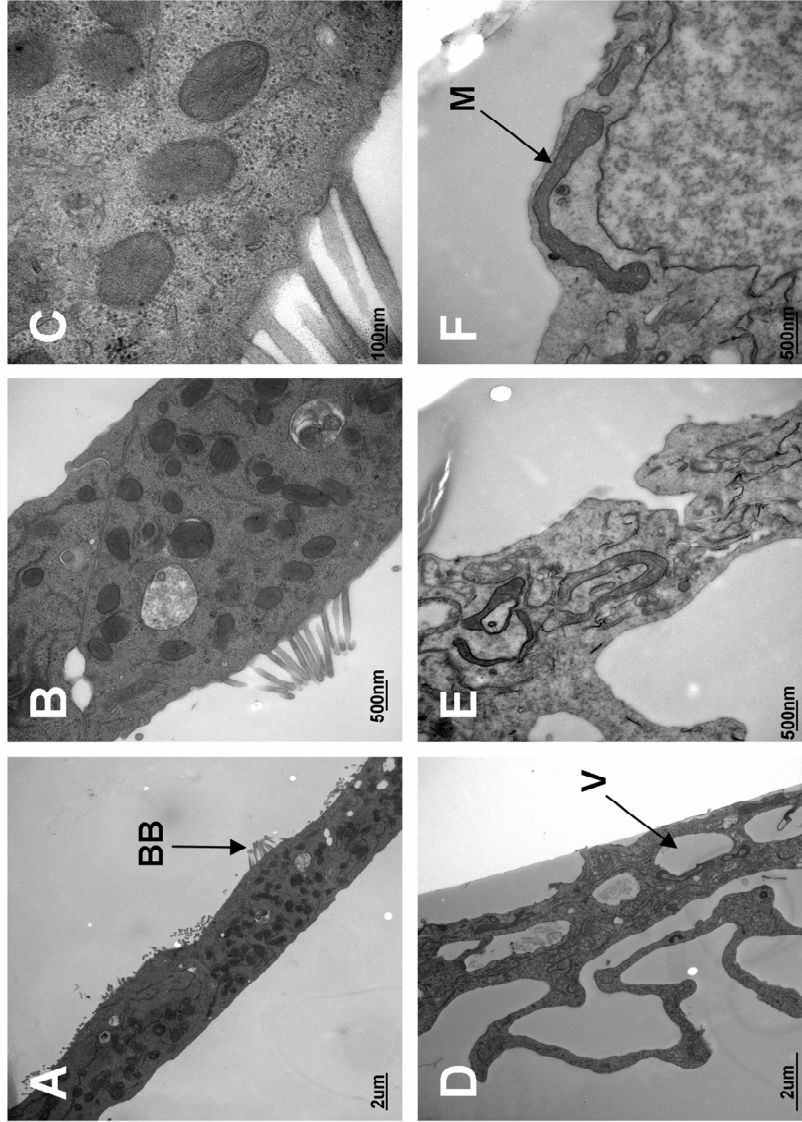


Figure 3.9. Electron microscopy of OK cells exposed to rotenone. OK cells form a confluent monolayer in culture, with an apical brush border (BB) (A-C). Following exposure to rotenone 10μM for 1 hour, extensive structural damage was observed in the cells, with loss of the brush border, and the appearance of numerous vacuoles (V) and abnormally shaped mitochondria (M) (D-F).

endocytosis in the proximal tubule'). In support of this hypothesis, blockade of glycolysis with 2-DG produced a much larger decrease in both cytosolic [ATP] and FA uptake. IAA is another established inhibitor of glycolysis; however, this agent proved to be highly toxic to the cells, leading to rapid necrosis, and therefore could not be used in conjunction with the 1 hour FA uptake assay. Greater vulnerability to IAA, compared to RC inhibition, again suggests that OK cells are predominantly dependent on anaerobic metabolism. However, it is unclear why 2-DG, another glycolytic inhibitor, was not as toxic as IAA; presumably the differences are due to the fact that the two agents target different steps in the glycolytic pathway, but this was not explored further in this project. Immortalised cells in culture tend to become increasingly anaerobic with time (Gstraunthaler *et al.*, 1999), due to The Warburg effect (Kim & Dang, 2006). This weakens their value as a model system to study metabolic phenomena in the PT, which has to be balanced against their many advantages.

3.8.2 Rotenone is highly toxic to OK cells

Rotenone had marked structural effects on the OK cells, with widespread cellular damage observed on EM, leading to an altered pattern of both FA and FD uptake. This means that rotenone had an effect on both receptor mediated and fluid phase endocytosis.

Exposure of rats to rotenone produces a phenotype similar to Parkinson's disease, with a characteristic loss of nigrostriatal dopaminergic neurons in the brain (Betarbet *et al.*, 2000); this has led to an epidemiological link between Parkinson's disease in humans and exposure to pesticides containing rotenone (Gorell *et al.*, 1998). Evidence has suggested that the toxicity of rotenone to neurons is mediated more via oxidative stress, rather than a drop in cytosolic ATP (Sherer *et al.*, 2003). The mechanism of the toxic effect of rotenone on OK cells in my study was unlikely to involve inhibition of complex I in the RC alone, as the effects were not mimicked by piericidin (another complex I inhibitor). Furthermore, although rotenone did cause a rise in ROS production (that was not observed with other RC inhibitors), this rise was obliterated by MnTBAP, which had no protective effect on the pattern of FA uptake.

Another established (although generally less well known) effect of rotenone, other than RC complex I inhibition, is toxicity to microtubules (Marshall & Himes, 1978). The similarity between the effects of rotenone and colchicine on FA uptake in OK cells suggests that the toxicity of the former may have been mediated via inhibition of microtubule proliferation; this was further supported by the protective effects of the microtubule stabilizing agent Taxol.

Inhibition of microtubule polymerization has been reported previously to reduce albumin uptake by OK cells (Gekle *et al.*, 1997). Microtubules are an important part of the cell cytoskeleton, and in addition to their structural role, they are also involved in key physiological processes, such as mitosis and transport of vesicles (via ATP dependent motor proteins such as kinesin and dynein). This latter role is thought to be important in trafficking ion transporters to the correct membrane in polarized cells, such as those of the renal epithelium (Hamm-Alvarez & Sheetz, 1998). Indeed, abnormal localization of megalin has been observed in the PT in rats exposed to the microtubule polymerization inhibitor colchicine (Gutmann *et al.*, 1989). Infusion of colchicine into rats in another study led to the observation of significant structural abnormalities in the PT on EM, which are likely to have inhibitory effects on normal endocytosis (Elkjaer *et al.*, 1995). Amongst the abnormalities reported were an increase in the size and number of intracellular endocytotic vesicles, which mirrors my findings in OK cells exposed to rotenone. The vesicles were reported to be in a more baso-lateral location than under control conditions and, conversely, mitochondria were found in sub-apical cytoplasm, rather than their usual baso-lateral distribution; findings that together highlight the importance of microtubules in determining normal cell polarity. Interestingly, structural abnormalities were not reported in mitochondria following colchicine exposure, perhaps suggesting that the abnormal appearance of mitochondria in OK cells exposed to rotenone in my study may have been related more to effects on the RC, rather than on microtubules. Immuno-fluorescence staining for AQP1 in rat kidney revealed that the normal apical membrane localization of this channel was altered by colchicine exposure, leading to a diffuse signal seen throughout the cytoplasm (Elkjaer *et al.*, 1995); resulting in images that were analogous to those of OK cells exposed to FA and rotenone in my study.

The toxic effect of rotenone on microtubule polymerisation is severe enough to arrest mitosis in cultured cells and is thought to be mediated via binding to tubulin in a manner analogous to colchicine (Brinkley *et al.*, 1974). Indeed, some have argued that it is actually the effect of rotenone on microtubules that explains its apparent selective toxicity to dopaminergic neurons (Ren & Feng, 2007). A wide variety of heavy metals have been implicated as environmental causes of renal tubular dysfunction (Wedeen & DeBroe, 2005); however, unlike PD, no epidemiological connection has been made to date between rotenone exposure and kidney disease in humans (although colchicine is used extensively in clinical practice for treating crystal arthropathies). Although my findings regarding the toxic effects of rotenone may, therefore, not relate directly to human disease, from an experimental viewpoint they raise an important issue related to the extra-mitochondrial effects of rotenone, as it is a commonly used reagent in studies investigating the effects of mitochondrial RC inhibition. They also reinforce the importance of microtubules in the function of polarised transporting epithelia, such as the PT.

3.8.3 The effect of mitochondrial respiratory chain inhibition on ROS production

In order to investigate other possible mediators of the effects of RC inhibition on endocytosis (aside from changes in ATP levels), I measured the effects of RC inhibitors on mitochondrial ROS production in OK cells, by using the ROS-sensitive dye mitoxox, which localizes to mitochondria. I found that inhibiting the RC with piericidin did not lead to a significant increase in ROS production, whilst CN actually decreased the rate.

A previous investigation of the effects of CN on ROS production in another renal cell line (LLC-MK2) reported an increase in ROS production and oxidative stress in response to CN (Hariharakrishnan *et al.*, 2009). However, the incubation period for that study was much longer (4 hours), the dye used to measure ROS (DCF) does not specifically measure mitochondrial ROS production and CN causes other potentially confounding effects (such as inhibition of the anti-oxidant enzyme SOD (Loven *et al.*, 1982)). The authors reported that LLC-MK2 cells were one of a number of renal-derived cell lines tested (they did not state which ones), and were found to be

particularly sensitive to the toxic effects of CN. Interestingly, they also found a large drop in cytosolic ATP levels in response to CN in these cells, implying a much greater dependence on aerobic metabolism compared with OK cells, perhaps explaining why the LLC-MK2 cells are so sensitive to CN. From a metabolic viewpoint, LLC-MK2 cells may, therefore, provide a more realistic model of PT cells *in vivo*; however, they lack the capacity for avid endocytosis of protein observed in OK cells.

Rotenone is thought to cause an increase in ROS production at complex I via inhibition of electron flow at the ubiquinone binding site, leading to an increased NADH/NAD⁺ ratio at the 'upstream' flavin binding site of complex I, which favours increased O₂⁻ formation (Hirst *et al.*, 2008). In contrast, rotenone tends to block the increase in ROS production observed during 'reverse electron flow' (e.g. during excess utilization of succinate as a substrate by complex II), by preventing electrons from reaching the flavin binding site (Hirst *et al.*, 2008). Given the fact that rotenone increased ROS production in the OK cells, it is therefore likely that electron flow is in the 'forward direction' in these cells under resting conditions. Differences between rotenone and piericidin in ROS generation at RC complex I have been reported before (Ohnishi *et al.*, 2005). Although both are thought to share a common binding domain with overlapping sites (Okun *et al.*, 1999), differences in the effects of the two reagents may be due to different conformational changes induced in the complex by binding of either reagent (Ino *et al.*, 2003). However, much still remains to be elucidated about the behaviour of complex I and the mechanisms of ROS generation at this site, particularly in different tissue types.

Chapter 4 – Results: Multi-photon imaging of mitochondrial function in live slices of rat kidney

4.1 Viability and orientation

Tissue was used for up to 6 hours following removal of the kidney. Various structures could be imaged by slicing at different levels (including cortical structures such as glomeruli and proximal and distal tubules, and medullary structures such as capillaries and the loops of Henle), and cell viability was confirmed by uptake and retention of the dye calcein-AM (Figure 4.1A-C). This dye enters cells and is cleaved to the fluorescent form by intracellular esterases, which are only active in live cells. Hence, it is a widely used and reliable marker of cell viability (Bratosin *et al.*, 2005). Structures were identified by their characteristic morphology, location, and green auto-fluorescence emission pattern at 800nm excitation (Figure 4.1D). PT cells emitted considerably greater autofluorescence in the green range than DT cells. The source(s) of this signal are unknown, although are likely to include oxidized flavoproteins (see below – ‘Autofluorescence measurements reveal that mitochondria in the proximal tubule are in a more oxidised state’). Autofluorescence in the green range appeared to vary in different sections of the PT, which may represent differences between different anatomical sections (S1, S2 and S3); however, this was not explored further in this project, partly due to a lack of specific markers for these segments.

Identification of tubules was confirmed in preliminary experiments by using fixed slices stained with specific antibodies (Figure 4.1E-F). PT cells were labelled using an antibody to aquaporin-1 (Sabolic *et al.*, 1992). As depicted, PT cells occupied the bulk of the volume of both the renal cortex and medullary rays. DT cells (thick ascending limb of the loop of Henle) were labelled with an antibody to Tamm Horsfall protein (Bachmann *et al.*, 1985). The red fluorescent signal from the DT antibodies can be contrasted with the green autofluorescence from the PT, which demonstrates the clear difference in size and morphology between the two tubule types (PT being much larger). Control specimens showed little or no signal. Given that identification of tubule types based on morphology was straightforward (at least

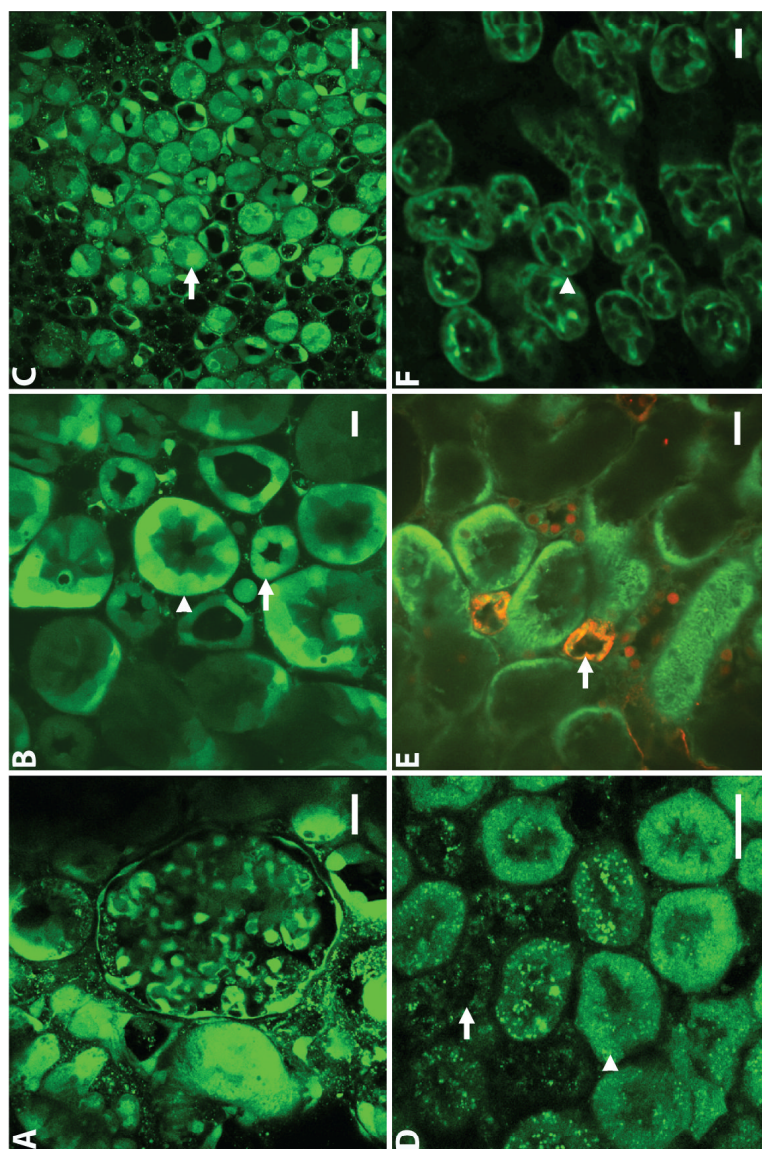


Figure 4.1. Structure and viability of rat kidney slices. Live rat kidney slice loaded with calcein and excited at 800nm to demonstrate viability, and showing glomerulus (A), cortical medullary ray (B) and medulla (C). In addition to differing morphology, proximal and distal tubules can be further distinguished by the green autofluorescence emission pattern when excited at 800nm (D). Antibody labeling in fixed slices of kidney was used in initial experiments to confirm the identity of nephron sections. Anti-Tamm-Horsfall protein (red) staining in distal tubules demonstrated the clear difference in morphology from proximal tubules (green autofluorescence) in the slice preparation (E). Anti-aquaporin-1 (green) staining was used to confirm the identity of proximal tubules (F). (Arrowhead: PT, Arrow: DT. Scale bar = 20µm).

PT versus DT, I was not able to resolve sub-sections on the PT), routine antibody staining to confirm identity was not performed in further experiments (this would also have required fixation of the live tissue).

4.2 Mitochondrial membrane potential is higher in distal tubules

$\Delta\psi_m$ lies at the heart of mitochondrial function, determining rates of ATP synthesis, ROS production, Ca^{2+} accumulation and protein import. The cationic lipophilic indicator TMRM was used to explore the distribution of $\Delta\psi_m$ in the tubules. The dye clearly concentrated in mitochondria, as expected, showing the characteristic distribution described in the literature, with mitochondria aligned in rows at the basolateral poles of the cells (Kaissling & Kriz, 1979) (Figure 4.2A). The signal intensity at any given pixel is a function of dye concentration, which in turn is a function of potential. The mitochondrial signal was isolated by applying threshold settings to remove the background cytoplasmic signal, so that values of pixels outside the mitochondria were excluded from measurements. The mean signal intensity in the remaining pixels within mitochondria was therefore independent of mitochondrial density in any given tubule. This is important as cell size and mitochondrial density vary along the length of the nephron.

The signal was clearly heterogeneous across the slice and was considerably higher in cells of the DT, giving a mean fluorescence intensity per x40 objective field of 1038 ± 80 A.U., compared with a mean in convoluted PT of 566 ± 23 A.U. ($p < 0.001$), which in turn was significantly higher than straight PT, where the mean was 385 ± 3 A.U. ($p < 0.001$; data are from 3 fields per slice, randomly selected using the bright field setting, from a total of 3 slices) (Figure 4.2B-C and E) and with all microscope settings kept constant. These observations suggest that mitochondria in the DT are more polarized compared with the PT. A similar pattern of signal was also observed using rhodamine 123 (Figure 4.2D), another cationic dye that functions in the same way as TMRM, showing that this difference was not specific for TMRM.

It has been shown previously that PT cells in isolated tubules are vulnerable to hypoxia, after which $\Delta\psi_m$ can be partially maintained by reversal of the F_1F_0 -ATPase

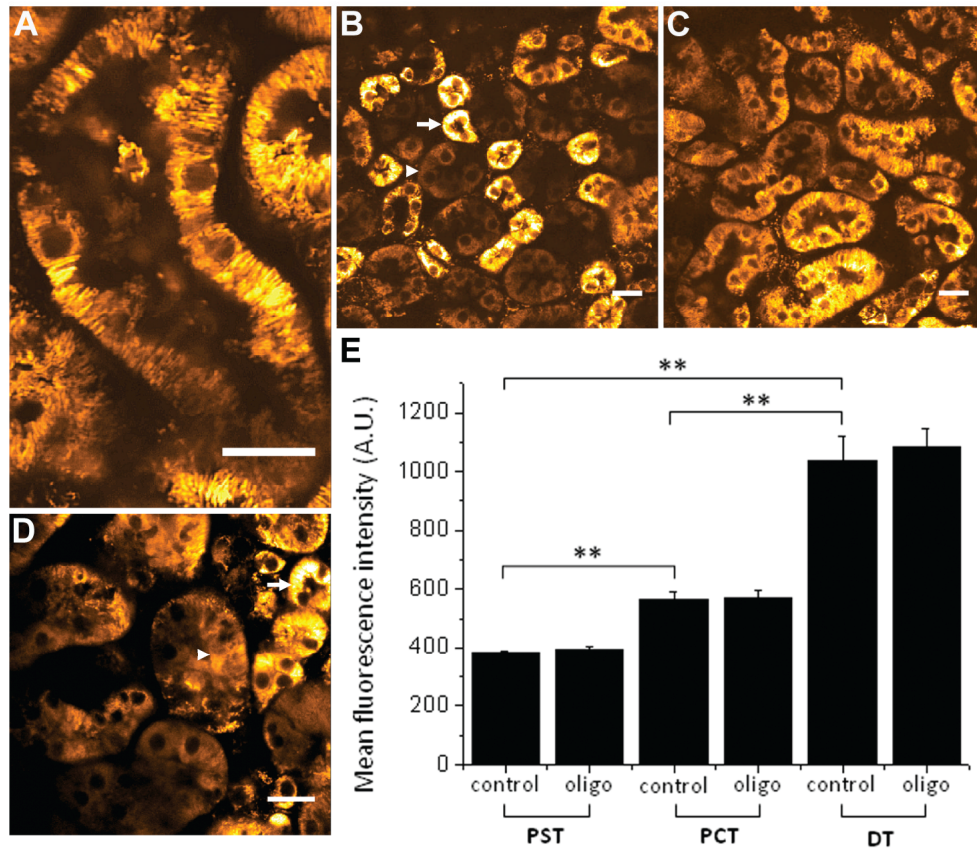


Figure 4.2. Measurement of mitochondrial membrane potential in renal tubules.

The proximal tubule contains a high density of mitochondria, which lie in a striated baso-lateral distribution (A). TMRM signal was consistently higher in distal tubules compared with proximal straight tubules in the medullary ray (B). The signal was greater in proximal convoluted than proximal straight tubules (C), but it was still not as high as in distal tubules. The pattern of signal was the same with Rhodamine-123, another $\Delta\psi_m$ dependent dye (D) (Arrowhead: PT, Arrow: DT. Scale bar = 20 μ m). Mean TMRM signal (\pm S.E.) for different tubule types is depicted, both before and 30 minutes after oligomycin (5 μ g/ml) (E). Data shown are from 3 randomly selected x40 objective fields per kidney slice, from a total of 3 slices per experiment (** $p < 0.001$).

(Feldkamp *et al.*, 2005a). Another possibility is that the lower potential reflects an increase in ATP turnover in PT compared with DT, in which case oligomycin may increase the potential in the PT more than in the DT. However, oligomycin (an inhibitor of ATPase and ATP synthase activity) addition (5 μ g/ml) had no significant effect on potential after 30 minutes and did not alter the differences in $\Delta\psi_m$ between PT and DT (Figure 4.2E).

4.3 TMRM signal remains higher in the distal tubule in the presence of efflux pump inhibitors

Both rhodamine 123 and TMRM are substrates for the MDR (Neyfakh, 1988). Extrusion of the dyes from the cells via the MDR could therefore provide an alternative explanation for differences in TMRM signal between tubule types. Verapamil, an inhibitor of MDR, enhanced loading of TMRM in both the PT and DT, with the fluorescence intensity rising in the PT from a mean value per x40 objective field of 357 ± 11 A.U. before verapamil, to 522 ± 65 A.U. after verapamil ($p < 0.03$); in the DT, rising from a mean of 613 ± 46 A.U. to 1054 ± 165 A.U. after verapamil ($p < 0.03$; in each case 3 randomly selected fields were imaged per slice, from a total of 3 slices). However, verapamil did not affect the clear signal differences between the PT and DT (Figure 4.3A). Cimetidine, an inhibitor of renal organic cation transporters (Wright, 2005), did not have any significant effect on TMRM loading (Figure 4.3B). Taken together, these results provide more evidence to support the notion that differences in TMRM signal between tubule types represent genuine differences in $\Delta\psi_m$, rather than artefact.

4.4 Mitochondrial membrane potential is better maintained in the distal tubule during anoxia

The PT is particularly vulnerable to ischaemia *in vivo*. By using an on-stage perfusion system, the effects of chemical anoxia (a model of *in vivo* ischemia) on mitochondrial function in renal tubules were imaged in real-time. Chemical anoxia was induced using a buffer (gassed with nitrogen rather than oxygen) containing

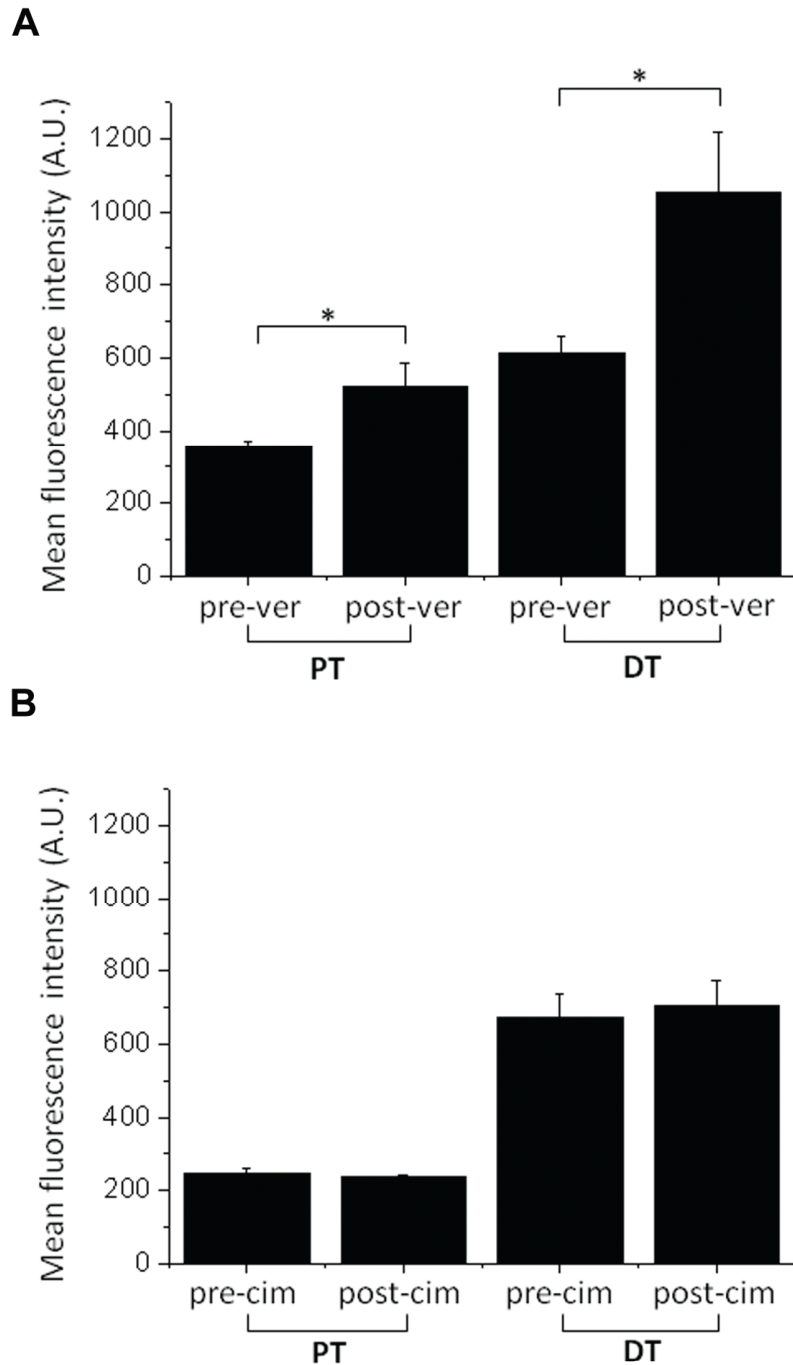


Figure 4.3. The effects of efflux pump inhibitors on TMRM signal in renal tubules. Loading of TMRM was enhanced by verapamil 10 μ M in both proximal and distal tubules (A), but not by cimetidine (B). Values given are mean (\pm S.E.) signal per x40 objective field, from 3 medullary ray regions (randomly selected using the bright field setting) per slice; from a total of 3 (verapamil) or 4 (cimetidine) slices per experiment (* $p < 0.03$).

sodium cyanide (CN) 1mM, which competes for oxygen at complex IV of the RC. $\Delta\psi_m$ in PT mitochondria fell rapidly in response to inhibition of respiration (Figure 4.4A). However, in cells of the DT, $\Delta\psi_m$ fell very slowly and was then maintained at a plateau for long periods. Even after 1 hour of chemical anoxia DT mitochondria still maintained a significant potential, as shown by a further response to the uncoupling agent FCCP (which causes complete depolarization of $\Delta\psi_m$) (Figure 4.4B). Values were normalised from 1 (the starting fluorescence signal) to 0 (the fluorescence signal post FCCP, taken as complete depolarization of $\Delta\psi_m$, i.e. 0mV), in order to make meaningful comparisons between PT and DT, as they have different resting TMRM signal intensities.

These differences between PT and DT were abolished by inhibition of the ATPase with oligomycin (5 μ g/ml), after which $\Delta\psi_m$ fell rapidly and completely depolarized in DT cells in response to chemical anoxia. This suggests that the ATPase in mitochondria of DT cells has a much greater capacity to pump protons - maintaining the membrane potential when the RC is compromised - compared with PT mitochondria.

4.5 ROS production is increased to a greater extent in proximal tubules by complex I inhibition

Mitochondria are a major source of intracellular ROS, which may play an important role in renal pathology. I measured rates of ROS generation in tubules using HET, which becomes fluorescent on oxidization by O_2^- . Hence, in cells producing ROS, HET fluorescence signal increases with time and the rate of increase is proportional to the rate of ROS production. Since the ROS-dependent oxidized product of HET binds to DNA, most of the signal change observed occurs in the nucleus; therefore, I measured the mean rate of fluorescence intensity change in the nuclei of renal tubular cells. Thus, the data acquired reflect the total rate of ROS production *per cell* and are not normalized to intracellular mitochondrial mass (see later discussion – ‘Reactive oxygen species production in renal tubules’). Unfortunately, I was not able to achieve adequate loading with the dye mitoxox in the slice model, so could not directly measure mitochondrial ROS production.

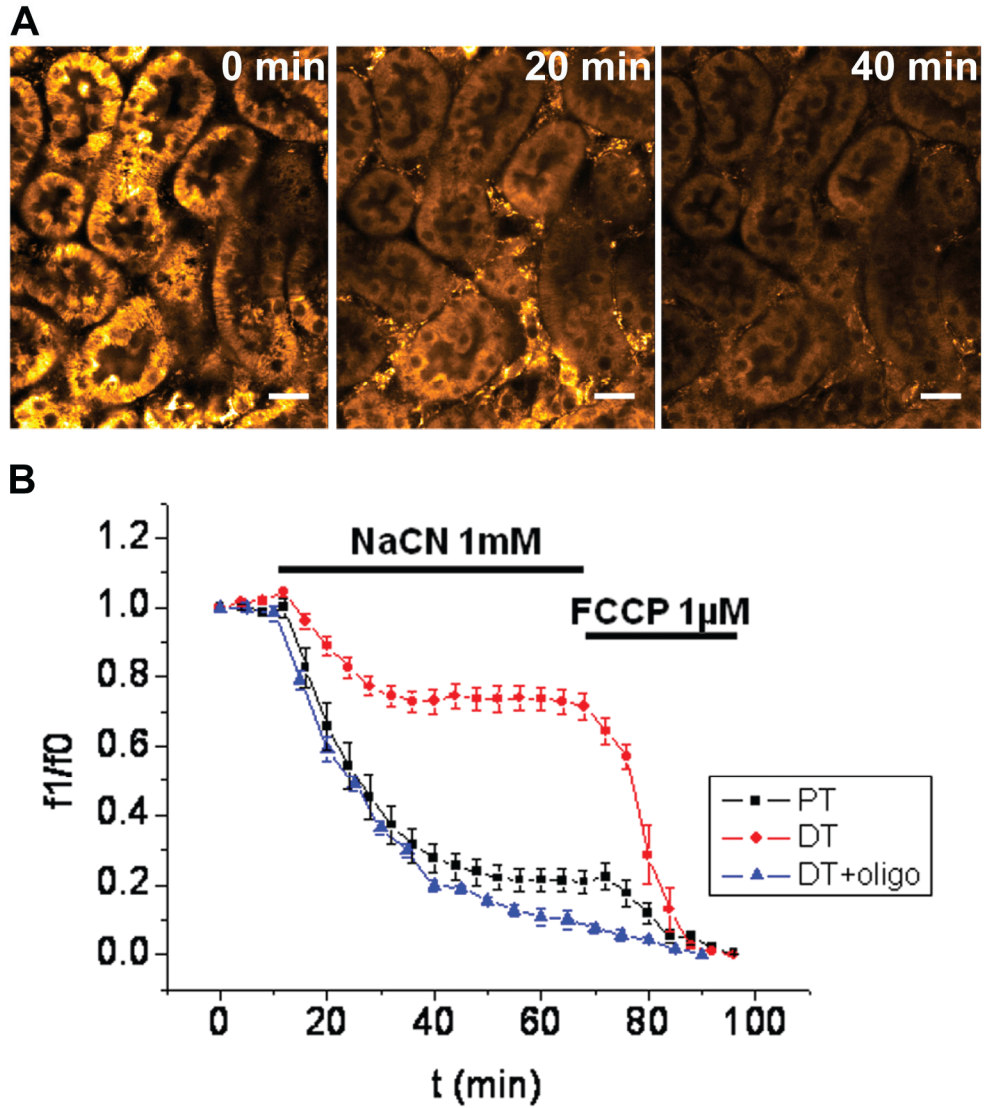


Figure 4.4. The effect of respiratory chain inhibition on mitochondrial membrane potential in renal tubules. Proximal tubules loaded with TMRM showed rapid depolarization of $\Delta\psi_m$ post chemical anoxia (**A**) (Scale bar = 20 μ m). In the distal tubule the decrease was slower, and $\Delta\psi_m$ was not completely depolarized after 60 minutes of anoxia (**B**). However, in the presence of oligomycin (5 μ g/ml), $\Delta\psi_m$ depolarized rapidly in distal tubular cells, when exposed to anoxia. Results displayed are mean (\pm S.E.) signal per tubule, from a total of 15 proximal tubules, 15 distal tubules without oligomycin and 29 distal tubules with oligomycin, from 3 separate slices for each experiment. The data were normalised from 1 (value at t=0, taken as resting $\Delta\psi_m$) to 0 (minimum value post FCCP, taken as 0mV).

Under resting conditions the basal rate of HET oxidation was higher in the PT cells (mean fluorescence intensity increase hour^{-1} $+70.9\% \pm 4.6$; $n=44$ cells from 4 separate slices) than in the DT cells (mean increase hour^{-1} $+34.3\% \pm 4.3$; $n=35$ cells from 4 separate slices, $p<0.01$) (Figure 4.5A).

Within mitochondria, complexes I and III of the RC are thought to be the main sources of ROS. Exposure to $10\mu\text{M}$ rotenone (an inhibitor of complex I of the RC) increased the rate of signal change in both tubule segments (Figure 4.5A and C), and the relative increase in the rate in the PT (mean rate post rotenone $501\% \pm 64$ of the control rate) was greater than that in the DT cells (mean rate post rotenone $162\% \pm 45$ of the control rate, $p<0.001$); consistent with a much bigger relative increase in ROS production in response to rotenone in the PT than in the DT. This observation could be explained by differences in either the amount or resting redox state of complex I in the two tubule segments (see below – ‘Autofluorescence measurements reveal mitochondria in the proximal tubule are in a more oxidised state’).

In an attempt to isolate the mitochondrial contribution to ROS production in the tubules, I repeated the experiments in the presence of apocynin $500\mu\text{M}$ (an inhibitor of NADPH oxidase, another major source of intracellular O_2^-). The HET fluorescence signal was greatly reduced in the presence of apocynin (implying significant NADPH oxidase activity at rest) and the microscope settings had to be adjusted to bring the signal back within the working range. In the presence of apocynin there was no longer any significant difference in the rate of signal change between PT cells (mean fluorescence intensity increase hour^{-1} $42.2\% \pm 3.8$; $n=35$ cells from 3 separate slices) and DT cells (mean increase hour^{-1} $51.3\% \pm 3.6$; $n=31$ cells from 3 separate slices, $p=0.14$). However, in response to rotenone there was again a significantly greater increase in the rate of signal change in the PT (mean rate post rotenone $703\% \pm 68$ of control rate) than in the DT (mean rate post rotenone $269\% \pm 74$, $p<0.001$) (Figure 4.5B); consistent with a bigger relative rise in the rate of ROS production in the PT in response to rotenone.

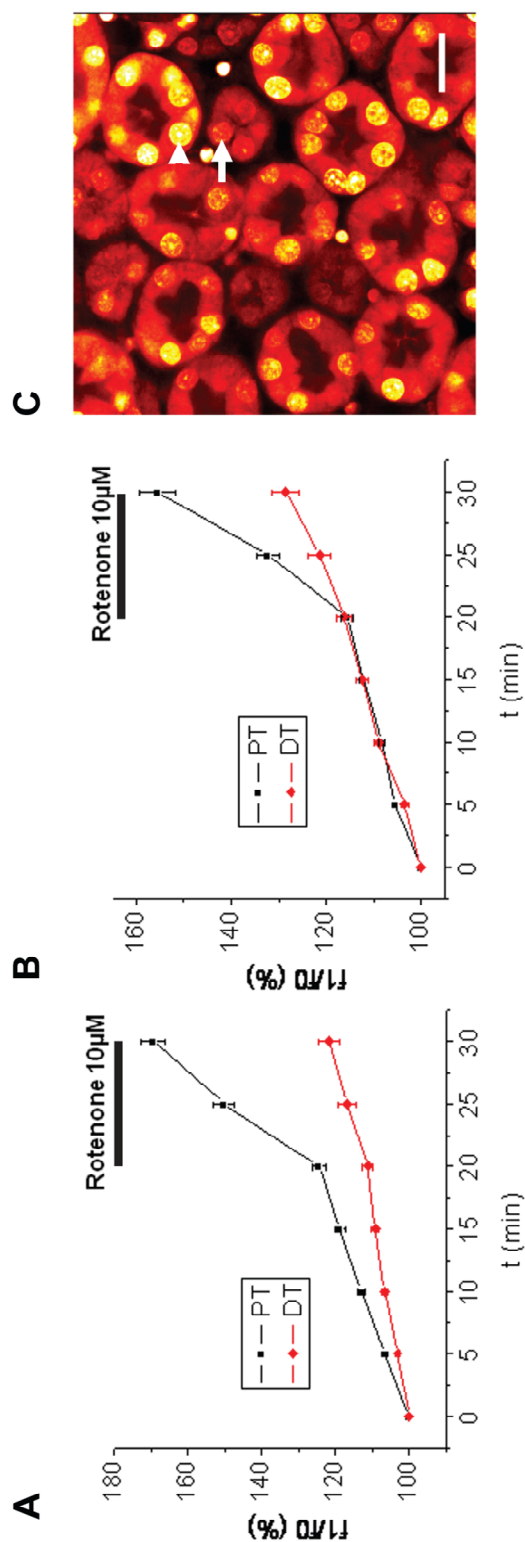


Figure 4.5. The rate of ROS production in renal tubules. Fluorescence signal increased over time in the nuclei of cells in kidney slices loaded with HET, due to the production of ROS, and the basal rate of ROS production was higher in the proximal than distal tubules (**A**). After 20 minutes, rotenone 10 μ M was added to the perfusate. This caused a relatively greater increase in the rate of ROS production in the proximal tubules than in the distal tubules. Values given are mean (\pm S.E.) fluorescence signal per nuclei (expressed as a percentage of the starting signal), from a total of 54 proximal and 26 distal tubular cells, from 4 separate slices. Experiments were repeated in the presence of apocynin 500 μ M, an inhibitor of NADPH oxidase. As expected, the rates of ROS production were lower, so different microscope settings were used. Under these conditions, the basal rate of ROS production was found to be similar in both tubule types, but again a relatively greater rise in the rate of ROS production was observed in proximal tubules in response to rotenone (**B**); mean values given are from a total of 37 proximal and 31 distal tubular cells, from 3 separate slices. A representative image is depicted of the HET signal 10 minutes post rotenone (in the absence of apocynin) (**C**). (Arrowhead: PT, Arrow: DT. Scale bar = 20 μ m).

4.6 Glutathione levels are higher in the proximal tubule than distal tubule

Steady state ROS production depends on a balance of ROS metabolism and catabolism. GSH is a major intracellular anti-oxidant able to reduce ROS. MCF forms a fluorescent adduct with GSH in a reaction catalyzed by GST, allowing measurement of GSH cellular content. A steady state fluorescence signal was reached by 50 minutes and the signal was significantly greater in the PT (mean fluorescence intensity increase per tubule after 60 minutes $+48.8\% \pm 2.5$, $n=40$ tubules from 4 separate slices) than in the DT (mean increase per tubule $+17.0\% \pm 3.6$, $n=26$ tubules from 4 separate slices, $p<0.001$) (Figure 4.6). These findings are consistent with a higher level of GSH in the PT than DT.

4.7 Autofluorescence measurements reveal that mitochondria in the proximal tubule are in a more oxidized state

Changes in $\Delta\psi_m$ and ROS production may reflect differences in oxygen consumption that might in turn reflect changes in the redox state of NADH and $FADH_2$, which are the substrates for complexes I and II of the RC, respectively. At 720nm excitation, the autofluorescence signal emitted between 435-485nm (blue) arose predominantly from mitochondrial NADH, while at 458nm excitation the signal emitted between 500-550nm (green) arose partly from FAD^{2+} . These interpretations were supported by the typical pattern of the signal, consisting of striations of signal at the basal pole of the cell, matching the known distribution of mitochondria in the tubule and the signal seen with TMRM; further confirmation was provided by the characteristic changes in signal observed in response to either RC inhibition or uncoupling (Figure 4.7A-F).

The resting NADH and FAD^{2+} fluorescence signals were calibrated in relation to the full available dynamic ranges, which were defined by inducing a maximally reduced state with a RC inhibitor (CN), and a maximally oxidized state with a RC uncoupler (FCCP). This allowed me to ‘calibrate’ the resting signal as a redox index. I

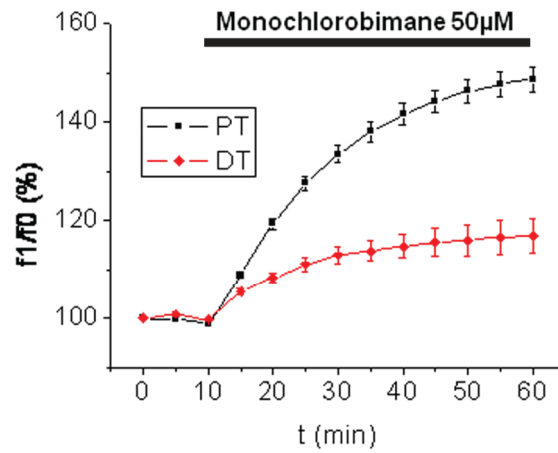
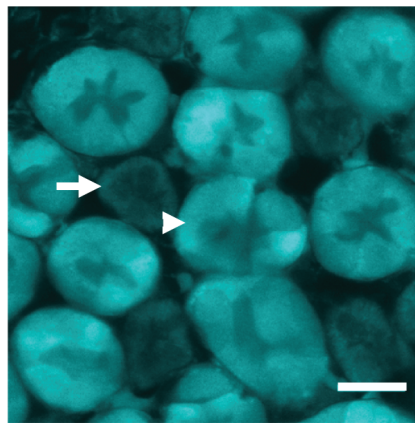
A**B**

Figure 4.6. Glutathione levels in renal tubules. Levels of the anti-oxidant glutathione were higher in the proximal than distal tubules, as measured using the fluorescent indicator monochlorobimane **(A)**. Steady state was reached after 50 minutes. Values given are mean (\pm S.E.) signal per tubule, from a total of 40 proximal and 26 distal tubules, from 4 separate slices. A representative image after 50 minutes is depicted **(B)**. (Arrowhead: PT, Arrow: DT. Scale bar = 20 μ m).

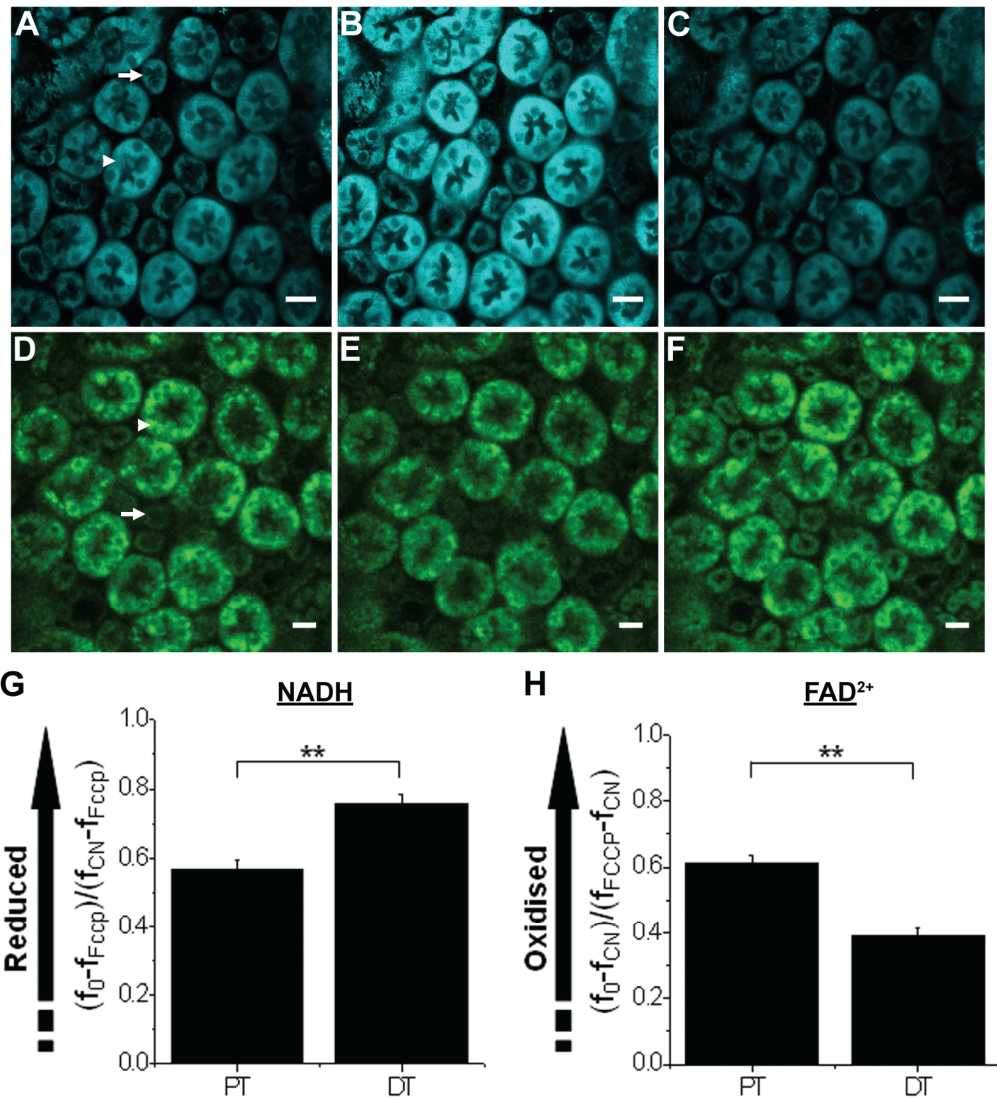


Figure 4.7. Mitochondrial redox state in renal tubules. Mitochondrial NADH was excited at 720nm (A). The identity of the signal was confirmed by an increase in response to the respiratory chain blocker cyanide (B) and a decrease in response to the respiratory chain uncoupler FCCP (C). FAD²⁺ was excited at 458nm (D), and reciprocal changes to NADH were observed in response to cyanide (E) and FCCP (F). (Arrowhead: PT, Arrow: DT. Scale bar = 20μm). Calibration of the NADH and FAD²⁺ signals with cyanide (maximally reduced state) and FCCP (maximally oxidized state) revealed that in the resting state mitochondria were more oxidized in proximal than distal tubules (G-H). Values given are mean (± S.E.) per tubule; from a total of 38 proximal and 29 distal tubules, from 5 separate slices, for NADH, and 43 proximal and 42 distal tubules, from 4 separate slices, for FAD²⁺ (** p<0.001).

generated single z-stack images at: (i) time zero; (ii) post 10 minutes of perfusion with CN⁻ 1mM, and following a 10-minute washout period; (iii) post 10 minutes of perfusion with FCCP 1μM.

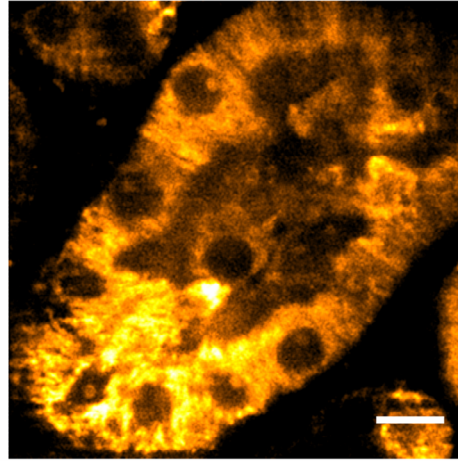
Using this method, I found the resting mitochondrial NADH pool to be in a more oxidized state in PT (mean value $[f_0 - f_{\text{FCCP}}]/[f_{\text{CN}} - f_{\text{FCCP}}]$ 0.57 ± 0.03 ; n=38 tubules from 5 separate slices) than in DT (mean value $[f_0 - f_{\text{FCCP}}]/[f_{\text{CN}} - f_{\text{FCCP}}]$ 0.76 ± 0.02 ; n=29 tubules from 5 separate slices, $p < 0.001$). Furthermore, this was mirrored by the finding of a more reduced FAD²⁺ pool in the DT (mean value $[f_0 - f_{\text{CN}}]/[f_{\text{FCCP}} - f_{\text{CN}}]$ 0.39 ± 0.02 , n=42 tubules from 4 separate slices) than in PT (mean value $[f_0 - f_{\text{CN}}]/[f_{\text{FCCP}} - f_{\text{CN}}]$ 0.61 ± 0.03 , n=43 tubules from 4 separate slices, $p < 0.001$) (Figure 4.7G-H). Overall, these data suggest that mitochondria in the PT are in a more oxidized state at rest, which might explain why a relatively greater response in ROS production was observed in this nephron segment following inhibition (and reduction) of complex I by rotenone.

4.8 Calcium signalling in the renal slice

As part of the overall aim to investigate differences in aspects of mitochondrial function in different tubule types, it was also intended to explore the effects of MD on Ca²⁺ signalling in different nephron segments; as a possible mechanism of how MD may lead to impaired PT transport. In order to visualise changes in intracellular Ca²⁺, slices were loaded with the fluorescent Ca²⁺ indicator Rhod-2 and excited at 900nm. Dye loading appeared to be predominantly in the mitochondria (Figure 4.8A), as the images resembled those of TMRM and NADH. Extracellular ATP is a physiological agonist that is known to initiate Ca²⁺ signals in the PT, via activation of purinergic receptors (Yamada *et al.*, 1996). In slices loaded with Rhod-2 an oscillating Ca²⁺ signal was elicited in PT cells in response to perfusion with a solution containing ATP 100μM (Figure 4.8B).

Unfortunately, due to difficulties in routinely achieving satisfactory dye loading with Rhod-2, it was not possible to create a reliable and reproducible assay of physiological Ca²⁺ signalling in the PT, which could then be used to explore the

A



B

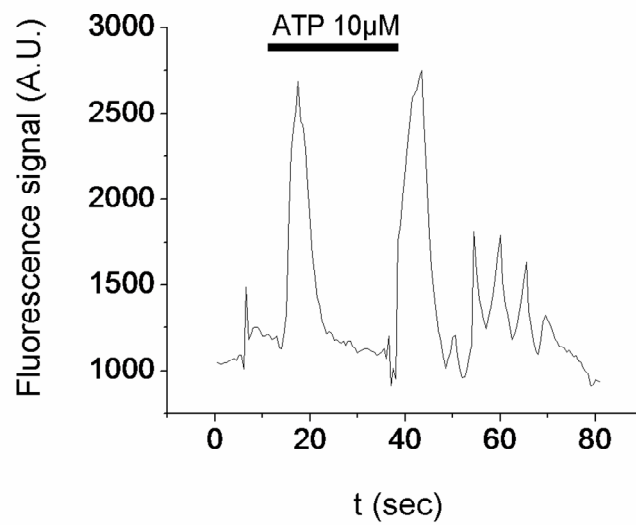


Figure 4.8. Calcium signalling in the proximal tubule, measured using Rhod2. The Ca^{2+} -sensitive dye Rhod-2 was loaded into live kidney slices and excited at 900nm. The emitted signal localised to mitochondria **(A)** (Scale bar = 10μm). An oscillating Ca^{2+} signal was recorded in response to the physiological agonist ATP 10μM **(B)**.

effects of MD and make comparisons to the DT. Other Ca^{2+} -sensitive dyes (Fluo-4 and Fura-2) were also tried as part of this work, as were agents that inhibit potential dye efflux pumps in the cell membrane (probenecid and sulfinpyrazone); however, none of these measures were effective.

4.9 Discussion

Multi-photon imaging of the kidney *in vivo* or *in vitro* is a powerful and relatively new approach to understanding basic renal physiology (Molitoris & Sandoval, 2005; Sipos *et al.*, 2007). Imaging of live, intact kidney slices is a useful technique to access all major nephron segments within the cortex and medulla (which is not possible *in vivo*), as well as to investigate mitochondrial function in what is a highly aerobic and heterogeneous tissue. Using this approach I have identified differences in $\Delta\psi_m$, ROS production, GSH levels and NADH/FAD²⁺ redox state between the PT and DT, at rest and in response to toxic stimuli.

4.9.1 Differences in mitochondrial membrane potential between proximal and distal tubules

I have observed a large and consistent difference in TMRM signal between the PT and DT, suggesting a difference in resting $\Delta\psi_m$. Furthermore, the TMRM signal appeared to vary between different sub-sections of the PT: it was larger in convoluted compared with straight segments, though not as large in either sub-segment when compared with the DT. I have tried to exclude a differential role of dye extrusion by transporters in the PT and DT, since I did not observe any changes in signal with cimetidine, an inhibitor of organic cation transport. Moreover, although verapamil (an inhibitor of the MDR) enhanced loading of TMRM, it did so in both PT and DT, and it did not affect the striking difference in signal between PT and DT; strongly suggesting a real difference in $\Delta\psi_m$. Another possible confounding factor affecting TMRM measurements would be a difference in ΔpH between the PT and DT mitochondria. PMF is ultimately responsible for driving ATP synthase activity and it consists of the sum of both $\Delta\psi_m$ and ΔpH ; it is therefore theoretically possible that PMF could be equal between PT and DT mitochondria if ΔpH was

much greater in the PT. However, experiments using nigericin (an agent that converts ΔpH to $\Delta\psi_m$ [by exchanging H^+ for K^+ across the inner mitochondrial membrane], so $\Delta\psi_m$ effectively then equals the PMF) in isolated tubules have shown that ΔpH makes very little contribution to the total PMF in PT mitochondria (Feldkamp *et al.*, 2009). This further supports the notion that variations in TMRM signal between tubule types reflect genuine differences in PMF.

Another possible confounding factor affecting mitochondrial TMRM uptake is any difference in cell membrane potential between the PT and DT. The concentration of TMRM in the cytosol ($[\text{TMRM}]_{\text{in}}$), is determined by the cell membrane potential and the extracellular TMRM concentration ($[\text{TMRM}]_{\text{out}}$), according to the Nernst equation:

$$\text{Cell membrane potential} = -61 \times \log_{10}([\text{TMRM}]_{\text{in}}/[\text{TMRM}]_{\text{out}})$$

Given a typical cell membrane potential of -60mV , it can be seen that $[\text{TMRM}]_{\text{in}}/[\text{TMRM}]_{\text{out}}$ will equal ~ 10 , but variations in membrane potential between different cell types will change this value, and therefore the concentration of TMRM to which mitochondria are exposed ($[\text{TMRM}]_{\text{in}}$). I did not attempt to make measurements of cell membrane potential in this project; however, published data indicate that there are no major differences between cells of PT and DT (Koeppen *et al.*, 1983).

Experiments were performed at room temperature, due to excessive movement of tissue at 37°C , which made it impossible to maintain the original focal plane in timed series experiments. This is a potentially confounding factor, as lowering temperature alters the permeability of cell membranes (Whittam & Willis, 1963), and the activity of ion transporters such as the Na^+/K^+ -ATPase (Willis & Ma, 1969). Accordingly, previous studies with renal cortical slices have shown that rates of ion transport and oxygen consumption are lower at 25°C than at 37°C (Whittam & Willis, 1963). Importantly, the effects of altering temperature may be more pronounced on some cellular processes than others; for example, in kidney cortical slices, Na^+/K^+ -ATPase activity appears to be more sensitive to a reduction in temperature than K^+ transport and Na^+ -sensitive respiration, especially in non-hibernating animals such as the rat

(although these effects were most pronounced at values below normal room temperature) (Willis & Ma, 1969).

Interestingly, differences in PT and DT signal have recently been reported *in vivo* during an investigation of the excretion of a fluorescent substrate for organic cation transport in the kidney (Horbelt *et al.*, 2007). Additionally, a study of $\Delta\psi_m$ in live kidney slices using confocal imaging of tissue loaded with tetramethyl rhodamine ethyl ester (TMRE) showed heterogeneity in signal among different cell types (Plotnikov *et al.*, 2007); but the investigators did not comment on the nature of these differences.

4.9.2 Differences between proximal and distal tubules in response to chemical anoxia

That mitochondrial function differs between the PT and DT is also suggested by differences in their respective responses to chemical anoxia (a model of *in vivo* ischaemia). It was demonstrated previously in isolated tubules that mitochondria depolarize rapidly in the PT in response to hypoxia (Feldkamp *et al.*, 2005b), and this deficit is maintained even after reoxygenation (Weinberg *et al.*, 2000). I found that in contrast to the PT, $\Delta\psi_m$ is surprisingly well maintained during anoxia in the DT; it is maintained at a plateau value for over 60 minutes, which is attributable to a reverse in activity of the ATP synthase (ATPase activity). This may be due to increased capacity for glycolytic ATP production. Alternatively, it may relate in part to differences in the expression level of the mitochondrial regulatory protein IF1 (see later – ‘Variation in mitochondrial function along the nephron’).

4.9.3 Reactive oxygen species production in renal tubules

ROS are thought to have wide-ranging physiological and patho-physiological effects in the kidney. I observed an increased basal rate of ROS production per cell in PT compared with DT. Given the higher resting $\Delta\psi_m$, it might be expected that mitochondrial ROS production would be greater in the DT; however, it is important to stress that I measured total cellular ROS production and this was not adjusted for

intracellular mitochondrial mass. Although the density of mitochondria in DT is generally a little higher than in PT, the ratio of mitochondrial volume to nuclear volume is much greater in the PT, because the cells are larger (Pfaller & Rittinger, 1980); therefore, it is likely that basal ROS production *per mitochondrion* is lower in the PT.

HEt is predominantly oxidized by O_2^- , and regional differences in the origins of O_2^- production (e.g., mitochondrial *versus* NADPH oxidase) in the kidney have been reported using tissue homogenates (Zou *et al.*, 2001); however, I observed differences in ROS production between different cell types within the same region of the kidney. The expression of different NADPH subunits varies among different tubule types (Gill & Wilcox, 2006), and this may therefore be an explanation for differences in basal O_2^- production. Indeed, in the presence of an NADPH oxidase inhibitor (apocynin) I did not observe significant differences in basal ROS production between PT and DT.

Although non-mitochondrial sources may contribute significantly to basal rates of ROS production in the renal tubular cells, the striking rise in ROS production observed following rotenone was likely to represent increased mitochondrial generation, given the known actions of rotenone on complex I of the RC (Hirst *et al.*, 2008). The fact that a much greater rise in ROS production occurred in the PT than the DT following rotenone exposure could be explained, at least in part, by a greater mitochondrial mass, per cell, in the PT. However, using an established calibration method (Duchen *et al.*, 2003), I have also shown that mitochondria in the PT are more oxidised at rest. Inhibition of complex I of the RC by rotenone is more likely to produce a greater change in the rate of ROS production in mitochondria that are in a more oxidized state, than in a more reduced state (Kushnareva *et al.*, 2002). The finding of a large increase in ROS production in the PT in response to inhibition of complex I could be of relevance in understanding the pathogenesis of some forms of FS, as evidence suggests that the activity of this complex is specifically impaired in cystine loaded renal tubules (a model of cystinosis) (Foreman *et al.*, 1995). Clearly, it would be interesting to investigate rates of ROS production in this and other models of FS.

ROS have been extensively implicated in the pathogenesis of ischaemic AKI and ATN (for review see (Nath & Norby, 2000)). Studies using mitochondria isolated from the cortex of rat kidneys revealed approximately 1.5 and 4 fold increases in ROS production in mitochondria derived from ischaemic and ischaemia-reperfused organs, respectively (Gonzalez-Flecha & Boveris, 1995). Furthermore, giving rats exogenous SOD appeared to be protective in a model of ischaemic AKI (Baker *et al.*, 1985). However, it should be noted that others have disputed the protective effects of anti-oxidants in ischaemic AKI (Gamelin & Zager, 1988), and anti-oxidants have yet to be proven to be beneficial in human AKI. Nevertheless, learning more about ROS production in the kidney in more detail is likely to improve our understanding of renal diseases (including those related to MD), and could lead to novel therapeutic strategies in the future. More recently it has been appreciated that ROS are also likely to have physiological roles in the kidney. For example, there is evidence that O_2^- can stimulate NaCl reabsorption in the TALH by increasing Na-K-2Cl co-transport (Juncos & Garvin, 2005), and O_2^- may also act as a mediator of tubulo-glomerular feedback at the macula densa (Liu *et al.*, 2007).

Elucidation of the mitochondrial contribution to ROS generation within renal tubular cells would be enhanced by fluorescent dyes that are specifically targeted to the mitochondria, such as mitosox; however, preliminary experiments using this dye in the rat kidney slice model revealed that the loading was generally poor, with a weak fluorescent signal that was insufficient to make meaningful measurements.

4.9.4 Glutathione in renal tubules

Using MCB, I found that levels of the anti-oxidant GSH were significantly higher in the PT than DT, which is consistent with previously published biochemical data (Brehe *et al.*, 1976). MCB is metabolized by GST and subtypes of this enzyme may vary along the rat nephron; the class α subtypes are selectively expressed in the PT and the class μ and class π subtypes in the DT (Rozell *et al.*, 1993). Differences in GST subtype expression among tubular segments could affect the rate of increase in fluorescence observed with MCB; however, I was unable to explore this further as

there are no selective inhibitors of the different GST subtypes. I therefore only used measurements of MCB fluorescence after a steady state signal was achieved, which reflects the total amount of GSH within cells, rather than the rate of GSH and MCB metabolism by GST.

4.9.5 Calcium dyes do not load effectively in the kidney slice model

The reasons for poor Ca^{2+} dye loading in the kidney slices are unclear, but may include extrusion of dyes from the renal cells via organic anion transporters (OATs). This is a well recognised phenomenon in various cell lines, where inhibitors of OATs, such as probenecid, can improve loading (Di *et al.*, 1990). However, I did not find any significant improvement in dye loading in the slices with probenecid. Extracellular esterases may cleave AM-ester dyes before they can enter cells and thus prevent loading (although another AM-ester dye [calcein] did load well into kidney slices). As new technologies in Ca^{2+} imaging become available, for example, transgenic animals expressing Ca^{2+} sensitive molecules (Tallini *et al.*, 2006), I may be able to re-explore this in the future.

Chapter 5 – Results: Subclinical renal tubular disease in patients with mitochondrial cytopathy

5.1 Demographics and clinical features

Twenty-two adult patients with mitochondrial cytopathy were recruited to the study. Demographics and clinical features including phenotype and underlying mutations are depicted in Table 5.1. The median age at recruitment was 41 years (range 18-68), and the median time since diagnosis was 20 years (range 3-53). A range of phenotypes were observed, with the most prevalent being Kearns-Sayre syndrome (and other myopathies) and progressive external ophthalmoplegia (PEO). Generally, the phenotypes reflected the types of mitochondrial cytopathy where survival into adulthood is observed, although no patients with the relatively common MELAS syndrome were recruited, and 2 patients with Leigh syndrome (often fatal in childhood/adolescence) were included. The presence of a pathological mutation affecting either mtDNA or nDNA was confirmed in all patients, with the exception of one who was included in the study on the basis of a typical phenotype of mitochondrial disease and clear biochemical evidence of decreased RC function. A range of underlying pathological genetic mutations from either blood or muscle were observed, the most common being mtDNA point mutations (n=13), followed by mtDNA deletions (typically associated with Kearns-Sayre and PEO) (n=5), and nDNA (poly) mutations (n=3). The most common point mtDNA mutation was A3243G in the TL1 gene.

A total of 10 patients had abnormal features on muscle histology (defined as the presence of one or more of: ragged red fibres, COX negative fibres, increased SDH staining and abnormal EM). RC function tests were performed on muscle tissue in 5 patients using standard spectrophotometric techniques (Department of Biochemistry, Institute of Neurology, UCL, UK); 4 patients had RC complex activities within normal limits, whilst 1 had clear decreases in the activity of complexes I and IV. The median serum creatinine was 65µmol/l (range 35-100, normal<120).

Phenotype	Age	Mutation	Abnormal Histology	RC function	SCr	RBP (n<18)	NAG (n<28)	Alb (n<2.5)	BP	DM	Rx
3243 carrier	55	TL1 A3243G blood		impaired	61	9.2	33.1	U	155/80	n	
Ataxia and deafness	38	TS1 7472insC blood			NA	12.9	20.0	U	NA	n	
Myopathy, neuropathy, deafness	34	Biochemical defect	y		88	658.1	46.3	4.07	150/70	n	
Kearns sayre	44	mtDNA deletion muscle	y		40	12.2	69.4	1.09	120/70	y	NSAID
Kearns sayre	25	mtDNA deletion muscle	y		36	13.3	37.9	1.05	140/80	n	statin
Kearns sayre	56	mtDNA deletion muscle	y		71	9.0	79.6	U	120/60	y	
Kearns sayre	30	TL1 A3243G blood			NA	21.7	31.1	U	112/62	n	
Kearns sayre	24	TL1 A3243G blood			38	15.1	38.0	1.69	98/60	n	
Leber's optic atrophy	25	ND4 muscle			98	3.8	9.7	4.83	NA	n	
Leigh	22	ND5 muscle			81	3.1	21.4	0.81	120/80	n	
Leigh	19	ATP6 T9176C muscle			NA	5.7	20.5	U	NA	n	
MERFF	58	TK A8344G muscle			35	120.0	68.4	3.70	130/75	n	
MERFF	32	TK A8344G muscle			74	8.7	73.0	0.72	110/75	n	valproate
MIDD, myopathy, neuropathy	50	TL1 A3243G blood	y	normal	65	7.6	74.2	1.17	124/70	y	
NARP	26	ATP6 T8993C blood	y		NA	1.8	14.3	0.77	NA	n	
Occipital blindness, ataxia, myoclonus	18	Poly			55	21.7	47.8	7.00	100/60	n	
PEO	59	Poly	y	normal	58	15.8	50.7	0.91	90/40	n	
PEO	68	mtDNA deletion muscle	y		NA	14.4	26.3	0.41	90/50	n	
PEO	56	ND4 muscle	y	normal	65	18.7	199.4	39.72	130/70	y	statin, ACEI
PEO and myopathy	56	mtDNA deletion muscle			100	51.6	17.6	1.71	130/70	n	
PEO and myopathy	52	TL2 muscle			NA	42.5	62.1	1.67	110/60	n	
SANDO	44	Poly	y	normal	81	16.8	34.9	1.89	150/100	n	

Table 5.1. Urinary results in patients with mitochondrial cytopathy. Abnormal histology relates to previous muscle biopsy. RC=respiratory chain, SCr=serum creatinine (μmol/l), RBP=urinary retinol binding protein/creatinine (μg/mmol), NAG=urinary N-acetyl-beta-D-glucosaminidase/creatinine (μmol/hr/mmol), Alb=urinary albumin/creatinine (mg/mmol), BP=blood pressure, DM=diabetes mellitus, Rx=potentially nephrotoxic therapy, MERFF=myoclonic epilepsy with ragged red fibres, MIDD=maternally inherited diabetes and deafness, NARP= neuropathy, ataxia and retinitis pigmentosa, PEO=progressive external ophthalmoplegia, SANDO= sensory ataxic neuropathy, dysarthria and ophthalmoplegia, Poly=polymerase gamma, NA=not available, U=undetected, NSAID=non-steroidal anti-inflammatory drug, ACEI=angiotensin converting enzyme inhibitor.

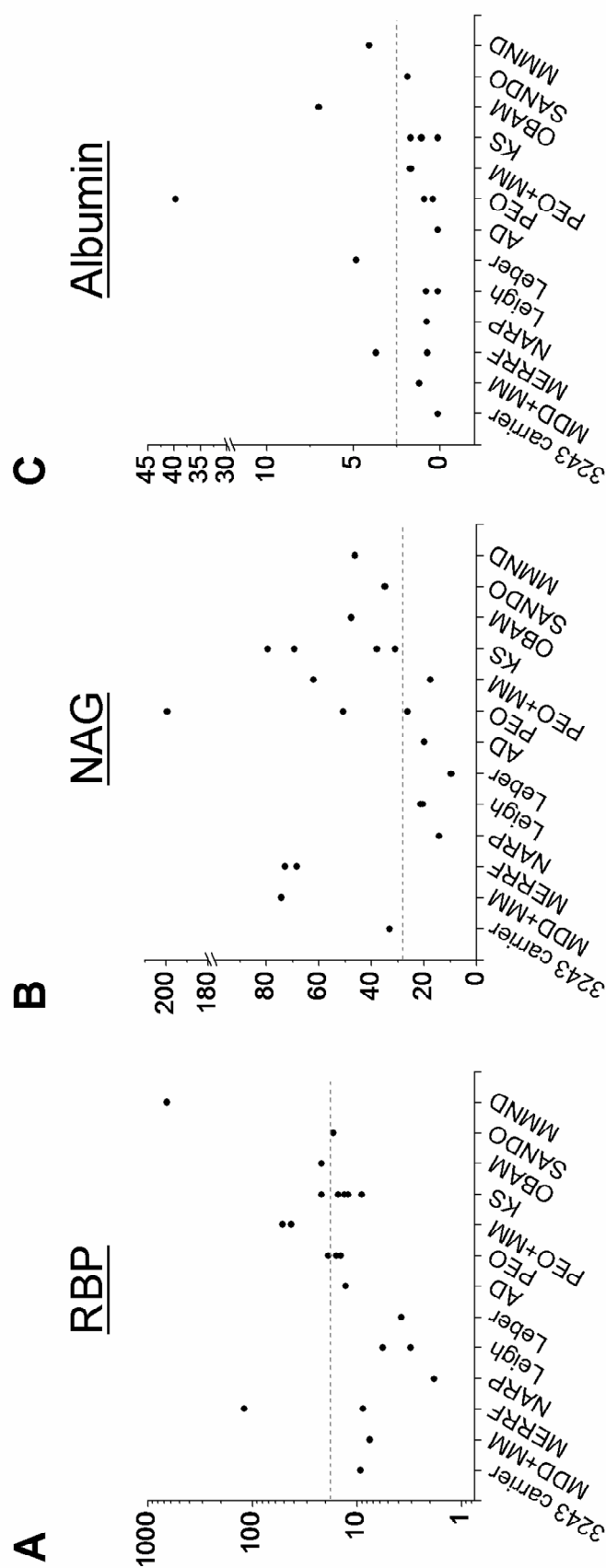
In terms of potentially confounding factors on renal function, median blood pressure was 120 mmHg systolic (range 90-155) and 70 mmHg diastolic (40-100), and a total of 3 patients had elevated blood pressure ($>140/90$). Diabetes had previously been diagnosed in 4 patients, and 4 patients were taking drugs that might affect renal function.

5.2 The prevalence of subclinical proteinuria is high in adult patients with mitochondrial cytopathy

The excretion of $U_{RBP/C}$, $U_{NAG/C}$ and $U_{A/C}$ by adult patients with mitochondrial disease is depicted according to clinical phenotype (Figure 5.1) and underlying genotype (Figure 5.2). Median $U_{RBP/C}$ was $13.8\mu\text{g}/\text{mmol}$ (range 1.8-658.1, normal <18), median $U_{NAG/C}$ was $38.0\mu\text{mol}/\text{hour}/\text{mmol}$ (range 9.7-199.4, normal <28) and median $U_{A/C}$ was $1.07\text{mg}/\text{mmol}$ (range 0.1-39.72, normal <2.5 [urinary albumin levels that were below the level of detection of the assay were assigned the value of 0.1]).

In total, 7/22 patients (32%) had elevated $U_{RBP/C}$ values above the normal range, across a range of phenotypes (1/2 MERFF, 1/3 PEO, 2/2 PEO and myopathy, 1/5 Kearns-Sayre, 1/1 occipital blindness, ataxia and myoclonus and 1/1 biochemical defect). The highest value ($658.1\mu\text{g}/\text{mmol}$) was found in the patient with impaired RC function; this was considerably greater than the next highest value ($120.0\mu\text{g}/\text{mmol}$) observed in the other patients.

With regards to $U_{NAG/C}$, a total of 15/22 patients (68%) had an elevated value above the normal range. However, $U_{NAG/C}$ can be increased in diabetes and 4/22 of the patients were diabetic (all of whom had an elevated $U_{NAG/C}$). Amongst the non-diabetic patients 11/18 (61%) had a $U_{NAG/C}$ above the normal range (1/1 A3243G carrier, 1 mitochondrial myopathy, neuropathy and deafness [biochemical defect], 3/4 Kearns-Sayre, 2/2 MERFF, 1/1 occipital blindness, ataxia and myoclonus, 1/2 PEO, 1/2 PEO and myopathy and 1/1 SANDO). Overall, 16/22 patients (73%) had evidence of a proximal tubular disorder (defined as elevated $U_{RBP/C}$ and/or $U_{NAG/C}$), including 12/18 (67%) of the non-diabetics.



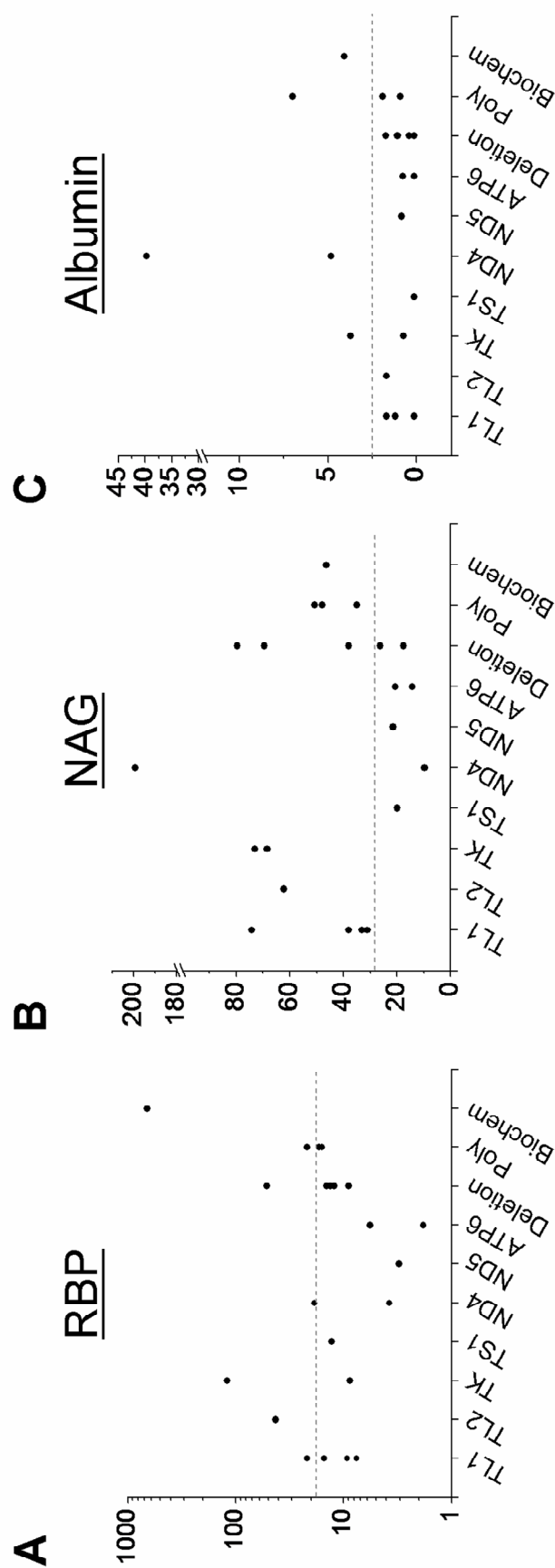


Figure 5.2. Urinary markers in patients with mitochondrial cytopathy, classified by underlying genetic mutation. The upper limits of the normal adult ranges are depicted as dotted lines for RBP ($n < 18 \mu\text{g}/\text{mmol}$) (A), NAG ($n < 28 \mu\text{g}/\text{hour}/\text{mmol}$) (B) and albumin ($n < 2.5 \text{mg}/\text{mmol}$) (C). All values are expressed as a ratio to urinary creatinine. Results are displayed according to genotype; sub-divided into mtDNA point mutations (in mtDNA genes TL1, TL2, TK, TS1, ND4, ND5 and ATP6), mtDNA single deletions (Deletion), rDNA mutations (Poly – polymerase gamma) and biochemical diagnosis (Biochem – no mutation identified but typical mitochondrial phenotype and impaired respiratory chain activity).

The proportion of patients with elevated $U_{A/C}$ (a marker of glomerular pathology) was 5/22 (23%). However, like $U_{NAG/C}$, $U_{A/C}$ can also be increased in diabetic patients, and the highest $U_{A/C}$ value observed in this study (39.72mg/mmol) was in a diabetic patient. Amongst the non-diabetic patients, 4/18 (22%) had a $U_{A/C}$ value above the normal range (1/1 mitochondrial myopathy, neuropathy and deafness, 1/1 Leber's optic atrophy, 1/1 MERFF and 1/1 occipital blindness, ataxia and myoclonus).

Unfortunately, due to the wide variety of phenotypes included in the study, and the relatively small number of patients within each group, I was unable to draw statistically significant conclusions about differences in either mean or median urinary values between phenotypes or genotypes.

5.3 Discussion

5.3.1 Subclinical proteinuria in adult patients with mitochondrial cytopathy

In this study I have demonstrated that the prevalence of subclinical renal proximal tubular disease is high in adult patients with mitochondrial cytopathy. Although a degree of albuminuria was also observed in the study participants, the prevalence was not as high as that of tubular dysfunction. This is of interest, as the literature to date had described predominantly cases of glomerular disease (FSGS) in adults with mitochondrial cytopathy, whilst children were reported to typically present with renal tubular disease (FS) (Hall *et al.*, 2008); as discussed earlier (chapter 1.4.6 – 'Differences between adults and children'), the reasons for these apparent differences are unclear.

To the best of my knowledge, this study is the first to systematically investigate renal phenotype in adults with mitochondrial disease, using sensitive markers of both PT and glomerular dysfunction. This might explain why I have found a different pattern of disease to that described in the literature to date, which has relied on isolated case reports of patients who have developed overt kidney disease detected by conventional clinical tests (such as serum creatinine and dipstick proteinuria). These

cases probably represent the more severe end of the spectrum, and it is likely from my results that there is a significant burden of undiagnosed subclinical renal tubular disease in adults with mitochondrial cytopathy. The true situation is further confounded by the difficulties that exist in reliably diagnosing mitochondrial disease, which mean that there are probably cases of unexplained kidney disease in the adult nephrology population that are not recognized to be due to MD.

Cases of PT dysfunction are often not detected in clinical practice until full-blown FS occurs, as screening tests for more subtle PT abnormalities (e.g. urinary LMWPs) are not yet widely available. In adult nephrology, in general, cases of FS are rare (with the exception of the recent concerns over TDF); hence, awareness of the possibility of underlying renal tubular dysfunction in adult patients with mitochondrial cytopathy is probably relatively low.

Unfortunately, I was not able to recruit sufficient numbers of patients to be able to draw any clear statistical conclusions about any associations between mitochondrial cytopathy phenotype, or underlying genetic mutation, and patterns of renal disease, and my findings are thus solely descriptive. There have been suggestions of possible associations between mtDNA deletion and PT dysfunction in children with mitochondrial disease (Martin-Hernandez *et al.*, 2005), but again the numbers involved were small and firm conclusions could not be reached. There does appear to be an emerging literature linking defective CoQ10 synthesis and nephrotic syndrome (glomerular disease) (Diomedi-Camassei *et al.*, 2007; Lopez *et al.*, 2006); the reasons for this remain unclear, but interestingly there is evidence for mitochondrial dysfunction in a hereditary form of nephrotic syndrome (congenital nephrotic syndrome of the Finnish type) (Holthofer *et al.*, 1999).

5.3.2 Difficulties of performing clinical studies related to mitochondrial cytopathy

Recruitment of adult patients with mitochondrial cytopathy is challenging, due to the relative rarity of the disease and the difficulty of establishing an exact genetic diagnosis in patients who have a clinical phenotype highly suggestive of mitochondrial disease. Although the entire mtDNA genome has been sequenced,

many nDNA genes affecting mitochondrial function remain to be discovered. However, with increasing awareness of the disease, and more convenient and readily available diagnostic techniques, the number of patients diagnosed with mitochondrial disease is likely to increase in the near future, potentially allowing more subjects to be recruited to renal studies such as this one. Furthermore, future studies on mitochondrial cytopathy may be enhanced by the recent decision by the NHS in the UK to nationally commission mitochondrial medicine services at three closely linked centres in London, Newcastle and Oxford (www.ncg.nhs.uk/ncg_services.htm).

5.3.3 Potential confounding factors

There are some potentially confounding factors in my study. Firstly, patients with mitochondrial cytopathy are susceptible to developing diabetes mellitus and/or the metabolic syndrome, and these may clearly then have effects on the kidney independently of the direct toxic effects of MD. Secondly, some patients were taking other therapies (e.g. NSAIDs, ACE inhibitors) that may have effects on renal function. Thirdly, due to the phenomenon of heteroplasmy, it is likely that the mtDNA mutant load varied between different patients, which may have a bearing on the resulting degree of renal dysfunction. At present, the only mechanism to measure the mtDNA mutant load in a solid organ is via a tissue biopsy, which involves significant risks and could not be justified for this sort of observational study. However, the technique of isolating renal epithelial cells from urine and measuring mtDNA mutant load in these is now being developed, and early studies suggest that the results correlate well with the mutant load in muscle in patients with mitochondrial disease (McDonnell *et al.*, 2004).

In addition to human studies such as mine, improved understanding of the effects of MD on the kidney will clearly be enhanced by the development of realistic animal models of mitochondrial cytopathy. To date this has proved problematic (as discussed in chapter 1.4.3), but newer models are currently in development that will hopefully address these historical problems and significantly enhance the field of mitochondrial research.

Chapter 6 – Results: Subclinical renal tubular disease in HIV infected patients

6.1 Demographics, HIV and treatment history

Patients recruited to the study were divided into 3 study groups: (1) anti-retroviral naïve (ARTN), (2) on ART and exposed to Tenofovir (TDF), and (3) on ART but with no history of TDF exposure (non-TDF). Table 6.1 contains the baseline demographics, ART history and laboratory blood tests, along with data on the prevalence of hypertension and potentially nephrotoxic non-HIV therapy in each group. The 3 groups were well matched for sex and ethnicity. As expected, the patients in the ARTN group were younger, and had higher plasma HIV RNA levels compared with the 2 treatment groups. Of the patients on ART, 94% (44/47 TDF, 31/33 non-TDF) had plasma HIV RNA levels <50 copies/ml. Only 1 patient had a HIV RNA level >400 copies/ml at the time of the study. There was no significant difference in CD4 count ($p>0.2$) among the study groups. The non-TDF group had received ART for a longer median time than the TDF group, although both groups had been treated with a similar median total number of ART drugs.

6.2 eGFR and serum phosphate

The median eGFR in all 3 groups was normal ($>90\text{ml/min/1.73m}^2$), and there were no significant differences among the groups ($p>0.9$). Only 1 patient in the study (in the TDF group) had an eGFR $<60\text{ml/min/1.73m}^2$. Median serum HPO_4^{2-} was lower in the TDF group (0.94 mmol/l [range 0.46-1.43]) than either the ARTN (0.99mmol/l [0.78-1.18]) or non-TDF (1.04 mmol/l [0.58-1.36]) groups (Figure 6.1); however, these differences were not statistically significant ($p>0.2$). The proportion of patients with HPO_4^{2-} values below the normal range ($<0.8\text{ mmol/l}$) was greater in the TDF group (11/43 [25.6%]) than either the ARTN (1/17 [5.9%]) or non-TDF (3/32 [9.4%]) groups; however, these differences were not statistically significant ($p>0.2$).

	ART naïve (n:19)	TDF exposed (n:47)	No TDF exposure (n:33)	p value
Age	36 (26-47)	43 (27-69)	43 (29-65)	p<0.05 (TDF v non-TDF p>0.9)
Sex: male % (n)	95 (18)	91 (43)	91 (30)	p>0.2
Ethnicity: white % (n)	68 (13)	83 (39)	82 (27)	p>0.2
Time on ART: months	-	44 (5-146)	86 (6-137)	P=0.04
Time on TDF: months	-	32 (3-68)	-	-
Proportion on Protease Inhibitor % (n)	-	47 (22)	33 (11)	p>0.2
Total number of ART drugs ever received (n)	-	5 (3-10)	4 (3-9)	p=0.1
Proportion exposed to minimum of 2 classes of ART % (n)	-	72 (34)	70 (23)	p>0.2
Proportion on any nephrotoxic drug % (n)	21 (4)	17 (8)	27 (9)	p>0.2
Hypertension % (n)	5 (1)	9 (4)	15 (5)	p>0.2
CD4 count (x10 ⁶ /l)	370 (20-860)	420 (120-1140)	440 (200-1060)	P=0.3
Viral load (copies/ml)	14,300 (600-430,000)	<50 (<50-80)	<50 (<50-4600)	p<0.01
eGFR (ml/min/1.73m ²)	100 (64-159)	99 (53-147)	98 (62-131)	(TDF v non-TDF p>0.9) p>0.9

Table 6.1. Baseline demographics, biochemistry, and medical and treatment history of HIV patients. Values given are median (and range) unless stated. Nephrotoxic drugs included NSAIDs, acyclovir, statins, ACE inhibitors, angiotensin II receptor blockers and valproate.

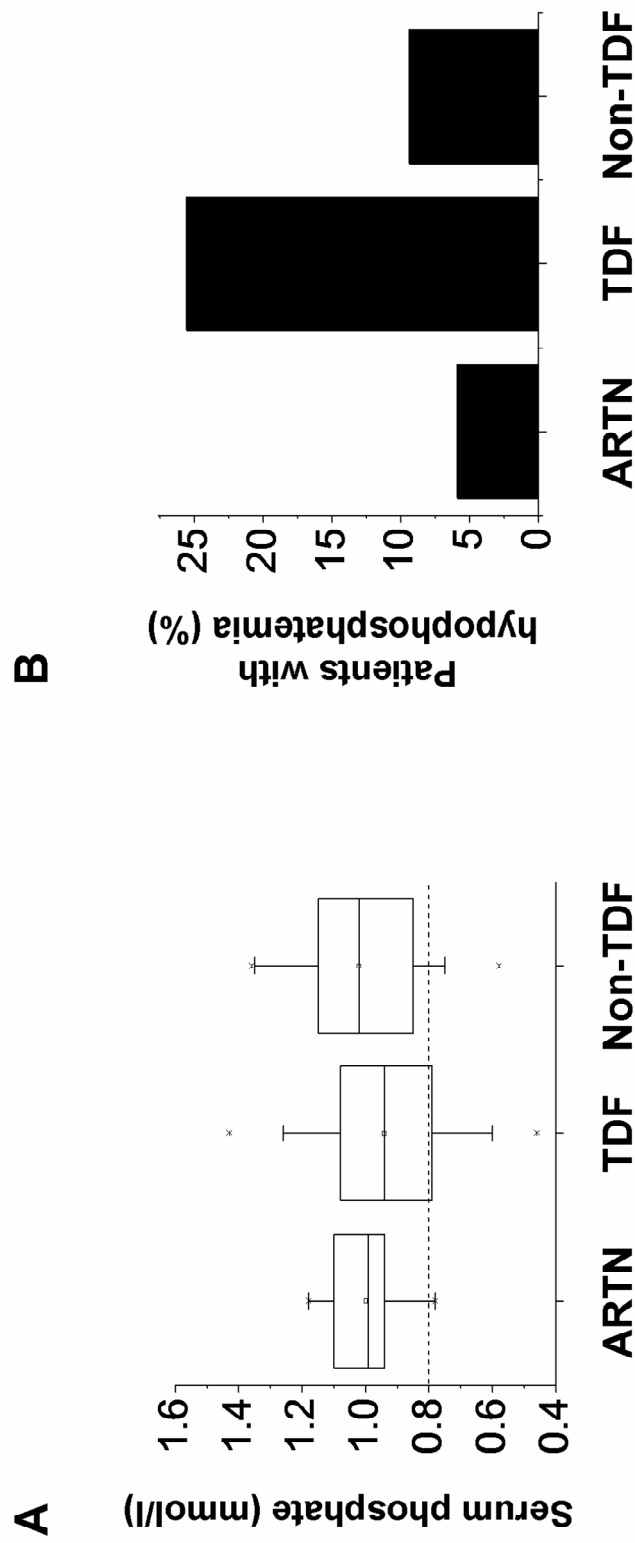


Figure 6.1. Serum phosphate in HIV patients. Mean serum phosphate was not significantly different between the different study groups ($p>0.2$) (A). Values given are mean (point), median (line), IQR (box), 5th/95th percentiles (error bars) and range (crosses). The dashed line represents the lower limit of the normal adult range ($n>0.8\text{mmol/l}$). The proportion of patients in the TDF group that had a serum phosphate value below the normal range was greater than in the ARTN and non-TDF groups (B), but this difference was not statistically significant ($p>0.2$).

6.3 Prevalence of sub-clinical proteinuria is high in HIV patients, especially in those exposed to Tenofovir

Urinary markers in HIV patients are depicted in Table 6.2.

	ARTN (n=19)	TDF (n=47)	non-TDF (n=33)	p
$U_{RBP/C}$ ($\mu\text{g}/\text{mmol}$)	10.4 (2.4-448.5)	24.2 (3.0-1972.4)	12.6 (3.5-693.4)	ARTN v TDF <0.03 ARTN v non-TDF >0.9 TDF v non-TDF <0.08
$U_{NAG/C}$ ($\mu\text{mol}/\text{hr}/\text{mmol}$)	24.7 (6.4-325.0)	44.6 (15.9-1226.2)	46.0 (1.4-958.9)	ARTN v TDF <0.01 ARTN v non-TDF <0.04 TDF v non-TDF >0.9
$U_{A/C}$ (mg/mmol)	0.8 (0-27.8)	1.0 (0-20.8)	1.2 (0.3-29.6)	ARTN v TDF >0.9 ARTN v non-TDF >0.9 TDF v non-TDF >0.9
$U_{P/C}$ (mg/mmol)	10.5 (0-38.0)	14.0 (6.0-64.0)	11.0 (0-51.0)	ARTN v TDF <0.07 ARTN v non-TDF >0.9 TDF v non-TDF <0.04

Table 6.2. Urinary markers in HIV patients. Values given are the median (and range), and are expressed as a ratio to urinary creatinine. ARTN=anti-retroviral naïve, TDF=exposed to Tenofovir, non-TDF=no exposure to Tenofovir.

$U_{RBP/C}$ was significantly different among the study groups ($p<0.02$) and was higher in the TDF group than in the ARTN group ($p<0.03$), and there was also a trend towards it being higher than in the non-TDF group ($p<0.08$) (Figure 6.2A). Within the TDF group there was no significant difference in $U_{RBP/C}$ between patients taking a protease inhibitor (29.0 $\mu\text{g}/\text{mmol}$ creatinine [4.0-1972.4], $n=22$) and those who were not (23.1 $\mu\text{g}/\text{mmol}$ creatinine [3.0-1028.3], $n=25$; $p>0.5$). Furthermore, there was no significant correlation between length of time on TDF and $U_{RBP/C}$ ($r_s=0.04$, $p>0.6$).

$U_{NAG/C}$ was also significantly different among the groups ($p<0.01$), and was higher in both TDF ($p<0.01$) and non-TDF ($p<0.04$) patients than in the ARTN group. However, there was no significant difference in $U_{NAG/C}$ between the TDF and

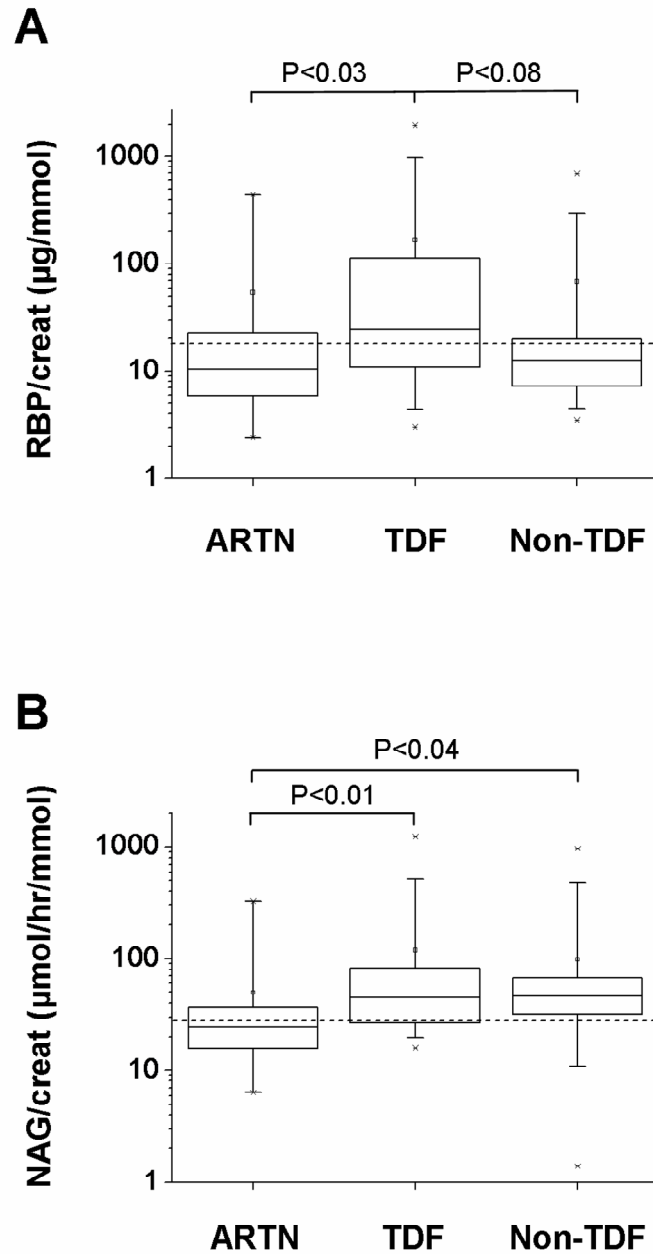


Figure 6.2. Urinary RBP and NAG in HIV patients. Urinary RBP excretion ($n < 18 \mu\text{g}/\text{mmol}$ creatinine) was higher in TDF patients than either anti-retroviral naïve (ARTN) or non-TDF patients (**A**). Urinary NAG excretion ($n < 28 \mu\text{mol}/\text{hour}/\text{mmol}$ creatinine) was higher in both TDF and non-TDF patients than ARTN patients (**B**). Values given are mean (point), median (line), IQR (box), 5th/95th percentiles (error bars) and range (crosses). Dotted lines denote upper limits of normal ranges.

non-TDF groups ($p>0.9$) (Figure 6.2B). Furthermore, there was no significant correlation between length of time on ART and $U_{NAG/C}$ ($r_s=0.11$, $p>0.2$).

There were no significant differences among the study groups in $U_{A/C}$ ($p>0.8$) (Figure 6.3A). However, there were differences in $U_{P/C}$ ($p<0.02$), with a trend towards a higher value in the TDF group than in the ARTN group ($p<0.07$) (Figure 6.3B). $U_{P/C}$ was significantly higher in the TDF group than the non-TDF group ($p<0.04$). There was no significant difference in $U_{P/C}$ between the non-TDF and ARTN groups ($p>0.9$). Overall, these results indicate that patients exposed to TDF have increased proteinuria.

6.4 Neither urine albumin/creatinine nor protein/creatinine ratio is sufficiently sensitive to detect all cases of subclinical nephropathy

The strongest correlation between urinary markers was found between $U_{RBP/C}$ and $U_{NAG/C}$, followed by (in descending order of association): $U_{NAG/C}$ and $U_{A/C}$, $U_{RBP/C}$ and $U_{A/C}$, $U_{RBP/C}$ and $U_{P/C}$, $U_{NAG/C}$ and $U_{P/C}$, and $U_{A/C}$ and $U_{P/C}$ (Table 6.3). Scatter plots comparing $U_{A/C}$ (the recommended screening tool of NICE, UK) with $U_{RBP/C}$, $U_{NAG/C}$ and $U_{P/C}$ are depicted (Figure 6.4) for each of the three study groups.

	$U_{RBP/C}$	$U_{NAG/C}$	$U_{A/C}$	$U_{P/C}$
$U_{RBP/C}$	-	0.60 ($p<0.01$)	0.53 ($p<0.01$)	0.33 ($p<0.01$)
$U_{NAG/C}$	0.60 ($p<0.01$)	-	0.56 ($p<0.01$)	0.26 ($p<0.02$)
$U_{A/C}$	0.53 ($p<0.01$)	0.56 ($p<0.01$)	-	0.20 ($p<0.06$)
$U_{P/C}$	0.33 ($p<0.01$)	0.26 ($p<0.02$)	0.20 ($p<0.06$)	-

Table 6.3. Correlation among urinary markers. Values given are the Spearman coefficients (range -1 to +1) and relevant p values.

Although there appeared to be some degree of correlation among urinary markers, the level of agreement between tests in detecting abnormal proteinuria (defined as

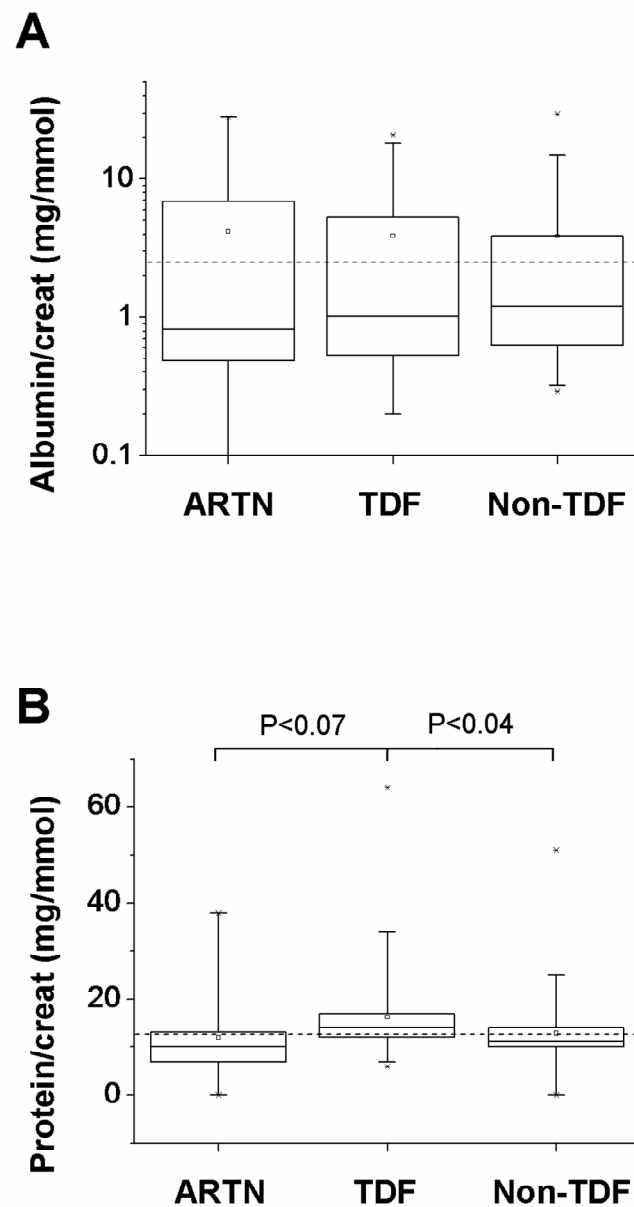


Figure 6.3. Urinary albumin and protein in HIV patients. Urinary albumin excretion ($n < 2.5 \text{ mg/mmol}$ creatinine) was not significantly different between the study groups **(A)**. Urinary protein/creatinine ratio ($n < 13 \text{ mg/mmol}$) was higher in TDF patients than either anti-retroviral naïve (ARTN) or non-TDF patients **(B)**. Values given are mean (point), median (line), IQR (box), 5th/95th percentiles (error bars) and range (crosses). Dotted lines denote upper limits of normal ranges.

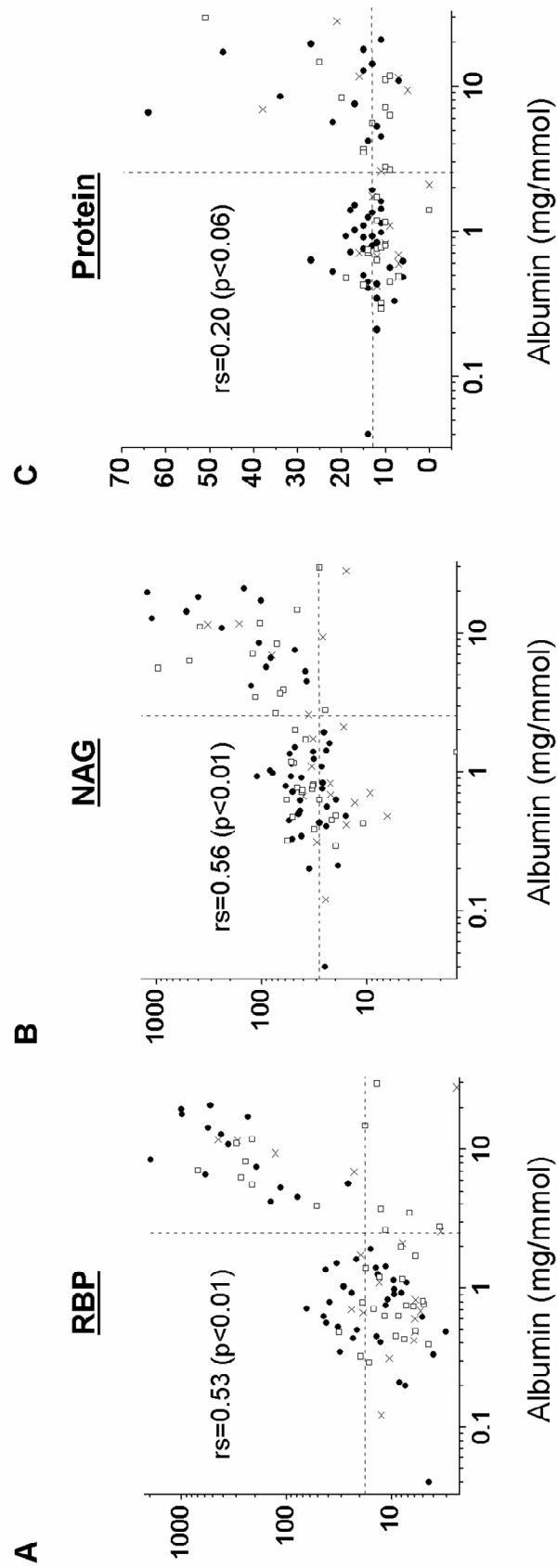


Figure 6.4. The relationship between urinary albumin and other urinary markers. Scatter plots are depicted for all three study groups (ARTN [x], TDF [•] and non-TDF [□]), showing the relationship between urinary albumin and urinary RBP (µg/mmol) (A), NAG (µmol/hr/mmol) (B) and protein (mg/mmol) (C). Values are expressed as ratios to urine creatinine.

above the normal range) was generally low (Table 6.4); this suggests that they were measuring different aspects of renal dysfunction in HIV patients.

	$U_{RBP/C}$	$U_{NAG/C}$	$U_{A/C}$	$U_{P/C}$
$U_{RBP/C}$	-	0.33	0.30	0.16
$U_{NAG/C}$	0.33	-	0.25	0.11
$U_{A/C}$	0.30	0.25	-	0.19
$U_{P/C}$	0.16	0.11	0.19	-

Table 6.4. Agreement among urinary markers in detecting abnormal proteinuria. Values given are the measures of agreement (κ [range 0 to 1]).

To evaluate the sensitivity of either $U_{P/C}$ or $U_{A/C}$ in detecting subclinical nephropathy, I compared the proportions of patients in each group with elevated values (above the normal upper limit) of $U_{P/C}$ or $U_{A/C}$, to the proportion with evidence of proximal tubular dysfunction (defined as elevated $U_{RBP/C}$ and/or $U_{NAG/C}$) (Figure 6.5). The proportion of patients in each group with proximal tubular dysfunction was considerably higher than the proportions with either elevated $U_{A/C}$ or $U_{P/C}$ (ARTN: 10/19 [52.6%] *versus* 6/19 [31.6%] *versus* 4/16 [25.0%]; TDF: 38/47 [80.9%] *versus* 14/47 [29.8%] *versus* 24/46 [52.2%]; non-TDF: 27/33 [81.8%] *versus* 13/33 [39.4%] *versus* 9/30 [30.0%]). This implies that either $U_{P/C}$ or $U_{A/C}$ testing alone cannot reliably detect patients with ART-associated renal tubular dysfunction.

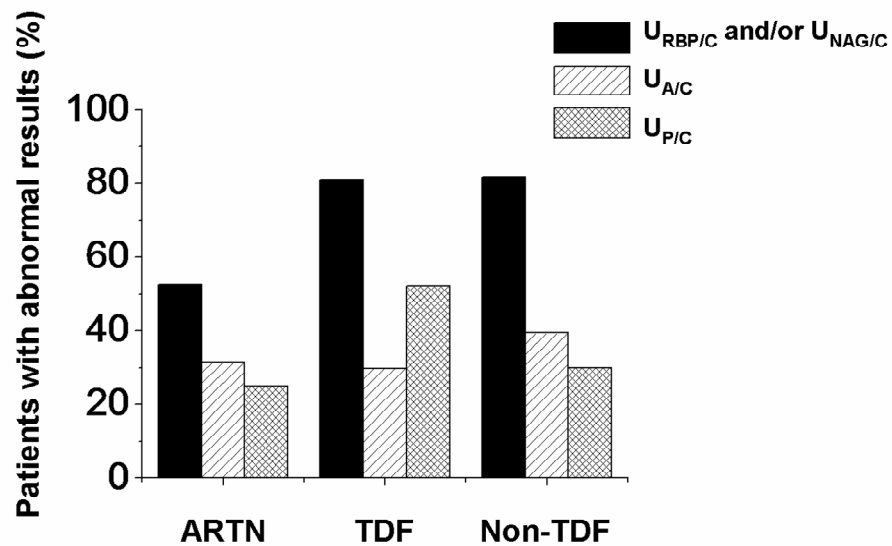


Figure 6.5. Sensitivity of either urinary albumin or protein in detecting subclinical renal tubular disease in HIV patients. The proportions of patients with an elevation (above the normal adult range) in either urinary albumin/creatinine ($U_{A/C}$) or protein/creatinine ($U_{P/C}$) were considerably lower than the proportion with abnormal tubular proteinuria (defined as elevated urinary RBP/creatinine [$U_{RBP/C}$] and/or NAG/creatinine [$U_{NAG/C}$]), in all three study groups. This suggests that neither albumin/creatinine nor protein/creatinine alone is sufficient to detect subclinical nephropathy in HIV patients. ARTN=anti-retroviral naïve, TDF=exposed to Tenofovir, non-TDF=never exposed to Tenofovir.

6.5 Discussion

6.5.1 Subclinical proteinuria in HIV patients

I have performed a cross-sectional study to investigate the nature and prevalence of subclinical nephropathy in HIV patients without overt renal disease. My results show that the prevalence of proximal tubular dysfunction (elevated $U_{RBP/C}$ and/or $U_{NAG/C}$) is high in both ART-naïve patients and those on ART. Patients exposed to TDF have increased $U_{RBP/C}$ and $U_{P/C}$ compared to ART-naïve patients and those taking other forms of ART.

Rates of tubular proteinuria were found to be high in HIV patients in a previous study (Kabanda *et al.*, 1996); however, no significant differences were found among different treatment groups. Subsequently, cross-sectional studies have demonstrated an association between TDF exposure and increased urinary excretion of beta-2-microglobulin in both children (Papaleo *et al.*, 2007) and adults (Gatanaga *et al.*, 2006). Furthermore, a small longitudinal study reported that excretion of urinary beta-2-microglobulin increased significantly in patients following the commencement of TDF therapy (Kinai & Hanabusa, 2005). Although widely used as a marker of proximal tubular dysfunction, urinary beta-2-microglobulin has drawbacks as a screening tool because of its pH dependence and enzymatic breakdown (Davey & Gosling, 1982); RBP is thought to be a more reliable low molecular weight protein to measure (Bernard & Lauwerys, 1981).

In my study, patients on ART (whether or not it included TDF) had significantly higher $U_{NAG/C}$ compared with ART-naïve patients; however, there were no significant differences in $U_{A/C}$ (a marker of glomerular disease). This suggests that there is a background level of proximal tubular damage in patients taking ART, which is not specific for TDF. However, I have found that patients taking TDF have higher $U_{RBP/C}$ than other HIV patients (whether or not they are on ART), which could be explained by a more specific inhibitory effect of TDF on proximal tubular uptake and/or transport of LMWPs. This is consistent with the association of this drug with FS in some case reports, and could also account for the increase in $U_{P/C}$ observed in patients taking TDF.

The finding that $U_{RBP/C}$ values in my study were not normally distributed, and did not correlate with length of time on treatment, suggests that TDF toxicity in the kidney may be an ‘all or none’ phenomenon. This may, in turn, relate to underlying pharmacogenomic factors; for example, it has recently been shown that ABCC2 (the gene which encodes MRP2, an efflux pathway for TDF) haplotypes are associated with PT dysfunction in TDF patients (Izzedine *et al.*, 2006). The significance of tubular proteinuria in predicting development of chronic kidney disease is currently unknown; although it has been suggested that increased delivery of LMWPs to distal parts of the nephron might have pathophysiological consequences (Kastner *et al.*, 2009; Norden *et al.*, 2001).

6.5.2 *Appropriate screening tests for renal tubular disease*

The level of agreement between the different urinary tests in my study in detecting abnormal proteinuria was generally low, and considerable numbers of patients with evidence of tubular dysfunction did not have a raised $U_{A/C}$ or $U_{P/C}$. Furthermore, the correlation between tubular markers and $U_{P/C}$ was also weak (although patients taking TDF did have significantly elevated $U_{P/C}$). Therefore, screening for increased urinary excretion of tubular proteins (such as $U_{RBP/C}$ and $U_{NAG/C}$) is likely to be a more appropriate strategy for monitoring patients taking TDF than more conventional clinical tests for nephropathy (i.e. $U_{P/C}$ or $U_{A/C}$). This will need to be assessed in prospective longitudinal studies, in order to identify those patients who are at increased risk of TDF-associated renal toxicity. Unfortunately, testing for urinary LMWP excretion is not widely available on a clinical basis in the UK; however, this may change in the future. In the meantime, other less sensitive but more readily available markers of PT function (such as fractional excretion of phosphate and urine dipstick for glycosuria) could be utilised for monitoring patients on ART.

6.5.3 *Serum phosphate in HIV patients*

Renal HPO_4^{2-} wasting is one of the features of FS. I did not observe significant differences in median serum HPO_4^{2-} among the study groups. However, there was a

non-significant increase in the proportion of patients with hypophosphataemia in the TDF group. This should be explored further in larger studies, as it is an important long-term consideration in patients taking TDF (where concern has tended to focus more on the development and progression of renal dysfunction *per se*, rather than the metabolic consequences of urinary LMWP and inorganic solute wasting). Patients taking ART have been shown previously to have reduced bone density compared to controls (Tebas *et al.*, 2000). The reasons for this are unclear, but may relate to increased osteoclastogenesis due to ART, mediated either via direct effects of the drugs or via changes in the levels of circulating cytokines that can act on osteoclasts (for review see (Pan *et al.*, 2006)). Renal fractional excretion of HPO_4^{2-} was not measured in this study, so I am unable to comment further on the mechanism of the effect of TDF on serum HPO_4^{2-} .

6.5.4 Study limitations and confounding factors

I do think there have been any major confounding factors in my study, as the different study groups were well matched and patients with diabetes or who were infected with Hepatitis B or C were excluded. The incidence of hypertension and use of potentially nephrotoxic non-HIV therapy was low in all groups. Although the non-TDF group had received ART for a longer median time than the TDF group, I do not think this weakens the findings. Indeed, it is quite possible that even bigger differences in relative toxicity would have been observed between the two treatment groups had they been more closely matched for duration of therapy.

My study was cross-sectional rather than longitudinal, and as such only associations between TDF exposure and renal tubular dysfunction can be demonstrated, and causality cannot be established. Furthermore, questions cannot be answered on progression of kidney disease in patients on TDF, or recovery following discontinuation. Prospective randomized controlled trials will be required to address these.

Chapter 7 - General discussion

7.1 The relationship between mitochondrial function and low molecular weight protein endocytosis in the proximal tubule

RC inhibition caused only small reductions in FA endocytosis and cytosolic ATP levels in OK cells, whereas much larger decreases were observed in both in response to blockade of glycolysis.

Evidence in the literature (from both renal and non-renal cell lines) suggests that a change in cytosolic ATP levels can have a significant effect on receptor mediated endocytosis at the cell membrane. The endocytosis and recycling of transferrin and its associated receptor in the MDCK renal cell line (which has properties more of the DT than PT) was found to be dependent on ATP levels (Podbilewicz & Mellman, 1990). Furthermore, uptake of radiolabelled transferrin in both K562 and Hela cells has been shown to be inhibited by ATP depletion, which was induced by exposing the cells to N₂, in the presence of 2-DG (Schmid & Carter, 1990). In the Cos7 cell line, the chloride channel CIC-2 was upregulated at the cell membrane by cellular ATP depletion, due to decreased endocytosis of the channel, possibly via a dynamin dependent process (Dhani *et al.*, 2008). The endocytosis of β -adrenergic receptors in response to catecholamines was also found to be ATP dependent (Liao & Perkins, 1993).

A variety of processes involved in the mechanism of endocytosis have been shown to be ATP dependent. For example, the exchange of free and bound clathrin in clathrin-coated pits requires ATP (Wu *et al.*, 2001). An intact actin cytoskeleton is important for endocytosis (Gekle *et al.*, 1997), and actin polymerisation is ATP dependent (ATP bound to monomeric [G] actin undergoes hydrolysis when polymeric [F] actin is formed (Korn *et al.*, 1987). The trafficking of endocytotic vesicles within cells along microtubules by the motor proteins kinesin and dynein is dependent on ATP (Oda *et al.*, 1995), and disruption of microtubule polymerisation has been reported to inhibit endocytosis of transferrin in a non-renal cell line (Jin & Snider, 1993). Microtubules may have a key role in receptor-ligand dissociation in endocytotic

vesicles in hepatocytes, again in an ATP dependent process (Goltz *et al.*, 1992). Furthermore, receptor recycling requires dissociation from ligands within the internalised vesicles; this process is enhanced by acidification of these endosomes, via an ATP dependent proton pump (Gluck *et al.*, 1996), and disruption of acidification leads to impaired protein endocytosis (Clague *et al.*, 1994).

A previous study on the effects of ATP depletion on fluid phase endocytosis (using the markers Lucifer Yellow and Horse-radish peroxidase [HSP], rather than dextran) reported that whilst CN decreased uptake, IAA had mixed effects, causing a decrease in HSP uptake but, surprisingly, an increase in Lucifer Yellow uptake (Kempson *et al.*, 1991). The authors speculated this may have been due to a non-endocytotic effect on Lucifer yellow uptake by IAA. I was unable to test the effects of IAA on endocytosis in OK cells, as I found it to be extremely toxic to the cells. Ifosfamide is a chemotherapeutic agent reported to cause FS (with *in vitro* evidence that its metabolites may inhibit mitochondrial RC function in a PT-derived cell line (Mohrmann *et al.*, 1993)); it was found to cause a decrease in cytosolic ATP in live renal cortical slices, which was associated with inhibition of uptake of HSP (Yaseen *et al.*, 2008).

In contrast to the above, other investigators have reported that ATP depletion does not affect receptor mediated endocytosis in intact cells (Larkin *et al.*, 1985), or that it may disrupt receptor recycling, but does not inhibit a single round of endocytosis (Clarke & Weigel, 1985). The differences observed between various studies in this field can perhaps be explained by a number of potentially confounding factors. Firstly, a variety of different cell models from different origins have been used, and endocytotic pathways and machinery may vary considerably between them (similar points could be made for the range of different ligands used). Secondly, as discussed previously, cell cultures can vary in their relative dependence on different ATP generating methods (aerobic versus anaerobic). Lastly, agents used to block either RC function or glycolysis could have important confounding effects of other aspects of cell function, affecting variables such as ROS production and Ca^{2+} signalling.

Exploring the relationship between cytosolic ATP and endocytosis further in OK cells will require a method to manipulate the former and then investigate the effect

on the latter, in a manner that does not lead to rapid cell death. Previous work in this area has been performed using disrupted cells where the concentration of ATP is much more easily controlled than in an intact functioning cell. Perhaps one approach would be to decrease cytosolic ATP rapidly with an agent like IAA, then add ATP in known concentrations to the culture medium; however, it is unclear how much ATP would be taken up by the cells, and extracellular ATP mediated signalling via purinergic receptors in the cell membrane would be a major potential confounding factor (experiments in another renal-derived cell line [WKPT] have revealed that extracellular ATP can have an inhibitory effect on LMWP uptake (Carvou *et al.*, 2007)). A possible solution to this problem might involve using caged ATP, which is not biologically active until a photosensitive bond has been broken; therefore, it can be introduced across cellular membranes and then activated within cells using a flash of ultraviolet light (McCray *et al.*, 1980).

To get around the problem of OK cells being relatively anaerobic, two strategies could be employed. The first is to try and make the OK cells switch to a greater dependence on aerobic metabolism. Various methods are available to try and achieve this, such as shaking culture flasks to increase aeration and lowering the culture medium glucose concentration to reduce the drive towards glycolysis (Griner & Schnellmann, 1994), but it is unclear how successful they generally are. An alternative approach would be to switch to primary tissue, but primary cultures of PT cells generally lose their phenotype within a few passages. Renal slices have been used to investigate amino acid (Rosenberg *et al.*, 1961) and HSP (Yaseen *et al.*, 2008) uptake in the PT, but they lack the normal architecture of the intact kidney and do not provide a model whereby LMWP endocytosis can be studied selectively at the apical PT membrane. Direct visualisation of LMWP endocytosis in the PT is now possible *in vivo* using multi-photon imaging (Molitoris & Sandoval, 2005); however, there are significant technological difficulties with this approach.

7.2 Variation in mitochondrial function along the nephron

Previous studies have shown that certain topographical patterns of injury are observed in the renal tubule, in diseases where MD is implicated in the pathogenesis.

For example, MD is thought to be central to the cellular injury that occurs following ischaemia-reperfusion (which is a major cause of AKI), and ischaemia-reperfusion in the isolated perfused kidney causes necrosis predominantly in the S3 portion of the PT (straight PT) (Shanley *et al.*, 1986c). Exposure to RC inhibitors in the same preparation causes maximal structural damage in the S1 segment of the convoluted PT (Shanley *et al.*, 1986a). This discrepancy may be partly explained by a relatively greater anaerobic capacity in the S3 segment, rendering it less vulnerable to RC inhibition (although still more vulnerable than DT). Furthermore, the importance of oxygen gradients *in vivo* must be considered. The S3 segment is situated in a relatively hypoxic environment in the inner cortex and outer medulla, and is thus more sensitive to changes in oxygen supply than the S1 segment, which is situated in the comparatively well oxygenated outer cortex. Accordingly, PT damage in hypoxic isolated perfused kidneys has been shown to be dependent on distance from arterial blood supply (i.e. less damage is observed in peri-arterial tubules (Shanley *et al.*, 1986b)).

Infusion of inhibitors of either the RC or the citric acid cycle into the isolated perfused kidney caused decreases in GRF, Na^+ reabsorption, ATP and oxygen consumption (QO_2) (Brezis *et al.*, 1985). RC inhibition caused a greater depletion of ATP in the cortex; whilst blockade of anaerobic glycolysis (with 2-DG) had the opposite effect (i.e. it depleted ATP to a greater extent in the medulla). This observation probably reflects the known gradient in aerobic dependence, which decreases from the cortex down to the medulla (Lee & Peter, 1969). Morphological changes were observed in the brush border of the PT following RC inhibition in the isolated perfused kidney, and the extent of these changes correlated with ATP levels. This provides another possible explanation for the impairment of LMWP uptake observed in patients with MD, as it is likely that effective endocytosis will be impeded by structural abnormalities in the apical membrane. It also highlights the important role that ATP may play in the mechanism. This was further supported by the fact that structural damage in the PT, due to citric acid cycle inhibitors, could be overcome by succinate, which bypasses the metabolic block and allows electrons to feed into the RC at complex II, consequently leading to restoration of ATP synthesis by mitochondria. Interestingly, very little structural damage was observed in the DT following infusion of RC inhibitors; although abnormalities were observed following

the addition of 2-DG. This is consistent with the notion that DT cells are protected from RC inhibitor induced damage by their ability to generate ATP via anaerobic metabolism.

Extensive damage in the DT has been reported in isolated perfused kidney models of *hypoxia* (rather than *anoxia*) (Brezis *et al.*, 1984a), and experiments involving isolated PT and DT cells suggested that the latter were more vulnerable to the effects of brief periods of oxygen deprivation (Lash & Tokarz, 1990). The reasons for this are unclear, but might include generation of ROS in the presence of a low oxygen tension; the DT appears to have a high $\Delta\psi_m$, and also a high density of mitochondria, both factors that could potentially lead to significant ROS formation during pathological states. Indeed, my measurements using HET in kidney slices suggested that ROS production *per mitochondrion* was likely to be higher in the DT than PT, although I did not investigate the effects of hypoxia on this. Ouabain (an inhibitor of the Na^+/K^+ -ATPase) is protective against CN induced cell toxicity in the DT, presumably because it helps to preserve cytosolic levels of ATP during metabolic inhibition (Brezis *et al.*, 1984b). It has also been reported to be protective in the PT, but to a lesser extent (Brezis *et al.*, 1985).

A greater capacity to generate ATP anaerobically may not be the only explanation for the difference in response of $\Delta\psi_m$ to RC inhibitors observed between DT and PT. Recently, new insights have been gained into a potentially important regulator of the mitochondrial ATP synthase, the nuclear-encoded mitochondrial protein IF1. This protein is thought to interact with and inhibit the enzyme, predominantly when the latter is acting in 'reverse mode' as an ATPase (i.e. breaking down ATP and maintaining $\Delta\psi_m$) (Green & Grover, 2000). This occurs when RC activity is impaired, and the mitochondria become net consumers of ATP. IF1 therefore has the effect of preserving ATP levels, at the expense of $\Delta\psi_m$, during times of RC compromise (such as in ischaemia). In cell culture models, IF1 overexpression appears protective against necrotic cell death when the RC is inhibited (Campanella *et al.*, 2008). Using immuno-staining of fixed kidney slices, it was recently demonstrated that the ratio of IF1 to its target molecule (the ATP5b subunit) is higher in PT than DT (Hall *et al.*, 2009), which might explain why $\Delta\psi_m$ depolarizes more rapidly in the PT during RC blockade. In addition to the known effects of IF1

in regulating ‘reverse’ ATP synthase (ATPase) activity, some recent evidence has also emerged to support a role for IF1 in modulating ‘forward’ activity. For example, it has been suggested that IF1 may promote dimerisation of ATP synthase molecules (Garcia *et al.*, 2006), and this might in turn increase the efficiency of the synthase (Strauss *et al.*, 2008). Increased proton flux through the ATP synthase due to greater efficiency will cause a lowering of $\Delta\psi_m$ (Campanella *et al.*, 2008); this could explain the lower resting $\Delta\psi_m$ observed in PT. However, if this were the case, it would be expected that oligomycin (which blocks the ATP synthase) would eliminate differences between the PT and DT, but oligomycin had no significant effect on $\Delta\psi_m$ in my experiments.

My findings in this project, along with the established literature, support the concept that mitochondrial function (and the response to inhibition of RC function) varies along the nephron. The question then arises, what might the teleological reasons be for such differences? The answer probably relates to the function of the different nephron segments. In the cortex, the role of the PT is to reabsorb vast amounts of water and solutes, via ATP-dependent transport mechanisms. The most efficient way to generate this ATP is by aerobic metabolism, and the PT (like other aerobic tissues such as the heart) is highly adapted to perform oxidative phosphorylation, principally using substrates that result in the maximum number of ATP molecules per molecule of fuel (e.g. fatty acids). The PT has also adapted to use a range of metabolic fuels that can be reclaimed from the renal filtrate, such as lactate, amino acids and even citric acid cycle intermediates, at the expense of losing the cellular machinery required to perform anaerobic glycolysis (Wirthensohn & Guder, 1986); thus, rendering itself vulnerable to any degree of RC compromise.

It is, therefore, not surprising that AKI and shut-down of kidney function is commonly observed clinically in response to significant circulatory disturbances (such as sepsis and hypotension). The mechanisms that lead to oliguria in AKI remain to be fully elucidated, but what is striking is that in the face of significant organ dysfunction, histological damage is rarely observed (Brun & Munck, 1957). This has led to the hypothesis that oliguria represents a protective ‘shutting-down’ of renal function (termed ‘acute renal success’ (Thurau & Boylan, 1976)), to minimise necrosis in tubules that have very little inherent resistance to RC

compromise. This concept could explain why historical interventions to improve tubular flow and urine output, such as vasodilators and diuretics, do not have beneficial effects on outcome. As a further protective mechanism against ischaemic insults, renal tubules appear to have significant regenerative capacity. The mechanisms that underlie this remain unclear (Bussolati *et al.*, 2008); but the fact is that many patients with severe AKI do recover kidney function in the weeks after the initial insult. The main clinical problems are the significant morbidity and mortality that occurs within those crucial few weeks of oligo-anuria.

The function of the DT in the Loop of Henle (TALH) is to concentrate the urine. Due to the counter-current mechanism that maintains osmotic gradients in the medulla, the blood flow to the medulla is necessarily sluggish, and consequently the TALH resides in a relatively hypoxic environment. It is therefore not surprising that it has evolved significant glycolytic capacity, and appears more resistant to RC compromise.

Thus, established differences in relative dependence on aerobic and anaerobic metabolism, between the PT and DT, relate to differences in function and the surrounding milieu. However, what is harder to explain (at least at present) is why there may be intrinsic differences in mitochondrial function (e.g. $\Delta\Psi_m$), as described in this study. Given that these findings are novel, and essentially unprecedented by similar investigations in the kidney, or any other organ, any putative explanation at this stage is necessarily speculative. $\Delta\Psi_m$ can be affected by a number of factors in intact cells such as substrate supply, proton leak across the mitochondrial inner membrane, and the ATP/ADP ratio (Nicholls, 2004). In the PT, a more oxidized state and lower $\Delta\Psi_m$ could be explained by a greater work load and more ATP hydrolysis to support the large amount of solute transport that occurs in this nephron segment. Therefore, I was surprised that differences in $\Delta\Psi_m$ were not corrected by inhibition of the mitochondrial ATPase with oligomycin, especially since I knew that oligomycin was working in the slice preparation from its profound effect on the DT in response to anoxia. However, it is unclear to what extent solute transport does occur in kidney slices *in vitro*. Indeed, if little transport is occurring under these conditions, then the intramitochondrial ATP/ADP ratio could be high. ATP can allosterically inhibit RC

complex IV activity in eukaryotic cells (Follmann *et al.*, 1998), and it has been suggested that this may provide a feedback mechanism; acting as a ‘brake’ on RC activity in the presence of a high ATP/ADP ratio, which will limit the size of $\Delta\Psi_m$ and hence prevent excessive ROS production (Kadenbach & Arnold, 1999; Lee *et al.*, 2001). In this setting, oligomycin would have relatively little effect on $\Delta\Psi_m$.

My data showed that mitochondrial RC substrates in the PT are in a more oxidised state at rest, with a lower $\Delta\Psi_m$; a scenario that would minimise ROS production in cells that have a high mitochondrial mass. The importance of this was illustrated by the dramatic rise in ROS production observed after a more reduced state at complex I induced by rotenone. One could speculate that $\Delta\Psi_m$ is kept relatively low in the PT by a degree of uncoupling between RC activity and ATP generation; it will, therefore, be of interest to explore the expression patterns of novel UCPs along the nephron. In contrast, it is perhaps more difficult to explain why $\Delta\Psi_m$ should be significantly higher in the DT in the resting state. These cells also have a high density of mitochondria, and significant ROS production would be expected with a high $\Delta\Psi_m$ in the DT. $\Delta\Psi_m$ is central to mitochondrial function, with effects on such crucial cellular processes as ATP generation, Ca^{2+} uptake and protein import. I can only speculate that other mitochondrial functions within the DT, which require a relatively higher $\Delta\Psi_m$, supersede in importance the increased risk of ROS production; clearly, this hypothesis will have to be explored further in future studies.

The observations made in this study have to be evaluated within the constraints of the kidney slice model. The slicing technique does result in some degree of trauma to the kidney, and natural osmotic gradients that exist in certain regions, such as the inner medulla, are lost. As metabolism is thought to be closely coupled to transport, and it is unclear to what extent transport is occurring in the slice preparation, some caution needs to be exercised in extrapolating my findings to the *in vivo* situation. However, kidney slices have been used historically for transport studies (Hong *et al.*, 1983; Rosenberg *et al.*, 1961; Yaseen *et al.*, 2008), confirming that some solute uptake does take place, and lending validity to the model.

Future *in vivo* studies will naturally be required to confirm or refute my findings in slices, which may include imaging mitochondrial function in whole intact kidneys. To do this, these studies will have to overcome the technical difficulties of applying imaging methods to the *in vivo* setting (e.g. achieving adequate dye loading). Possible alternative approaches to fluorescence microscopy for studying renal metabolism *in vivo* include functional MRI imaging (Bianchi *et al.*, 2007) and urinary metabonomics (Vilasi *et al.*, 2007) (which essentially provides a readout of metabolic activity in the intact kidney).

7.3 Renal dysfunction in adult patients with mitochondrial cytopathy or HIV

My studies have revealed that patients with either mitochondrial cytopathy or HIV have high rates of subclinical proximal tubular disease. Proteinuria (Kannel *et al.*, 1984) and chronic kidney disease (Foley *et al.*, 1998) are both significant risk factors for the development of cardiovascular disease, the leading cause of death in the western world. Given that patients with mitochondrial cytopathy and HIV are prone to developing the metabolic syndrome, another important cardiovascular risk factor, the finding of renal disease in these patients may be of significance when considering their long-term health. This becomes increasingly important as the life expectancy of patients with HIV continues to rise, due to more potent therapy. Indeed, we may well be witnessing a shift in the epidemiology of renal disease attributed to HIV, from conditions related to the direct toxic effects of the virus (e.g. HIVAN and immune complex mediated nephritis) to tubular disorders caused by drug toxicity (such as FS due to TDF) (Wyatt & Klotman, 2006; Roling *et al.*, 2006). My study provided evidence that, even in patients not exposed to TDF, there was a background level of PT toxicity likely to be due to ART.

Whether or not patients with subclinical tubular proteinuria are likely to progress to develop overt kidney disease, or even end-stage renal failure, is currently unknown; longitudinal follow-up studies over a significant period of time will obviously be required to answer this question. However, it has been postulated that the existence of abnormally high concentrations of bioactive peptides (e.g. insulin and parathyroid

hormone) in distal parts of the nephron, due to impaired PT uptake, could have a toxic effect of tubular cells (Norden *et al.*, 2001). This has been supported by experimental evidence suggesting that proteinuria in rodents may have downstream effects on ENaC activity in the collecting duct (Kastner *et al.*, 2009), and thus on the function of the distal nephron. Arguing against this hypothesis is the existence of hereditary forms of FS that produce marked tubular proteinuria, but do not progress to any significant deterioration in renal function over a number of years (Tolaymat *et al.*, 1992).

Diagnosis of kidney disease in clinical practice has traditionally relied on fairly crude markers of renal function, such as serum creatinine and urine dipstick (for albumin). Not only are these relatively insensitive tests that will miss more subtle abnormalities, they are also primarily markers of glomerular disease and are not specifically designed to screen for PT dysfunction. It is, therefore, likely that they will miss the burden of tubular disease detected using more sensitive markers in studies such as mine. In recognition of this, interest is growing in the development of more sensitive urinary biomarkers of kidney disease, which may detect subtle kidney injury at an earlier stage than traditional tests. This may be an advantage in acute conditions, where an early diagnosis and intervention may change the outcome; whereas, previously, waiting for a significant rise in creatinine to occur may have led to the establishment of irreversible disease. For example, the usage of urinary neutrophil gelatinase associated lipocalin (NGAL) (Mishra *et al.*, 2003) and kidney injury molecule (KIM) (Liangos *et al.*, 2007) have attracted much interest in recent years as potential early diagnostic tests for AKI. Furthermore, by testing a range of biomarkers, some qualitative information may be gleaned about the pattern of disease taking place within a kidney as well as the severity. Analysis of the urinary proteome (which involves the rapid measurement of the levels of a number of different proteins) has shown that it appears to differ between different classes of lupus nephritis (Oates *et al.*, 2005). This requires further validation, but the potential of this technology is clear; that clinical nephrology may move on from biopsy based diagnosis (and all the inherent risks to the patient that entails), to non-invasive techniques involving detailed screening of urine. Urine proteomic screening is likely to eventually become a routine tool in evaluating the potential nephrotoxicity of

newly developed medicines, which could help to prevent the kind of unexpected problems encountered with drugs such as TDF.

Another advantage of analysing an entire proteome is that it includes peptides that may be decreased in the urine of FS patients, due to impaired synthesis or release by damaged PT, as well as the traditional markers of abnormal PT uptake that are usually increased in the urine (such as RBP) (Drube *et al.*, 2009). As LMWPs are thought to be taken up by the PT via a common pathway (the megalin/cubulin system), it was assumed that the proteome of FS patients would be similar, no matter what the underlying aetiology. However, recent studies have provided evidence that the urinary proteome does actually vary according to the cause of PT dysfunction (Vilasi *et al.*, 2007). It is, therefore, possible that future urine proteomic screening of TDF patients, and comparison to the proteomes associated with other forms of FS, may provide clues as to the underlying mechanism of PT toxicity due to TDF. Variation in urine proteome could also explain why some forms of FS lead to worsening kidney disease but others don't; perhaps progression of disease depends on which proteins are being taken up or released by the PT, rather than the overall amount of proteinuria.

List of abbreviations

ADP	Adenosine diphosphate
AKI	Acute kidney injury
ANT	Adenine nucleoside transporter
AQP	Aquaporin
ART	Anti-retroviral therapy
ATP	Adenosine triphosphate
AZT	Zidovudine
COX	Cytochrome c oxidase
CN	Cyanide
ddI	Didanosine
2-DG	2-Deoxyglucose
$\Delta\Psi_m$	Mitochondrial membrane potential
DT	Distal tubule
eGFR	Estimated glomerular filtration rate
EM	Electron microscopy
ER	Endoplasmic reticulum
FA	FITC-albumin
FAD ²⁺	Oxidised flavoproteins
FCCP	Carbonyl cyanide p-(trifluoromethoxy) phenylhydrazone
FD	FITC-dextran
FS	Fanconi syndrome
FSGS	Focal segmental glomerulosclerosis
GSH	Glutathione
GST	Glutathione-s-transferase
HAART	Highly active anti-retroviral therapy
HEt	Dihydroethidium (hydroethidine)
HIV	Human immunodeficiency virus
HIVAN	Human immunodeficiency virus associated nephropathy
HPO ₄ ²⁻	Inorganic phosphate
HSP	Horse-radish peroxidase
IMM	Inner mitochondrial membrane

IP3	Inositol triphosphate
MCB	Monochlorobimane
MD	Mitochondrial dysfunction
MDR	Multi-drug resistance transporter
MDRD	Modification of Diet in Renal Disease
MELAS	Mitochondrial encephalo-myopathy with lactic acidosis and stroke
MERFF	Myoclonic epilepsy with ragged red fibres
Mg Green	Magnesium green
MIDD	Maternally inherited diabetes and deafness
MRP	Multi-drug resistance-associated protein
mtDNA	Mitochondrial DNA
NADH	Nicotinamide adenine dinucleotide
NADPH oxidase	Nicotinamide adenine dinucleotide phosphate oxidase
NAG	N-acetyl-beta-D-glucosaminidase
nDNA	Nuclear DNA
NO	Nitric Oxide
NRTI	Nucleoside reverse transcriptase inhibitor
O ₂ ⁻	Superoxide
OK	Opossum kidney cell
PAN	Puromycin aminonucleoside nephrosis
PCT	Proximal convoluted tubule
PI	Protease inhibitor
PMF	Proton motive force
Pol-γ	DNA Polymerase Gamma
PST	Proximal straight tubule
PT	Proximal tubule
RBP	Retinol binding protein
RC	Respiratory chain
ROI	Region of interest
SOD	Superoxide dismutase
TALH	Thick ascending limb of the loop of Henle
TDF	Tenofovir

THP	Tamm Horsfall Protein
TMRM	Tetramethyl rhodamine methyl ester
$U_{A/C}$	Urine albumin/creatinine ratio
UCP	Uncoupling protein
$U_{NAG/C}$	Urine N-acetyl-beta-D-glucosaminidase/creatinine ratio
$U_{P/C}$	Urine protein/creatinine ratio
$U_{RBP/C}$	Urine retinol binding protein/creatinine ratio

References

- Abramov AY, Scorziello A, & Duchen MR (2007). Three distinct mechanisms generate oxygen free radicals in neurons and contribute to cell death during anoxia and reoxygenation. *J Neurosci* 27, 1129-1138.
- Affourtit C & Brand MD (2008). On the role of uncoupling protein-2 in pancreatic beta cells. *Biochim Biophys Acta* 1777, 973-979.
- Axmacher N, Winterer J, Stanton PK, Draguhn A, & Muller W (2004). Two-photon imaging of spontaneous vesicular release in acute brain slices and its modulation by presynaptic GABAA receptors. *Neuroimage* 22, 1014-1021.
- Bachmann S, Koeppen-Hagemann I, & Kriz W (1985). Ultrastructural localization of Tamm-Horsfall glycoprotein (THP) in rat kidney as revealed by protein A-gold immunocytochemistry. *Histochemistry* 83, 531-538.
- Bacic D, Schulz N, Biber J, Kaissling B, Murer H, & Wagner CA (2003). Involvement of the MAPK-kinase pathway in the PTH-mediated regulation of the proximal tubule type IIa Na⁺/Pi cotransporter in mouse kidney. *Pflügers Arch* 446, 52-60.
- Bagnasco S, Good D, Balaban R, & Burg M (1985). Lactate production in isolated segments of the rat nephron. *Am J Physiol* 248, F522-F526.
- Baker GL, Corry RJ, & Autor AP (1985). Oxygen free radical induced damage in kidneys subjected to warm ischemia and reperfusion. Protective effect of superoxide dismutase. *Ann Surg* 202, 628-641.
- Balaban RS, Soltoff SP, Storey JM, & Mandel LJ (1980). Improved renal cortical tubule suspension: spectrophotometric study of O₂ delivery. *Am J Physiol* 238, F50-F59.
- Barany P, Wibom R, Hultman E, & Bergstrom J (1991). ATP production in isolated muscle mitochondria from haemodialysis patients: effects of correction of anaemia with erythropoietin. *Clin Sci (Lond)* 81, 645-653.
- Barbier O, Jacquillet G, Tauc M, Cougnon M, & Poujeol P (2005). Effect of heavy metals on, and handling by, the kidney. *Nephron Physiol* 99, 105-110.
- Barditch-Crovo P, Deeks SG, Collier A, Safrin S, Coakley DF, Miller M, Kearney BP, Coleman RL, Lamy PD, Kahn JO, McGowan I, & Lietman PS (2001). Phase I/II

trial of the pharmacokinetics, safety, and antiretroviral activity of tenofovir disoproxil fumarate in human immunodeficiency virus-infected adults. *Antimicrob Agents Chemother* 45, 2733-2739.

Bastide B, Snoeckx K, & Mounier Y (2002). ADP-ribose stimulates the calcium release channel RyR1 in skeletal muscle of rat. *Biochem Biophys Res Commun* 296, 1267-1271.

Bayona-Bafaluy MP, Blits B, Battersby BJ, Shoubridge EA, & Moraes CT (2005). Rapid directional shift of mitochondrial DNA heteroplasmy in animal tissues by a mitochondrially targeted restriction endonuclease. *Proc Natl Acad Sci U S A* 102, 14392-14397.

Bernard AM & Lauwerys RR (1981). Retinol binding protein in urine: a more practical index than urinary beta 2-microglobulin for the routine screening of renal tubular function. *Clin Chem* 27, 1781-1782.

Bernard AM, Moreau D, & Lauwerys R (1982). Comparison of retinol-binding protein and beta 2-microglobulin determination in urine for the early detection of tubular proteinuria. *Clin Chim Acta* 126, 1-7.

Betarbet R, Sherer TB, MacKenzie G, Garcia-Osuna M, Panov AV, & Greenamyre JT (2000). Chronic systemic pesticide exposure reproduces features of Parkinson's disease. *Nat Neurosci* 3, 1301-1306.

Bianchi MC, Sgandurra G, Tosetti M, Battini R, & Cioni G (2007). Brain magnetic resonance in the diagnostic evaluation of mitochondrial encephalopathies. *Biosci Rep* 27, 69-85.

Biesecker G, Karimi S, Desjardins J, Meyer D, Abbott B, Bendele R, & Richardson F (2003). Evaluation of mitochondrial DNA content and enzyme levels in tenofovir DF-treated rats, rhesus monkeys and woodchucks. *Antiviral Res* 58, 217-225.

Bindokas VP, Jordan J, Lee CC, & Miller RJ (1996). Superoxide production in rat hippocampal neurons: selective imaging with hydroethidine. *J Neurosci* 16, 1324-1336.

Birkus G, Hitchcock MJ, & Cihlar T (2002). Assessment of mitochondrial toxicity in human cells treated with tenofovir: comparison with other nucleoside reverse transcriptase inhibitors. *Antimicrob Agents Chemother* 46, 716-723.

Birn H, Fyfe JC, Jacobsen C, Mounier F, Verroust PJ, Orskov H, Willnow TE, Moestrup SK, & Christensen EI (2000). Cubilin is an albumin binding protein important for renal tubular albumin reabsorption. *J Clin Invest* 105, 1353-1361.

Bockenbauer D, Bokenkamp A, van't HW, Levchenko E, Kist-van Holthe JE, Tasic V, & Ludwig M (2008). Renal phenotype in Lowe Syndrome: a selective proximal tubular dysfunction. *Clin J Am Soc Nephrol* 3, 1430-1436.

Bootman MD, Collins TJ, Peppiatt CM, Prothero LS, MacKenzie L, de SP, Travers M, Tovey SC, Seo JT, Berridge MJ, Ciccolini F, & Lipp P (2001). Calcium signalling--an overview. *Semin Cell Dev Biol* 12, 3-10.

Bourdon A, Minai L, Serre V, Jais JP, Sarzi E, Aubert S, Chretien D, de LP, Paquis-Flucklinger V, Arakawa H, Nakamura Y, Munnich A, & Rotig A (2007). Mutation of RRM2B, encoding p53-controlled ribonucleotide reductase (p53R2), causes severe mitochondrial DNA depletion. *Nat Genet* 39, 776-780.

Bratosin D, Mitrofan L, Palii C, Estaquier J, & Montreuil J (2005). Novel fluorescence assay using calcein-AM for the determination of human erythrocyte viability and aging. *Cytometry A* 66, 78-84.

Brehe JE, Chan AW, Alvey TR, & Burch HB (1976). Effect of methionine sulfoximine on glutathione and amino acid levels in the nephron. *Am J Physiol* 231, 1536-1540.

Brezis M, Rosen S, Silva P, & Epstein FH (1984a). Selective vulnerability of the medullary thick ascending limb to anoxia in the isolated perfused rat kidney. *J Clin Invest* 73, 182-190.

Brezis M, Rosen S, Spokes K, Silva P, & Epstein FH (1984b). Transport-dependent anoxic cell injury in the isolated perfused rat kidney. *Am J Pathol* 116, 327-341.

Brezis M, Shanley P, Silva P, Spokes K, Lear S, Epstein FH, & Rosen S (1985). Disparate mechanisms for hypoxic cell injury in different nephron segments. Studies in the isolated perfused rat kidney. *J Clin Invest* 76, 1796-1806.

Brinkley BR, Barham SS, Barranco SC, & Fuller GM (1974). Rotenone inhibition of spindle microtubule assembly in mammalian cells. *Exp Cell Res* 85, 41-46.

Brodehl J (1992). Fanconi syndrome., ed. Edelmann CM, pp. 1841-1872. Little Brown, Boston.

Brown WM, George M, Jr., & Wilson AC (1979). Rapid evolution of animal mitochondrial DNA. *Proc Natl Acad Sci U S A* 76, 1967-1971.

Brun & Munck (1957). Lesions of the kidney in acute renal failure following shock. *Lancet* 272, 603-607.

Bussolati B, Tetta C, & Camussi G (2008). Contribution of stem cells to kidney repair. *Am J Nephrol* 28, 813-822.

Calcraft PJ, Ruas M, Pan Z, Cheng X, Arredouani A, Hao X, Tang J, Rietdorf K, Teboul L, Chuang KT, Lin P, Xiao R, Wang C, Zhu Y, Lin Y, Wyatt CN, Parrington J, Ma J, Evans AM, Galione A, & Zhu MX (2009). NAADP mobilizes calcium from acidic organelles through two-pore channels. *Nature* 459, 596-600.

Camello-Almaraz C, Salido GM, Pariente JA, & Camello PJ (2002). Role of mitochondria in Ca^{2+} oscillations and shape of Ca^{2+} signals in pancreatic acinar cells. *Biochem Pharmacol* 63, 283-292.

Campanella M, Casswell E, Chong S, Farah Z, Wieckowski MR, Abramov AY, Tinker A, & Duchen MR (2008). Regulation of mitochondrial structure and function by the F_1F_0 -ATPase inhibitor protein, IF1. *Cell Metab* 8, 13-25.

Campanella M, Seraphim A, Abeti R, Casswell E, Echave P, & Duchen MR (2009). IF1, the endogenous regulator of the F_1F_0 -ATP synthase, defines mitochondrial volume fraction in HeLa cells by regulating autophagy. *Biochim Biophys Acta*.

Carvou N, Norden AG, Unwin RJ, & Cockcroft S (2007). Signalling through phospholipase C interferes with clathrin-mediated endocytosis. *Cell Signal* 19, 42-51.

Cetinkaya I, Schlatter E, Hirsch JR, Herter P, Harms E, & Kleta R (2002). Inhibition of Na^{+} -dependent transporters in cystine-loaded human renal cells: electrophysiological studies on the Fanconi syndrome of cystinosis. *J Am Soc Nephrol* 13, 2085-2093.

Chelikani P, Fita I, & Loewen PC (2004). Diversity of structures and properties among catalases. *Cell Mol Life Sci* 61, 192-208.

Chomyn A, Martinuzzi A, Yoneda M, Daga A, Hurko O, Johns D, Lai ST, Nonaka I, Angelini C, & Attardi G (1992). MELAS mutation in mtDNA binding site for transcription termination factor causes defects in protein synthesis and in respiration but no change in levels of upstream and downstream mature transcripts. *Proc Natl Acad Sci U S A* 89, 4221-4225.

Christensen EI, Devuyst O, Dom G, Nielsen R, Van der SP, Verroust P, Leruth M, Guggino WB, & Courtoy PJ (2003). Loss of chloride channel CLC-5 impairs endocytosis by defective trafficking of megalin and cubilin in kidney proximal tubules. *Proc Natl Acad Sci U S A* 100, 8472-8477.

Christensen EI & Gburek J (2004). Protein reabsorption in renal proximal tubule-function and dysfunction in kidney pathophysiology. *Pediatr Nephrol* 19, 714-721.

Ciancio G, Pollack A, Taupier MA, Block NL, & Irvin GL, III (1988). Measurement of cell-cycle phase-specific cell death using Hoechst 33342 and propidium iodide: preservation by ethanol fixation. *J Histochem Cytochem* 36, 1147-1152.

Cihlar T, Ho ES, Lin DC, & Mulato AS (2001). Human renal organic anion transporter 1 (hOAT1) and its role in the nephrotoxicity of antiviral nucleotide analogs. *Nucleosides Nucleotides Nucleic Acids* 20, 641-648.

Clague MJ, Urbe S, Aniento F, & Gruenberg J (1994). Vacuolar ATPase activity is required for endosomal carrier vesicle formation. *J Biol Chem* 269, 21-24.

Clarke BL & Weigel PH (1985). Recycling of the asialoglycoprotein receptor in isolated rat hepatocytes. ATP depletion blocks receptor recycling but not a single round of endocytosis. *J Biol Chem* 260, 128-133.

Conaldi PG, Biancone L, Bottelli A, Wade-Evans A, Racusen LC, Boccellino M, Orlandi V, Serra C, Camussi G, & Toniolo A (1998). HIV-1 kills renal tubular epithelial cells in vitro by triggering an apoptotic pathway involving caspase activation and Fas upregulation. *J Clin Invest* 102, 2041-2049.

Coor C, Salmon RF, Quigley R, Marver D, & Baum M (1991). Role of adenosine triphosphate (ATP) and NaK ATPase in the inhibition of proximal tubule transport with intracellular cystine loading. *J Clin Invest* 87, 955-961.

Cote HC, Magil AB, Harris M, Scarth BJ, Gadawski I, Wang N, Yu E, Yip B, Zalunardo N, Werb R, Hogg R, Harrigan PR, & Montaner JS (2006). Exploring mitochondrial nephrotoxicity as a potential mechanism of kidney dysfunction among HIV-infected patients on highly active antiretroviral therapy. *Antivir Ther* 11, 79-86.

Dada LA, Chandel NS, Ridge KM, Pedemonte C, Bertorello AM, & Sznajder JI (2003). Hypoxia-induced endocytosis of Na,K-ATPase in alveolar epithelial cells is mediated by mitochondrial reactive oxygen species and PKC-zeta. *J Clin Invest* 111, 1057-1064.

Davenport A (2004). Carnitine: a false dawn in the treatment of muscle weakness in end-stage renal failure patients? *Nephron Clin Pract* 97, c33-c34.

Davey PG & Gosling P (1982). beta 2-Microglobulin instability in pathological urine. *Clin Chem* 28, 1330-1333.

de la Prada FJ, Prados AM, Tugores A, Uriol M, Saus C, & Morey A (2006). [Acute renal failure and proximal renal tubular dysfunction in a patient with acquired immunodeficiency syndrome treated with tenofovir]. *Nefrologia* 26, 626-630.

Delplace M (1983). [Renal manifestations of Sjogren's syndrome. Review of the literature starting with a case]. *Sem Hop* 59, 1693-1698.

Denk W & Svoboda K (1997). Photon upmanship: why multiphoton imaging is more than a gimmick. *Neuron* 18, 351-357.

Dhani SU, Kim CP, Huan LJ, & Bear CE (2008). ATP depletion inhibits the endocytosis of ClC-2. *J Cell Physiol* 214, 273-280.

Di VF, Steinberg TH, & Silverstein SC (1990). Inhibition of Fura-2 sequestration and secretion with organic anion transport blockers. *Cell Calcium* 11, 57-62.

DiCataldo A., Palumbo M, Pittala D, Renis M, Schiliro G, Russo A, Ragusa R, Mollica F, & Li VS (1999). Deletions in the mitochondrial DNA and decrease in the oxidative phosphorylation activity of children with Fanconi syndrome secondary to antineoplastic therapy. *Am J Kidney Dis* 34, 98-106.

Dickie P, Felser J, Eckhaus M, Bryant J, Silver J, Marinos N, & Notkins AL (1991). HIV-associated nephropathy in transgenic mice expressing HIV-1 genes. *Virology* 185, 109-119.

Diesel W, Emms M, Knight BK, Noakes TD, Swanepoel CR, van Zyl SR, Kaschula RO, & Sinclair-Smith CC (1993). Morphologic features of the myopathy associated with chronic renal failure. *Am J Kidney Dis* 22, 677-684.

Diomedes-Camassei F, Di GS, Santorelli FM, Caridi G, Piemonte F, Montini G, Ghiggeri GM, Murer L, Barisoni L, Pastore A, Muda AO, Valente ML, Bertini E, & Emma F (2007). COQ2 Nephropathy: A Newly Described Inherited Mitochondriopathy with Primary Renal Involvement. *J Am Soc Nephrol* 18, 2773-2780.

Drube J, Schiffer E, Mischak H, Kemper MJ, Neuhaus T, Pape L, Lichtinghagen R, & Ehrich JH (2009). Urinary proteome pattern in children with renal Fanconi syndrome. *Nephrol Dial Transplant*.

Duchen MR (2004). Mitochondria in health and disease: perspectives on a new mitochondrial biology. *Mol Aspects Med* 25, 365-451.

Duchen MR & Biscoe TJ (1992). Relative mitochondrial membrane potential and $[Ca^{2+}]_i$ in type I cells isolated from the rabbit carotid body. *J Physiol* 450, 33-61.

Duchen MR, Surin A, & Jacobson J (2003). Imaging mitochondrial function in intact cells. *Methods Enzymol* 361, 353-389.

Dumollard R, Duchen M, & Carroll J (2007). The role of mitochondrial function in the oocyte and embryo. *Curr Top Dev Biol* 77, 21-49.

Dyall SD, Brown MT, & Johnson PJ (2004). Ancient invasions: from endosymbionts to organelles. *Science* 304, 253-257.

Edelstein CL, Alkhunaizi AA, & Schrier RW (1997). The role of calcium in the pathogenesis of acute renal failure. *Ren Fail* 19, 199-207.

Elkjaer ML, Birn H, Agre P, Christensen EI, & Nielsen S (1995). Effects of microtubule disruption on endocytosis, membrane recycling and polarized distribution of Aquaporin-1 and gp330 in proximal tubule cells. *Eur J Cell Biol* 67, 57-72.

Fatokun AA, Stone TW, & Smith RA (2008). Oxidative stress in neurodegeneration and available means of protection. *Front Biosci* 13, 3288-3311.

Feldkamp T, Kribben A, & Weinberg JM (2005a). F1FO-ATPase activity and ATP dependence of mitochondrial energization in proximal tubules after hypoxia/reoxygenation. *J Am Soc Nephrol* 16, 1742-1751.

Feldkamp T, Kribben A, & Weinberg JM (2005b). Assessment of mitochondrial membrane potential in proximal tubules after hypoxia-reoxygenation. *Am J Physiol Renal Physiol* 288, F1092-F1102.

Feldkamp T, Weinberg JM, Horbelt M, Von KC, Witzke O, Nurnberger J, & Kribben A (2009). Evidence for involvement of nonesterified fatty acid-induced protonophoric uncoupling during mitochondrial dysfunction caused by hypoxia and reoxygenation. *Nephrol Dial Transplant* 24, 43-51.

Foley RN, Parfrey PS, & Sarnak MJ (1998). Clinical epidemiology of cardiovascular disease in chronic renal disease. *Am J Kidney Dis* 32, S112-S119.

Follmann K, Arnold S, Ferguson-Miller S, & Kadenbach B (1998). Cytochrome c oxidase from eucaryotes but not from procaryotes is allosterically inhibited by ATP. *Biochem Mol Biol Int* 45, 1047-1055.

Foreman JW, Benson LL, Wellons M, Avner ED, Sweeney W, Nissim I, & Nissim I (1995). Metabolic studies of rat renal tubule cells loaded with cystine: the cystine dimethylester model of cystinosis. *J Am Soc Nephrol* 6, 269-272.

Franzini-Armstrong C & Protasi F (1997). Ryanodine receptors of striated muscles: a complex channel capable of multiple interactions. *Physiol Rev* 77, 699-729.

Friedman AL, Trygstad CW, & Chesney RW (1978). Autosomal dominant Fanconi syndrome with early renal failure. *Am J Med Genet* 2, 225-232.

Gamelin LM & Zager RA (1988). Evidence against oxidant injury as a critical mediator of postischemic acute renal failure. *Am J Physiol* 255, F450-F460.

Garcia JJ, Morales-Rios E, Cortes-Hernandez P, & Rodriguez-Zavala JS (2006). The inhibitor protein (IF1) promotes dimerization of the mitochondrial F1F0-ATP synthase. *Biochemistry* 45, 12695-12703.

Gatanaga H, Tachikawa N, Kikuchi Y, Teruya K, Genka I, Honda M, Tanuma J, Yazaki H, Ueda A, Kimura S, & Oka S (2006). Urinary beta2-microglobulin as a possible sensitive marker for renal injury caused by tenofovir disoproxil fumarate. *AIDS Res Hum Retroviruses* 22, 744-748.

Gekle M, Mildenerger S, Freudinger R, Schwerdt G, & Silbernagl S (1997). Albumin endocytosis in OK cells: dependence on actin and microtubules and regulation by protein kinases. *Am J Physiol* 272, F668-F677.

Gekle M, Mildenerger S, Freudinger R, & Silbernagl S (1995). Endosomal alkalization reduces Jmax and Km of albumin receptor-mediated endocytosis in OK cells. *Am J Physiol* 268, F899-F906.

Gerbitz KD, van den Ouweland JM, Maassen JA, & Jaksch M (1995). Mitochondrial diabetes mellitus: a review. *Biochim Biophys Acta* 1271, 253-260.

Ghiculescu RA & Kubler PA (2006). Aminoglycoside-associated Fanconi syndrome. *Am J Kidney Dis* 48, e89-e93.

Gill PS & Wilcox CS (2006). NADPH oxidases in the kidney. *Antioxid Redox Signal* 8, 1597-1607.

Ginsberg JM, Chang BS, Matarese RA, & Garella S (1983). Use of single voided urine samples to estimate quantitative proteinuria. *N Engl J Med* 309, 1543-1546.

Gluck SL, Underhill DM, Iyori M, Holliday LS, Kostrominova TY, & Lee BS (1996). Physiology and biochemistry of the kidney vacuolar H⁺-ATPase. *Annu Rev Physiol* 58, 427-445.

Goltz JS, Wolkoff AW, Novikoff PM, Stockert RJ, & Satir P (1992). A role for microtubules in sorting endocytic vesicles in rat hepatocytes. *Proc Natl Acad Sci U S A* 89, 7026-7030.

Gonzalez-Flecha B & Boveris A (1995). Mitochondrial sites of hydrogen peroxide production in reperused rat kidney cortex. *Biochim Biophys Acta* 1243, 361-366.

Gorell JM, Johnson CC, Rybicki BA, Peterson EL, & Richardson RJ (1998). The risk of Parkinson's disease with exposure to pesticides, farming, well water, and rural living. *Neurology* 50, 1346-1350.

Green DW & Grover GJ (2000). The IF(1) inhibitor protein of the mitochondrial F(1)F(0)-ATPase. *Biochim Biophys Acta* 1458, 343-355.

Griffith OW & Meister A (1979). Glutathione: interorgan translocation, turnover, and metabolism. *Proc Natl Acad Sci U S A* 76, 5606-5610.

Griner RD & Schnellmann RG (1994). Decreasing glycolysis increases sensitivity to mitochondrial inhibition in primary cultures of renal proximal tubule cells. *In Vitro Cell Dev Biol Anim* 30A, 30-34.

Gruber J, Schaffer S, & Halliwell B (2008). The mitochondrial free radical theory of ageing--where do we stand? *Front Biosci* 13, 6554-6579.

Gstraunthaler G, Seppi T, & Pfaller W (1999). Impact of culture conditions, culture media volumes, and glucose content on metabolic properties of renal epithelial cell cultures. Are renal cells in tissue culture hypoxic? *Cell Physiol Biochem* 9, 150-172.

Guarnieri G, Situlin R, & Biolo G (2001). Carnitine metabolism in uremia. *Am J Kidney Dis* 38, S63-S67.

Gucer S, Talim B, Asan E, Korkusuz P, Ozen S, Unal S, Kalkanoglu SH, Kale G, & Caglar M (2005). Focal segmental glomerulosclerosis associated with mitochondrial cytopathy: report of two cases with special emphasis on podocytes. *Pediatr Dev Pathol* 8, 710-717.

Guery B, Choukroun G, Noel LH, Clavel P, Rotig A, Lebon S, Rustin P, Bellane-Chantelot C, Mougenot B, Grunfeld JP, & Chauveau D (2003). The spectrum of systemic involvement in adults presenting with renal lesion and mitochondrial tRNA(Leu) gene mutation. *J Am Soc Nephrol* 14, 2099-2108.

Guillausseau PJ, Massin P, Dubois-LaFargue D, Timsit J, Virally M, Gin H, Bertin E, Blickle JF, Bouhanick B, Cahen J, Caillat-Zucman S, Charpentier G, Chedin P, Derrien C, Ducluzeau PH, Grimaldi A, Guerci B, Kaloustian E, Murat A, Olivier F, Paques M, Paquis-Flucklinger V, Porokhov B, Samuel-Lajeunesse J, & Vialettes B (2001). Maternally inherited diabetes and deafness: a multicenter study. *Ann Intern Med* 134, 721-728.

Gullans SR, Brazy PC, Soltoff SP, Dennis VW, & Mandel LJ (1982). Metabolic inhibitors: effects on metabolism and transport in the proximal tubule. *AJP - Renal Physiology* 243, F133-F140.

Gutmann EJ, Niles JL, McCluskey RT, & Brown D (1989). Colchicine-induced redistribution of an apical membrane glycoprotein (gp330) in proximal tubules. *Am J Physiol* 257, C397-C407.

Hackbarth H, Buttner D, Jarck D, Pothmann M, Messow C, & Gartner K (1983). Distribution of glomeruli in the renal cortex of Munich Wistar Fromter (MWF) rats. *Ren Physiol* 6, 63-71.

Hagiwara M, Yamagata K, Capaldi RA, & Koyama A (2006). Mitochondrial dysfunction in focal segmental glomerulosclerosis of puromycin aminonucleoside nephrosis. *Kidney Int* 69, 1146-1152.

Hall AM, Unwin RJ, Hanna MG, & Duchon MR (2008). Renal function and mitochondrial cytopathy (MC): more questions than answers? *QJM* 101, 755-766.

Hall AM, Unwin RJ, Parker N, & Duchon MR (2009). Multiphoton imaging reveals differences in mitochondrial function between nephron segments. *J Am Soc Nephrol* 20, 1293-1302.

Hamm-Alvarez SF & Sheetz MP (1998). Microtubule-dependent vesicle transport: modulation of channel and transporter activity in liver and kidney. *Physiol Rev* 78, 1109-1129.

Hansrote S, Croul S, Selak M, Kalman B, & Schwartzman RJ (2002). External ophthalmoplegia with severe progressive multiorgan involvement associated with the mtDNA A3243G mutation. *J Neurol Sci* 197, 63-67.

Hariharakrishnan J, Satpute RM, Prasad GB, & Bhattacharya R (2009). Oxidative stress mediated cytotoxicity of cyanide in LLC-MK2 cells and its attenuation by alpha-ketoglutarate and N-acetyl cysteine. *Toxicol Lett* 185, 132-141.

Headley RN, King JS, Jr., Cooper MR, & Felts JH (1972). Multiple myeloma presenting as adult Fanconi syndrome. *Clin Chem* 18, 293-295.

Helm M, Florentz C, Chomyn A, & Attardi G (1999). Search for differences in post-transcriptional modification patterns of mitochondrial DNA-encoded wild-type and mutant human tRNA^{Lys} and tRNA^{Leu}(UUR). *Nucleic Acids Res* 27, 756-763.

Hervouet E & Godinot C (2006). Mitochondrial disorders in renal tumors. *Mitochondrion* 6, 105-117.

Hirst J, King MS, & Pryde KR (2008). The production of reactive oxygen species by complex I. *Biochem Soc Trans* 36, 976-980.

Holthofer H, Kretzler M, Haltia A, Solin ML, Taanman JW, Schagger H, Kriz W, Kerjaschki D, & Schlondorff D (1999). Altered gene expression and functions of mitochondria in human nephrotic syndrome. *FASEB J* 13, 523-532.

Hong SK, Haspel HC, Sonenberg M, & Goldinger JM (1983). Effects of gossypol on PAH transport in the rabbit kidney slice. *Toxicol Appl Pharmacol* 71, 430-435.

Hoopes RR, Jr., Shrimpton AE, Knohl SJ, Hueber P, Hoppe B, Matyus J, Simckes A, Tasic V, Toenshoff B, Suchy SF, Nussbaum RL, & Scheinman SJ (2005). Dent Disease with mutations in OCRL1. *Am J Hum Genet* 76, 260-267.

Horbelt M, Wotzlaw C, Sutton TA, Molitoris BA, Philipp T, Kribben A, Fandrey J, & Pietruck F (2007). Organic cation transport in the rat kidney in vivo visualized by time-resolved two-photon microscopy. *Kidney Int* 72, 422-429.

Hoschele D (2006). Cell culture models for the investigation of NRTI-induced mitochondrial toxicity. Relevance for the prediction of clinical toxicity. *Toxicol In Vitro* 20, 535-546.

Hsu BY, Wehrli SL, Yandrasitz JR, Fenstermacher EA, Palmieri MJ, Rea CT, McNamara PD, Bovee KC, & Segal S (1994). Renal brush border membrane lipid

composition in Basenji dogs with spontaneous idiopathic Fanconi syndrome. *Metabolism* 43, 1073-1078.

Huisman MT, Smit JW, Crommentuyn KM, Zelcer N, Wiltshire HR, Beijnen JH, & Schinkel AH (2002). Multidrug resistance protein 2 (MRP2) transports HIV protease inhibitors, and transport can be enhanced by other drugs. *AIDS* 16, 2295-2301.

Imai E & Iwatani H (2007). The continuing story of renal repair with stem cells. *J Am Soc Nephrol* 18, 2423-2424.

Imaoka T, Kusuhara H, Adachi M, Schuetz JD, Takeuchi K, & Sugiyama Y (2007). Functional involvement of multidrug resistance-associated protein 4 (MRP4/ABCC4) in the renal elimination of the antiviral drugs adefovir and tenofovir. *Mol Pharmacol* 71, 619-627.

Ino T, Nishioka T, & Miyoshi H (2003). Characterization of inhibitor binding sites of mitochondrial complex I using fluorescent inhibitor. *Biochim Biophys Acta* 1605, 15-20.

Ishibashi F (2006). Chronic high glucose inhibits albumin reabsorption by lysosomal alkalization in cultured porcine proximal tubular epithelial cells (LLC-PK1). *Diabetes Res Clin Pract* 72, 223-230.

Iwasaki N, Babazono T, Tsuchiya K, Tomonaga O, Suzuki A, Togashi M, Ujihara N, Sakka Y, Yokokawa H, Ogata M, Nihei H, & Iwamoto Y (2001). Prevalence of A-to-G mutation at nucleotide 3243 of the mitochondrial tRNA(Leu(UUR)) gene in Japanese patients with diabetes mellitus and end stage renal disease. *J Hum Genet* 46, 330-334.

Izzedine H, Hulot JS, Villard E, Goyenvallée C, Dominguez S, Ghosn J, Valantin MA, Lechat P, & Deray AG (2006). Association between ABCC2 gene haplotypes and tenofovir-induced proximal tubulopathy. *J Infect Dis* 194, 1481-1491.

Izzedine H, Hulot JS, Vittecoq D, Gallant JE, Staszewski S, Launay-Vacher V, Cheng A, & Deray G (2005a). Long-term renal safety of tenofovir disoproxil fumarate in antiretroviral-naïve HIV-1-infected patients. Data from a double-blind randomized active-controlled multicentre study. *Nephrol Dial Transplant* 20, 743-746.

Izzedine H, Launay-Vacher V, & Deray G (2005c). Fanconi syndrome associated with didanosine therapy. *AIDS* 19, 844-845.

Izzedine H, Launay-Vacher V, & Deray G (2005b). Antiviral drug-induced nephrotoxicity. *Am J Kidney Dis* 45, 804-817.

Izzedine H, Launay-Vacher V, Isnard-Bagnis C, & Deray G (2003). Drug-induced Fanconi's syndrome. *Am J Kidney Dis* 41, 292-309.

Jacobson J, Duchen MR, Hothersall J, Clark JB, & Heales SJ (2005). Induction of mitochondrial oxidative stress in astrocytes by nitric oxide precedes disruption of energy metabolism. *J Neurochem* 95, 388-395.

Jager S, Handschin C, St-Pierre J, & Spiegelman BM (2007). AMP-activated protein kinase (AMPK) action in skeletal muscle via direct phosphorylation of PGC-1alpha. *Proc Natl Acad Sci U S A* 104, 12017-12022.

James AM, Wei YH, Pang CY, & Murphy MP (1996). Altered mitochondrial function in fibroblasts containing MELAS or MERRF mitochondrial DNA mutations. *Biochem J* 318 (Pt 2), 401-407.

Jin M & Snider MD (1993). Role of microtubules in transferrin receptor transport from the cell surface to endosomes and the Golgi complex. *J Biol Chem* 268, 18390-18397.

Jobsis PD, Rothstein EC, & Balaban RS (2007). Limited utility of acetoxymethyl (AM)-based intracellular delivery systems, in vivo: interference by extracellular esterases. *J Microsc* 226, 74-81.

Jones R, Stebbing J, Nelson M, Moyle G, Bower M, Mandalia S, & Gazzard B (2004). Renal dysfunction with tenofovir disoproxil fumarate-containing highly active antiretroviral therapy regimens is not observed more frequently: a cohort and case-control study. *J Acquir Immune Defic Syndr* 37, 1489-1495.

Juncos R & Garvin JL (2005). Superoxide enhances Na-K-2Cl cotransporter activity in the thick ascending limb. *Am J Physiol Renal Physiol* 288, F982-F987.

Kabanda A, Vandercam B, Bernard A, Lauwerys R, & van Ypersele de SC (1996). Low molecular weight proteinuria in human immunodeficiency virus-infected patients. *Am J Kidney Dis* 27, 803-808.

Kadenbach B (2003). Intrinsic and extrinsic uncoupling of oxidative phosphorylation. *Biochim Biophys Acta* 1604, 77-94.

Kadenbach B & Arnold S (1999). A second mechanism of respiratory control. *FEBS Lett* 447, 131-134.

Kaissling B & Kriz W (1979). Structural analysis of the rabbit kidney. *Adv Anat Embryol Cell Biol* 56, 1-123.

Kalansooriya A, Holbrook I, Jennings P, & Whiting PH (2007). Serum cystatin C, enzymuria, tubular proteinuria and early renal insult in type 2 diabetes. *Br J Biomed Sci* 64, 121-123.

Kannel WB, Stampfer MJ, Castelli WP, & Verter J (1984). The prognostic significance of proteinuria: the Framingham study. *Am Heart J* 108, 1347-1352.

Karadottir R, Cavelier P, Bergersen LH, & Attwell D (2005). NMDA receptors are expressed in oligodendrocytes and activated in ischaemia. *Nature* 438, 1162-1166.

Kastner C, Pohl M, Sendeski M, Stange G, Wagner CA, Jensen BL, Patzak A, Bachmann S, & Theilig F (2009). Effects of receptor-mediated endocytosis and tubular protein composition on volume retention in experimental glomerulonephritis. *Am J Physiol Renal Physiol*.

Keelan J, Allen NJ, Antcliff D, Pal S, & Duchon MR (2001). Quantitative imaging of glutathione in hippocampal neurons and glia in culture using monochlorobimane. *J Neurosci Res* 66, 873-884.

Kempson SA, Kunkler KJ, & Murer H (1991). Iodoacetate action on endocytic uptake of different fluid-phase markers by OK renal epithelial cells. *Biochim Biophys Acta* 1091, 324-328.

Khan SM, Smigrodzki RM, & Swerdlow R (2006). Cell and Animal Models of mtDNA Biology: Progress and Prospects. *Am J Physiol Cell Physiol*.

Kim JW & Dang CV (2006). Cancer's molecular sweet tooth and the Warburg effect. *Cancer Res* 66, 8927-8930.

Kinai E & Hanabusa H (2005). Renal tubular toxicity associated with tenofovir assessed using urine-beta 2 microglobulin, percentage of tubular reabsorption of phosphate and alkaline phosphatase levels. *AIDS* 19, 2031-2033.

Kirichok Y, Krapivinsky G, & Clapham DE (2004). The mitochondrial calcium uniporter is a highly selective ion channel. *Nature* 427, 360-364.

Knepper MA, Wade JB, Terris J, Ecelbarger CA, Marples D, Mandon B, Chou CL, Kishore BK, & Nielsen S (1996). Renal aquaporins. *Kidney Int* 49, 1712-1717.

Koeppen BM, Giebisch G, & Biagi BA (1983). Electrophysiology of mammalian renal tubules: inferences from intracellular microelectrode studies. *Annu Rev Physiol* 45, 497-517.

Kohler JJ, Hosseini SH, Hoying-Brandt A, Green E, Johnson DM, Russ R, Tran D, Raper CM, Santoianni R, & Lewis W (2009). Tenofovir renal toxicity targets mitochondria of renal proximal tubules. *Lab Invest* 89, 513-519.

Korn ED, Carlier MF, & Pantaloni D (1987). Actin polymerization and ATP hydrolysis. *Science* 238, 638-644.

Kozyraki R, Fyfe J, Verroust PJ, Jacobsen C, Utry-Varsat A, Gburek J, Willnow TE, Christensen EI, & Moestrup SK (2001). Megalin-dependent cubilin-mediated endocytosis is a major pathway for the apical uptake of transferrin in polarized epithelia. *Proc Natl Acad Sci U S A* 98, 12491-12496.

Kozyraki R, Kristiansen M, Silahtaroglu A, Hansen C, Jacobsen C, Tommerup N, Verroust PJ, & Moestrup SK (1998). The human intrinsic factor-vitamin B12 receptor, cubilin: molecular characterization and chromosomal mapping of the gene to 10p within the autosomal recessive megaloblastic anemia (MGA1) region. *Blood* 91, 3593-3600.

Krauss S, Zhang CY, & Lowell BB (2005). The mitochondrial uncoupling-protein homologues. *Nat Rev Mol Cell Biol* 6, 248-261.

Kujoth GC, Hiona A, Pugh TD, Someya S, Panzer K, Wohlgemuth SE, Hofer T, Seo AY, Sullivan R, Jobling WA, Morrow JD, Van RH, Sedivy JM, Yamasoba T, Tanokura M, Weindruch R, Leeuwenburgh C, & Prolla TA (2005). Mitochondrial DNA mutations, oxidative stress, and apoptosis in mammalian aging. *Science* 309, 481-484.

Kushnareva Y, Murphy AN, & Andreyev A (2002). Complex I-mediated reactive oxygen species generation: modulation by cytochrome c and NAD(P)⁺ oxidation-reduction state. *Biochem J* 368, 545-553.

Ladewig T, Kloppenburg P, Lalley PM, Zipfel WR, Webb WW, & Keller BU (2003). Spatial profiles of store-dependent calcium release in motoneurons of the nucleus hypoglossus from newborn mouse. *J Physiol* 547, 775-787.

Lapsley M, Akers K, & Norden AG (1998). Sensitive assays for urinary retinol-binding protein and beta-2-glycoprotein-1 based on commercially available standards. *Ann Clin Biochem* 35 (Pt 1), 115-119.

Larkin JM, Donzell WC, & Anderson RG (1985). Modulation of intracellular potassium and ATP: effects on coated pit function in fibroblasts and hepatocytes. *J Cell Physiol* 124, 372-378.

Lash LH (2005). Role of glutathione transport processes in kidney function. *Toxicol Appl Pharmacol* 204, 329-342.

Lash LH, Hagen TM, & Jones DP (1986). Exogenous glutathione protects intestinal epithelial cells from oxidative injury. *Proc Natl Acad Sci U S A* 83, 4641-4645.

Lash LH & Tokarz JJ (1990). Oxidative stress in isolated rat renal proximal and distal tubular cells. *Am J Physiol* 259, F338-F347.

Launay-Vacher V, Izzedine H, Karie S, Hulot JS, Baumelou A, & Deray G (2006). Renal tubular drug transporters. *Nephron Physiol* 103, 97-106.

LeBel CP, Ischiropoulos H, & Bondy SC (1992). Evaluation of the probe 2',7'-dichlorofluorescein as an indicator of reactive oxygen species formation and oxidative stress. *Chem Res Toxicol* 5, 227-231.

Lee I, Bender E, Arnold S, & Kadenbach B (2001). New control of mitochondrial membrane potential and ROS formation--a hypothesis. *Biol Chem* 382, 1629-1636.

Lee JB & Peter HM (1969). Effect of oxygen tension on glucose metabolism in rabbit kidney cortex and medulla. *Am J Physiol* 217, 1464-1471.

Lee YJ & Han HJ (2006). Role of ATP in DNA synthesis of renal proximal tubule cells: involvement of calcium, MAPKs, and CDKs. *Am J Physiol Renal Physiol* 291, F98-106.

Lee YJ, Park SH, Jeung TO, Kim KW, Lee JH, & Han HJ (2005). Effect of adenosine triphosphate on phosphate uptake in renal proximal tubule cells: involvement of PKC and p38 MAPK. *J Cell Physiol* 205, 68-76.

Leheste JR, Rolinski B, Vorum H, Hilpert J, Nykjaer A, Jacobsen C, Aucouturier P, Moskaug JO, Otto A, Christensen EI, & Willnow TE (1999). Megalin knockout mice as an animal model of low molecular weight proteinuria. *Am J Pathol* 155, 1361-1370.

Levey AS, Bosch JP, Lewis JB, Greene T, Rogers N, & Roth D (1999). A more accurate method to estimate glomerular filtration rate from serum creatinine: a new prediction equation. Modification of Diet in Renal Disease Study Group. *Ann Intern Med* 130, 461-470.

Lewis W & Dalakas MC (1995). Mitochondrial toxicity of antiviral drugs. *Nat Med* 1, 417-422.

Leyssens A, Nowicky AV, Patterson L, Crompton M, & Duchen MR (1996). The relationship between mitochondrial state, ATP hydrolysis, $[Mg^{2+}]_i$ and $[Ca^{2+}]_i$ studied in isolated rat cardiomyocytes. *J Physiol* 496 (Pt 1), 111-128.

Li JY, Hsieh RH, Peng NJ, Lai PH, Lee CF, Lo YK, & Wei YH (2007). A follow-up study in a Taiwanese family with mitochondrial myopathy, encephalopathy, lactic acidosis and stroke-like episodes syndrome. *J Formos Med Assoc* 106, 528-536.

Li N, Yi FX, Spurrier JL, Bobrowitz CA, & Zou AP (2002). Production of superoxide through NADH oxidase in thick ascending limb of Henle's loop in rat kidney. *Am J Physiol Renal Physiol* 282, F1111-F1119.

Liangos O, Perianayagam MC, Vaidya VS, Han WK, Wald R, Tighiouart H, MacKinnon RW, Li L, Balakrishnan VS, Pereira BJ, Bonventre JV, & Jaber BL (2007). Urinary N-acetyl-beta-(D)-glucosaminidase activity and kidney injury molecule-1 level are associated with adverse outcomes in acute renal failure. *J Am Soc Nephrol* 18, 904-912.

Liao JF & Perkins JP (1993). Differential effects of antimycin A on endocytosis and exocytosis of transferrin also are observed for internalization and externalization of beta-adrenergic receptors. *Mol Pharmacol* 44, 364-370.

Lino M, Binaut R, Noel LH, Patey N, Rustin P, Daniel L, Serpaggi J, Varaut A, Vanhille P, Knebelmann B, Grunfeld JP, & Fakhouri F (2005). Tubulointerstitial nephritis and Fanconi syndrome in primary biliary cirrhosis. *Am J Kidney Dis* 46, e41-e46.

Liu R, Garvin JL, Ren Y, Pagano PJ, & Carretero OA (2007). Depolarization of the macula densa induces superoxide production via NAD(P)H oxidase. *Am J Physiol Renal Physiol* 292, F1867-F1872.

Lonlay P, Valnot I, Barrientos A, Gorbatyuk M, Tzagoloff A, Taanman JW, Benayoun E, Chretien D, Kadhon N, Lombes A, de Baulny HO, Niaudet P, Munnich A, Rustin P, & Rotig A (2001). A mutant mitochondrial respiratory chain

assembly protein causes complex III deficiency in patients with tubulopathy, encephalopathy and liver failure. *Nat Genet* 29, 57-60.

Lopez LC, Schuelke M, Quinzii CM, Kanki T, Rodenburg RJ, Naini A, DiMauro S, & Hirano M (2006). Leigh syndrome with nephropathy and CoQ10 deficiency due to decaprenyl diphosphate synthase subunit 2 (PDSS2) mutations. *Am J Hum Genet* 79, 1125-1129.

Loven DP, Schedl HP, Oberley LW, Wilson HD, Bruch L, & Niehaus CL (1982). Superoxide dismutase activity in the intestine of the streptozotocin-diabetic rat. *Endocrinology* 111, 737-742.

Lowik MM, Hol FA, Steenbergen EJ, Wetzels JF, & van den Heuvel LP (2005). Mitochondrial tRNA^{Leu(UUR)} mutation in a patient with steroid-resistant nephrotic syndrome and focal segmental glomerulosclerosis. *Nephrol Dial Transplant* 20, 336-341.

Lundin AP, Stein RA, Brown CD, LaBelle P, Kalman FS, Delano BG, Heneghan WF, Lazarus NA, Krasnow N, & Friedman EA (1987). Fatigue, acid-base and electrolyte changes with exhaustive treadmill exercise in hemodialysis patients. *Nephron* 46, 57-62.

Maagaard A, Holberg-Petersen M, Kollberg G, Oldfors A, Sandvik L, & Bruun JN (2006). Mitochondrial (mt)DNA changes in tissue may not be reflected by depletion of mtDNA in peripheral blood mononuclear cells in HIV-infected patients. *Antivir Ther* 11, 601-608.

Malik A, Abraham P, & Malik N (2005). Acute renal failure and Fanconi syndrome in an AIDS patient on tenofovir treatment--case report and review of literature. *J Infect* 51, E61-E65.

Mandemakers W, Morais VA, & De SB (2007). A cell biological perspective on mitochondrial dysfunction in Parkinson disease and other neurodegenerative diseases. *J Cell Sci* 120, 1707-1716.

Manwaring N, Jones MM, Wang JJ, Rochtchina E, Howard C, Mitchell P, & Sue CM (2007). Population prevalence of the MELAS A3243G mutation. *Mitochondrion* 7, 230-233.

Marshall LE & Himes RH (1978). Rotenone inhibition of tubulin self-assembly. *Biochim Biophys Acta* 543, 590-594.

Marshansky V, Ausiello DA, & Brown D (2002). Physiological importance of endosomal acidification: potential role in proximal tubulopathies. *Curr Opin Nephrol Hypertens* 11, 527-537.

Martin-Hernandez E, Garcia-Silva MT, Vara J, Campos Y, Cabello A, Muley R, Del Hoyo P, Martin MA, & Arenas J (2005). Renal pathology in children with mitochondrial diseases. *Pediatr Nephrol* 20, 1299-1305.

Mayevsky A & Chance B (2007). Oxidation-reduction states of NADH in vivo: from animals to clinical use. *Mitochondrion* 7, 330-339.

McCormack JG, Halestrap AP, & Denton RM (1990). Role of calcium ions in regulation of mammalian intramitochondrial metabolism. *Physiol Rev* 70, 391-425.

McCray JA, Herbette L, Kihara T, & Trentham DR (1980). A new approach to time-resolved studies of ATP-requiring biological systems; laser flash photolysis of caged ATP. *Proc Natl Acad Sci U S A* 77, 7237-7241.

McDonnell MT, Schaefer AM, Blakely EL, McFarland R, Chinnery PF, Turnbull DM, & Taylor RW (2004). Noninvasive diagnosis of the 3243A > G mitochondrial DNA mutation using urinary epithelial cells. *Eur J Hum Genet* 12, 778-781.

McTigue M, Ting GO, & Weiner MW (1983). Relationship between sodium transport and oxygen consumption in the isolated perfused rat kidney. *Ren Physiol* 6, 112-129.

Miller RF, Shahmonesh M, Hanna MG, Unwin RJ, Schapira AH, & Weller IV (2003). Polyphenotypic expression of mitochondrial toxicity caused by nucleoside reverse transcriptase inhibitors. *Antivir Ther* 8, 253-257.

Mingardi G, Bizzi A, Cini M, Licini R, Mecca G, & Garattini S (1980). Carnitine balance in hemodialyzed patients. *Clin Nephrol* 13, 269-270.

Mirabella M, Di GS, Silvestri G, Tonali P, & Servidei S (2000). Apoptosis in mitochondrial encephalomyopathies with mitochondrial DNA mutations: a potential pathogenic mechanism. *Brain* 123 (Pt 1), 93-104.

Miro O, Marrades RM, Roca J, Sala E, Masanes F, Campistol JM, Torregrosa JV, Casademont J, Wagner PD, & Cardellach F (2002). Skeletal muscle mitochondrial function is preserved in young patients with chronic renal failure. *Am J Kidney Dis* 39, 1025-1031.

Mishra J, Ma Q, Prada A, Mitsniefes M, Zahedi K, Yang J, Barasch J, & Devarajan P (2003). Identification of neutrophil gelatinase-associated lipocalin as a novel early urinary biomarker for ischemic renal injury. *J Am Soc Nephrol* 14, 2534-2543.

Mitchell P (1961). Coupling of phosphorylation to electron and hydrogen transfer by a chemi-osmotic type of mechanism. *Nature* 191, 144-148.

Moestrup SK, Kozyraki R, Kristiansen M, Kaysen JH, Rasmussen HH, Brault D, Pontillon F, Goda FO, Christensen EI, Hammond TG, & Verroust PJ (1998). The intrinsic factor-vitamin B12 receptor and target of teratogenic antibodies is a megalin-binding peripheral membrane protein with homology to developmental proteins. *J Biol Chem* 273, 5235-5242.

Mohrmann M, Pauli A, Walkenhorst H, Schonfeld B, & Brandis M (1993). Effect of ifosfamide metabolites on sodium-dependent phosphate transport in a model of proximal tubular cells (LLC-PK1) in culture. *Ren Physiol Biochem* 16, 285-298.

Molitoris BA & Sandoval RM (2005). Intravital multiphoton microscopy of dynamic renal processes. *Am J Physiol Renal Physiol* 288, F1084-F1089.

Mollace V, Nottet HS, Clayette P, Turco MC, Muscoli C, Salvemini D, & Perno CF (2001). Oxidative stress and neuroAIDS: triggers, modulators and novel antioxidants. *Trends Neurosci* 24, 411-416.

Moore GE, Parsons DB, Stray-Gundersen J, Painter PL, Brinker KR, & Mitchell JH (1993). Uremic myopathy limits aerobic capacity in hemodialysis patients. *Am J Kidney Dis* 22, 277-287.

Morel-Maroger Striker LJ, D'Amico G, Preud'homme J, & Striker GE (1994). Monoclonal Gammopathies, mixed cryoglobulinemias, and lymphomas. In *Renal Pathology*, eds. Tisher CC & Brenner BM.

Morris RC, Jr. (1968). An experimental renal acidification defect in patients with hereditary fructose intolerance. II. Its distinction from classic renal tubular acidosis; its resemblance to the renal acidification defect associated with the Fanconi syndrome of children with cystinosis. *J Clin Invest* 47, 1648-1663.

Moslemi AR & Darin N (2007). Molecular genetic and clinical aspects of mitochondrial disorders in childhood. *Mitochondrion* 7, 241-252.

Moudy AM, Handran SD, Goldberg MP, Ruffin N, Karl I, Kranz-Eble P, DeVivo DC, & Rothman SM (1995). Abnormal calcium homeostasis and mitochondrial polarization in a human encephalomyopathy. *Proc Natl Acad Sci U S A* 92, 729-733.

Murphy MP (2009). How mitochondria produce reactive oxygen species. *Biochem J* 417, 1-13.

Nakada K, Inoue K, & Hayashi JI (2001). Mito-mice: animal models for mitochondrial DNA-based diseases. *Semin Cell Dev Biol* 12, 459-465.

Nan DN, Fernandez-Ayala M, Infante J, Matorras P, & Gonzalez-Macias J (2002). Progressive cardiomyopathy as manifestation of mitochondrial disease. *Postgrad Med J* 78, 298-299.

Nath KA & Norby SM (2000). Reactive oxygen species and acute renal failure. *Am J Med* 109, 665-678.

Neiberger RE, George JC, Perkins LA, Theriaque DW, Hutson AD, & Stacpoole PW (2002). Renal manifestations of congenital lactic acidosis. *Am J Kidney Dis* 39, 12-23.

Nelson I, Hanna MG, Wood NW, & Harding AE (1997). Depletion of mitochondrial DNA by ddC in untransformed human cell lines. *Somat Cell Mol Genet* 23, 287-290.

Neyfakh AA (1988). Use of fluorescent dyes as molecular probes for the study of multidrug resistance. *Exp Cell Res* 174, 168-176.

Niaudet P (1998). Mitochondrial disorders and the kidney. *Arch Dis Child* 78, 387-390.

Niaudet P & Rotig A (1996). Renal involvement in mitochondrial cytopathies. *Pediatr Nephrol* 10, 368-373.

Niaudet P & Rotig A (1997). The kidney in mitochondrial cytopathies. *Kidney Int* 51, 1000-1007.

Nicholls DG (2006). The physiological regulation of uncoupling proteins. *Biochim Biophys Acta* 1757, 459-466.

Nicholls DG (2004). Mitochondrial membrane potential and aging. *Aging Cell* 3, 35-40.

Nicholls DG & Rial E (1999). A history of the first uncoupling protein, UCP1. *J Bioenerg Biomembr* 31, 399-406.

Niculescu-Duvaz I, Phanish MK, Colville-Nash P, & Dockrell ME (2007). The TGFbeta1-induced fibronectin in human renal proximal tubular epithelial cells is p38 MAP kinase dependent and Smad independent. *Nephron Exp Nephrol* 105, e108-e116.

Nisoli E, Falcone S, Tonello C, Cozzi V, Palomba L, Fiorani M, Pisconti A, Brunelli S, Cardile A, Francolini M, Cantoni O, Carruba MO, Moncada S, & Clementi E (2004). Mitochondrial biogenesis by NO yields functionally active mitochondria in mammals. *Proc Natl Acad Sci U S A* 101, 16507-16512.

Norden AG, Lapsley M, Igarashi T, Kelleher CL, Lee PJ, Matsuyama T, Scheinman SJ, Shiraga H, Sundin DP, Thakker RV, Unwin RJ, Verroust P, & Moestrup SK (2002). Urinary megalin deficiency implicates abnormal tubular endocytic function in Fanconi syndrome. *J Am Soc Nephrol* 13, 125-133.

Norden AG, Lapsley M, Lee PJ, Pusey CD, Scheinman SJ, Tam FW, Thakker RV, Unwin RJ, & Wrong O (2001). Glomerular protein sieving and implications for renal failure in Fanconi syndrome. *Kidney Int* 60, 1885-1892.

Norden AG, Scheinman SJ, schodt-Lanckman MM, Lapsley M, Nortier JL, Thakker RV, Unwin RJ, & Wrong O (2000). Tubular proteinuria defined by a study of Dent's (CLCN5 mutation) and other tubular diseases. *Kidney Int* 57, 240-249.

O'Rourke B, Ramza BM, & Marban E (1994). Oscillations of membrane current and excitability driven by metabolic oscillations in heart cells. *Science* 265, 962-966.

Oates JC, Varghese S, Bland AM, Taylor TP, Self SE, Stanislaus R, Almeida JS, & Arthur JM (2005). Prediction of urinary protein markers in lupus nephritis. *Kidney Int* 68, 2588-2592.

Oberbauer R, Rohrmoser M, Regele H, Muhlbacher F, & Mayer G (1999). Apoptosis of tubular epithelial cells in donor kidney biopsies predicts early renal allograft function. *J Am Soc Nephrol* 10, 2006-2013.

Oda H, Stockert RJ, Collins C, Wang H, Novikoff PM, Satir P, & Wolkoff AW (1995). Interaction of the microtubule cytoskeleton with endocytic vesicles and cytoplasmic dynein in cultured rat hepatocytes. *J Biol Chem* 270, 15242-15249.

Ohnishi ST, Ohnishi T, Muranaka S, Fujita H, Kimura H, Uemura K, Yoshida K, & Utsumi K (2005). A possible site of superoxide generation in the complex I segment of rat heart mitochondria. *J Bioenerg Biomembr* 37, 1-15.

Okun JG, Lummen P, & Brandt U (1999). Three classes of inhibitors share a common binding domain in mitochondrial complex I (NADH:ubiquinone oxidoreductase). *J Biol Chem* 274, 2625-2630.

Pan G, Yang Z, Ballinger SW, & McDonald JM (2006). Pathogenesis of osteopenia/osteoporosis induced by highly active anti-retroviral therapy for AIDS. *Ann N Y Acad Sci* 1068, 297-308.

Papadopoulou LC, Sue CM, Davidson MM, Tanji K, Nishino I, Sadlock JE, Krishna S, Walker W, Selby J, Glerum DM, Coster RV, Lyon G, Scalais E, Lebel R, Kaplan P, Shanske S, De V, Bonilla E, Hirano M, DiMauro S, & Schon EA (1999). Fatal infantile cardioencephalomyopathy with COX deficiency and mutations in SCO2, a COX assembly gene. *Nat Genet* 23, 333-337.

Papaleo A, Warszawski J, Salomon R, Jullien V, Veber F, Dechaux M, & Blanche S (2007). Increased beta-2 microglobulinuria in human immunodeficiency virus-1-infected children and adolescents treated with tenofovir. *Pediatr Infect Dis J* 26, 949-951.

Parrish AE (1981). The effect of minimal exercise on the blood lactate in azotemic subjects. *Clin Nephrol* 16, 35-39.

Parrish AR, Gandolfi AJ, & Brendel K (1995). Precision-cut tissue slices: applications in pharmacology and toxicology. *Life Sci* 57, 1887-1901.

Pavenstadt H, Kriz W, & Kretzler M (2003). Cell biology of the glomerular podocyte. *Physiol Rev* 83, 253-307.

Petersen OH, Michalak M, & Verkhratsky A (2005). Calcium signalling: past, present and future. *Cell Calcium* 38, 161-169.

Petrescu I & Tarba C (1997). Uncoupling effects of diclofenac and aspirin in the perfused liver and isolated hepatic mitochondria of rat. *Biochim Biophys Acta* 1318, 385-394.

Peyriere H, Reynes J, Rouanet I, Daniel N, de Boever CM, Mauboussin JM, Leray H, Moachon L, Vincent D, & Salmon-Ceron D (2004). Renal tubular dysfunction associated with tenofovir therapy: report of 7 cases. *J Acquir Immune Defic Syndr* 35, 269-273.

Pfaller W & Rittinger M (1980). Quantitative morphology of the rat kidney. *Int J Biochem* 12, 17-22.

Piwon N, Gunther W, Schwake M, Bosl MR, & Jentsch TJ (2000). CIC-5 Cl⁻ - channel disruption impairs endocytosis in a mouse model for Dent's disease. *Nature* 408, 369-373.

Plotnikov EY, Kazachenko AV, Vyssokikh MY, Vasileva AK, Tcvirkun DV, Isaev NK, Kirpatovsky VI, & Zorov DB (2007). The role of mitochondria in oxidative and nitrosative stress during ischemia/reperfusion in the rat kidney. *Kidney Int.*

Podbilewicz B & Mellman I (1990). ATP and cytosol requirements for transferrin recycling in intact and disrupted MDCK cells. *EMBO J* 9, 3477-3487.

Price RG (1992). The role of NAG (N-acetyl-beta-D-glucosaminidase) in the diagnosis of kidney disease including the monitoring of nephrotoxicity. *Clin Nephrol* 38 Suppl 1, S14-S19.

Quimby D & Brito MO (2005). Fanconi syndrome associated with use of tenofovir in HIV-infected patients: a case report and review of the literature. *AIDS Read* 15, 357-364.

Quinzii C, Naini A, Salviati L, Trevisson E, Navas P, DiMauro S, & Hirano M (2006). A mutation in para-hydroxybenzoate-polyprenyl transferase (COQ2) causes primary coenzyme Q10 deficiency. *Am J Hum Genet* 78, 345-349.

Rabkin R, Yagil C, & Frank B (1989). Basolateral and apical binding, internalization, and degradation of insulin by cultured kidney epithelial cells. *Am J Physiol* 257, E895-E902.

Rahman S, Hargreaves I, Clayton P, & Heales S (2001). Neonatal presentation of coenzyme Q10 deficiency. *J Pediatr* 139, 456-458.

Raychowdhury R, Niles JL, McCluskey RT, & Smith JA (1989). Autoimmune target in Heymann nephritis is a glycoprotein with homology to the LDL receptor. *Science* 244, 1163-1165.

Reardon W, Ross RJ, Sweeney MG, Luxon LM, Pembrey ME, Harding AE, & Trembath RC (1992). Diabetes mellitus associated with a pathogenic point mutation in mitochondrial DNA. *Lancet* 340, 1376-1379.

Reinecke F, Levanets O, Olivier Y, Louw R, Semete B, Grobler A, Hidalgo J, Smeitink J, Olckers A, & Van der Westhuizen FH (2006). Metallothionein isoform 2A expression is inducible and protects against ROS-mediated cell death in rotenone-treated HeLa cells. *Biochem J* 395, 405-415.

Reitsma-Bierens WC (1993). Renal complications in glycogen storage disease type I. *Eur J Pediatr* 152 Suppl 1, S60-S62.

Ren Y & Feng J (2007). Rotenone selectively kills serotonergic neurons through a microtubule-dependent mechanism. *J Neurochem* 103, 303-311.

Rich PR (2003). The molecular machinery of Keilin's respiratory chain. *Biochem Soc Trans* 31, 1095-1105.

Rifkin BS & Perazella MA (2004). Tenofovir-associated nephrotoxicity: Fanconi syndrome and renal failure. *Am J Med* 117, 282-284.

Robinson KM, Janes MS, Pehar M, Monette JS, Ross MF, Hagen TM, Murphy MP, & Beckman JS (2006). Selective fluorescent imaging of superoxide in vivo using ethidium-based probes. *Proc Natl Acad Sci U S A* 103, 15038-15043.

Roling J, Schmid H, Fischereder M, Draenert R, & Goebel FD (2006). HIV-associated renal diseases and highly active antiretroviral therapy-induced nephropathy. *Clin Infect Dis* 42, 1488-1495.

Rosenberg, Blair, & Segal (1961). Transport of amino acids by slices of rat-kidney cortex. *Biochim Biophys Acta* 54, 479-488.

Roth KS, Carter BE, & Higgins ES (1991). Succinylacetone effects on renal tubular phosphate metabolism: a model for experimental renal Fanconi syndrome. *Proc Soc Exp Biol Med* 196, 428-431.

Rotig A (2003). Renal disease and mitochondrial genetics. *J Nephrol* 16, 286-292.

Rotig A, Appelkvist EL, Geromel V, Chretien D, Kadhon N, Edery P, Lebeideau M, Dallner G, Munnich A, Ernster L, & Rustin P (2000). Quinone-responsive multiple respiratory-chain dysfunction due to widespread coenzyme Q10 deficiency. *Lancet* 356, 391-395.

Rotig A & Munnich A (2003). Genetic features of mitochondrial respiratory chain disorders. *J Am Soc Nephrol* 14, 2995-3007.

Rozell B, Hansson HA, Guthenberg C, Tahir MK, & Mannervik B (1993). Glutathione transferases of classes alpha, mu and pi show selective expression in different regions of rat kidney. *Xenobiotica* 23, 835-849.

Rusanen H, Majamaa K, & Hassinen IE (2000). Increased activities of antioxidant enzymes and decreased ATP concentration in cultured myoblasts with the 3243A-->G mutation in mitochondrial DNA. *Biochim Biophys Acta* 1500, 10-16.

Russo LM, Sandoval RM, Campos SB, Molitoris BA, Comper WD, & Brown D (2009). Impaired tubular uptake explains albuminuria in early diabetic nephropathy. *J Am Soc Nephrol* 20, 489-494.

Russo LM, Sandoval RM, McKee M, Osicka TM, Collins AB, Brown D, Molitoris BA, & Comper WD (2007). The normal kidney filters nephrotic levels of albumin retrieved by proximal tubule cells: retrieval is disrupted in nephrotic states. *Kidney Int* 71, 504-513.

Russo P & O'Regan S (1990). Visceral pathology of hereditary tyrosinemia type I. *Am J Hum Genet* 47, 317-324.

Sabolic I, Valenti G, Verbavatz JM, Van Hoek AN, Verkman AS, Ausiello DA, & Brown D (1992). Localization of the CHIP28 water channel in rat kidney. *Am J Physiol* 263, C1225-C1233.

Sachse A & Wolf G (2007). Angiotensin II-induced reactive oxygen species and the kidney. *J Am Soc Nephrol* 18, 2439-2446.

Sala E, Noyszewski EA, Campistol JM, Marrades RM, Dreha S, Torregrossa JV, Beers JS, Wagner PD, & Roca J (2001). Impaired muscle oxygen transfer in patients with chronic renal failure. *Am J Physiol Regul Integr Comp Physiol* 280, R1240-R1248.

Salviati L, Sacconi S, Murer L, Zacchello G, Franceschini L, Laverda AM, Basso G, Quinzii C, Angelini C, Hirano M, Naini AB, Navas P, DiMauro S, & Montini G (2005). Infantile encephalomyopathy and nephropathy with CoQ10 deficiency: a CoQ10-responsive condition. *Neurology* 65, 606-608.

Sangkhathat S, Kusafuka T, Yoneda A, Kuroda S, Tanaka Y, Sakai N, & Fukuzawa M (2005). Renal cell carcinoma in a pediatric patient with an inherited mitochondrial mutation. *Pediatr Surg Int* 21, 745-748.

Saumoy M, Vidal F, Peraire J, Saulea S, Veia AM, Vilades C, Ribera E, & Richart C (2004). Proximal tubular kidney damage and tenofovir: a role for mitochondrial toxicity? *AIDS* 18, 1741-1742.

Scaglia F, Vogel H, Hawkins EP, Vladutiu GD, Liu LL, & Wong LJ (2003). Novel homoplasmic mutation in the mitochondrial tRNA^{Tyr} gene associated with atypical

mitochondrial cytopathy presenting with focal segmental glomerulosclerosis. *Am J Med Genet A* 123, 172-178.

Schmid SL & Carter LL (1990). ATP is required for receptor-mediated endocytosis in intact cells. *J Cell Biol* 111, 2307-2318.

Schmiedel J, Jackson S, Schafer J, & Reichmann H (2003). Mitochondrial cytopathies. *J Neurol* 250, 267-277.

Schooley RT, Ruane P, Myers RA, Beall G, Lampiris H, Berger D, Chen SS, Miller MD, Isaacson E, & Cheng AK (2002). Tenofovir DF in antiretroviral-experienced patients: results from a 48-week, randomized, double-blind study. *AIDS* 16, 1257-1263.

Schrader J, Luders S, Kulschewski A, Hammersen F, Zuchner C, Venneklaas U, Schrandt G, Schnieders M, Rangoonwala B, Berger J, Dominiak P, & Zidek W (2006). Microalbuminuria and tubular proteinuria as risk predictors of cardiovascular morbidity and mortality in essential hypertension: final results of a prospective long-term study (MARPLE Study)*. *J Hypertens* 24, 541-548.

Schulman JD & Schneider JA (1976). Cystinosis and the Fanconi syndrome. *Pediatr Clin North Am* 23, 779-793.

Schurman SJ & Scheinman SJ (2009). Inherited cerebrorenal syndromes. *Nat Rev Nephrol* 5, 529-538.

Shah AJ, Sahgal V, Quintanilla AP, Subramani V, Singh H, & Hughes R (1983). Muscle in chronic uremia--a histochemical and morphometric study of human quadriceps muscle biopsies. *Clin Neuropathol* 2, 83-89.

Shanley PF, Brezis M, Spokes K, Silva P, Epstein FH, & Rosen S (1986b). Hypoxic injury in the proximal tubule of the isolated perfused rat kidney. *Kidney Int* 29, 1021-1032.

Shanley PF, Brezis M, Spokes K, Silva P, Epstein FH, & Rosen S (1986a). Differential responsiveness of proximal tubule segments to metabolic inhibitors in the isolated perfused rat kidney. *Am J Kidney Dis* 7, 76-83.

Shanley PF, Rosen MD, Brezis M, Silva P, Epstein FH, & Rosen S (1986c). Topography of focal proximal tubular necrosis after ischemia with reflow in the rat kidney. *Am J Pathol* 122, 462-468.

Sherer TB, Betarbet R, Testa CM, Seo BB, Richardson JR, Kim JH, Miller GW, Yagi T, Matsuno-Yagi A, & Greenamyre JT (2003). Mechanism of toxicity in rotenone models of Parkinson's disease. *J Neurosci* 23, 10756-10764.

Shirley DG & Unwin RJ (2005). The structure and function of tubules. In *Oxford Textbook of Clinical Nephrology*, eds. Davison, Grunfeld, Cameron, Ponticelli, Ritz, Winnearls, & Ypersele.

Sidaway JE, Davidson RG, McTaggart F, Orton TC, Scott RC, Smith GJ, & Brunskill NJ (2004). Inhibitors of 3-hydroxy-3-methylglutaryl-CoA reductase reduce receptor-mediated endocytosis in opossum kidney cells. *J Am Soc Nephrol* 15, 2258-2265.

Simeoni M, Boyde A, Shirley DG, Capasso G, & Unwin RJ (2004). Application of red laser video-rate scanning confocal microscopy to in vivo assessment of tubular function in the rat: selective action of diuretics on tubular diameter. *Exp Physiol* 89, 181-185.

Simmons CF, Jr., Bogusky RT, & Humes HD (1980). Inhibitory effects of gentamicin on renal mitochondrial oxidative phosphorylation. *J Pharmacol Exp Ther* 214, 709-715.

Singer M, De S, V, Vitale D, & Jeffcoate W (2004). Multiorgan failure is an adaptive, endocrine-mediated, metabolic response to overwhelming systemic inflammation. *Lancet* 364, 545-548.

Sipos A, Toma I, Kang JJ, Rosivall L, & Peti-Peterdi J (2007). Advances in renal (patho)physiology using multiphoton microscopy. *Kidney Int*.

Skinner R (2003). Chronic ifosfamide nephrotoxicity in children. *Med Pediatr Oncol* 41, 190-197.

Soltoff SP (1986). ATP and the regulation of renal cell function. *Annu Rev Physiol* 48, 9-31.

Spat A, Bradford PG, McKinney JS, Rubin RP, & Putney JW, Jr. (1986). A saturable receptor for 32P-inositol-1,4,5-triphosphate in hepatocytes and neutrophils. *Nature* 319, 514-516.

Sproule DM & Kaufmann P (2008). Mitochondrial encephalopathy, lactic acidosis, and strokelike episodes: basic concepts, clinical phenotype, and therapeutic management of MELAS syndrome. *Ann N Y Acad Sci* 1142, 133-158.

Strauss M, Hofhaus G, Schroder RR, & Kuhlbrandt W (2008). Dimer ribbons of ATP synthase shape the inner mitochondrial membrane. *EMBO J* 27, 1154-1160.

Streb H, Irvine RF, Berridge MJ, & Schulz I (1983). Release of Ca^{2+} from a nonmitochondrial intracellular store in pancreatic acinar cells by inositol-1,4,5-trisphosphate. *Nature* 306, 67-69.

Taanman JW (1999). The mitochondrial genome: structure, transcription, translation and replication. *Biochim Biophys Acta* 1410, 103-123.

Taft DR (2004). The isolated perfused rat kidney model: a useful tool for drug discovery and development. *Curr Drug Discov Technol* 1, 97-111.

Takahashi A, Camacho P, Lechleiter JD, & Herman B (1999). Measurement of intracellular calcium. *Physiol Rev* 79, 1089-1125.

Takebayashi S, Jimi S, Segawa M, & Takaki A (2003). Mitochondrial DNA deletion of proximal tubules is the result of itai-itai disease. *Clin Exp Nephrol* 7, 18-26.

Tallini YN, Ohkura M, Choi BR, Ji G, Imoto K, Doran R, Lee J, Plan P, Wilson J, Xin HB, Sanbe A, Gulick J, Mathai J, Robbins J, Salama G, Nakai J, & Kotlikoff MI (2006). Imaging cellular signals in the heart in vivo: Cardiac expression of the high-signal Ca^{2+} indicator GCaMP2. *Proc Natl Acad Sci U S A* 103, 4753-4758.

Tebas P, Powderly WG, Claxton S, Marin D, Tantisiriwat W, Teitelbaum SL, & Yarasheski KE (2000). Accelerated bone mineral loss in HIV-infected patients receiving potent antiretroviral therapy. *AIDS* 14, F63-F67.

Territo PR, Mootha VK, French SA, & Balaban RS (2000). Ca^{2+} activation of heart mitochondrial oxidative phosphorylation: role of the F(0)/F(1)-ATPase. *Am J Physiol Cell Physiol* 278, C423-C435.

Thakkar H, Lowe PA, Price CP, & Newman DJ (1998). Measurement of the kinetics of protein uptake by proximal tubular cells using an optical biosensor. *Kidney Int* 54, 1197-1205.

Thakker RV (2000). Pathogenesis of Dent's disease and related syndromes of X-linked nephrolithiasis. *Kidney Int* 57, 787-793.

Thirumurugan A, Thewles A, Gilbert RD, Hulton SA, Milford DV, Lote CJ, & Taylor CM (2004). Urinary L-lactate excretion is increased in renal Fanconi syndrome. *Nephrol Dial Transplant* 19, 1767-1773.

Thurau K & Boylan JW (1976). Acute renal success. The unexpected logic of oliguria in acute renal failure. *Am J Med* 61, 308-315.

Tolaymat A, Sakarcan A, & Neiberger R (1992). Idiopathic Fanconi syndrome in a family. Part I. Clinical aspects. *J Am Soc Nephrol* 2, 1310-1317.

Trachootham D, Lu W, Ogasawara MA, Nilsa RD, & Huang P (2008). Redox regulation of cell survival. *Antioxid Redox Signal* 10, 1343-1374.

Trifunovic A, Wredenberg A, Falkenberg M, Spelbrink JN, Rovio AT, Bruder CE, Bohlooly Y, Gidlöf S, Oldfors A, Wibom R, Tornell J, Jacobs HT, & Larsson NG (2004). Premature ageing in mice expressing defective mitochondrial DNA polymerase. *Nature* 429, 417-423.

Trollinger DR, Cascio WE, & Lemasters JJ (1997). Selective loading of Rhod 2 into mitochondria shows mitochondrial Ca²⁺ transients during the contractile cycle in adult rabbit cardiac myocytes. *Biochem Biophys Res Commun* 236, 738-742.

Utsch B, Bokenkamp A, Benz MR, Besbas N, Dotsch J, Franke I, Frund S, Gök F, Hoppe B, Karle S, Kuwertz-Broking E, Laube G, Neb M, Nuutinen M, Ozaltın F, Rascher W, Ring T, Tasic V, van Wijk JA, & Ludwig M (2006). Novel OCRL1 mutations in patients with the phenotype of Dent disease. *Am J Kidney Dis* 48, 942-14.

Valnot I, von Kleist-Retzow JC, Barrientos A, Gorbatyuk M, Taanman JW, Mehaye B, Rustin P, Tzagoloff A, Munnich A, & Rotig A (2000). A mutation in the human heme A:farnesyltransferase gene (COX10) causes cytochrome c oxidase deficiency. *Hum Mol Genet* 9, 1245-1249.

Van't Hoff W (2005). Fanconi syndrome. In *Oxford Textbook of Clinical Nephrology*, eds. Davison, Grunfeld, Cameron, Ponticelli, Ritz, Winearls, & Ypersele, Oxford University Press.

Vaux EC, Taylor DJ, Altmann P, Rajagopalan B, Graham K, Cooper R, Bonomo Y, & Styles P (2004). Effects of carnitine supplementation on muscle metabolism by the use of magnetic resonance spectroscopy and near-infrared spectroscopy in end-stage renal disease. *Nephron Clin Pract* 97, c41-c48.

Verroust PJ, Birn H, Nielsen R, Kozyraki R, & Christensen EI (2002). The tandem endocytic receptors megalin and cubilin are important proteins in renal pathology. *Kidney Int* 62, 745-756.

Vickers AE, Rose K, Fisher R, Saulnier M, Sahota P, & Bentley P (2004). Kidney slices of human and rat to characterize cisplatin-induced injury on cellular pathways and morphology. *Toxicol Pathol* 32, 577-590.

Vidal F, Domingo JC, Guallar J, Saumoy M, Cordobilla B, Sanchez de la RR, Giralt M, Alvarez ML, Lopez-Dupla M, Torres F, Villarroya F, Cihlar T, & Domingo P (2006). In vitro cytotoxicity and mitochondrial toxicity of tenofovir alone and in combination with other antiretrovirals in human renal proximal tubule cells. *Antimicrob Agents Chemother* 50, 3824-3832.

Vilasi A, Cutillas PR, Maher AD, Zirah SF, Capasso G, Norden AW, Holmes E, Nicholson JK, & Unwin RJ (2007). Combined proteomic and metabonomic studies in three genetic forms of the renal Fanconi syndrome. *Am J Physiol Renal Physiol* 293, F456-F467.

Villarroya F, Domingo P, & Giralt M (2007). Lipodystrophy in HIV 1-infected patients: lessons for obesity research. *Int J Obes (Lond)* 31, 1763-1776.

Wada T, Tanji N, Ozawa A, Wang J, Shimamoto K, Sakayama K, & Yokoyama M (2006). Mitochondrial DNA mutations and 8-hydroxy-2'-deoxyguanosine Content in Japanese patients with urinary bladder and renal cancers. *Anticancer Res* 26, 3403-3408.

Wahlstedt-Froberg V, Pettersson T, Aminoff M, Dugue B, & Grasbeck R (2003). Proteinuria in cubilin-deficient patients with selective vitamin B12 malabsorption. *Pediatr Nephrol* 18, 417-421.

Walsh SB, Shirley DG, Wrong OM, & Unwin RJ (2007). Urinary acidification assessed by simultaneous furosemide and fludrocortisone treatment: an alternative to ammonium chloride. *Kidney Int* 71, 1310-1316.

Walton RJ & Bijvoet OL (1975). Nomogram for derivation of renal threshold phosphate concentration. *Lancet* 2, 309-310.

Wang SS, Devuyst O, Courtoy PJ, Wang XT, Wang H, Wang Y, Thakker RV, Guggino S, & Guggino WB (2000). Mice lacking renal chloride channel, CLC-5, are a model for Dent's disease, a nephrolithiasis disorder associated with defective receptor-mediated endocytosis. *Hum Mol Genet* 9, 2937-2945.

Wanner C & Horl WH (1988). Carnitine abnormalities in patients with renal insufficiency. Pathophysiological and therapeutical aspects. *Nephron* 50, 89-102.

Wedeen RP & DeBroe ME (2005). Nephrotoxic metals. Oxford University Press.

Weinberg JM, Venkatachalam MA, Roeser NF, & Nissim I (2000). Mitochondrial dysfunction during hypoxia/reoxygenation and its correction by anaerobic metabolism of citric acid cycle intermediates. *Proc Natl Acad Sci U S A* 97, 2826-2831.

Weinberger MH, Aoi W, & Henry DP (1975). Direct effect of beta-adrenergic stimulation on renin release by the rat kidney slice in vitro. *Circ Res* 37, 318-324.

Whittam & Willis (1963). Ion movements and oxygen consumption in kidney cortex slices. *J Physiol* 168, 158-177.

Wiederkehr A & Wollheim CB (2006). Minireview: implication of mitochondria in insulin secretion and action. *Endocrinology* 147, 2643-2649.

Wilcox CS (2002). Reactive oxygen species: roles in blood pressure and kidney function. *Curr Hypertens Rep* 4, 160-166.

Willis JS & Ma LN (1969). Cold resistance of Na- K-ATPase of renal cortex of the hamster, a hibernating mammal. *Am J Physiol* 217, 321-326.

Winkler HH, Bygrave FL, & Lehninger AL (1968). Characterization of the atractyloside-sensitive adenine nucleotide transport system in rat liver mitochondria. *J Biol Chem* 243, 20-28.

Wirthensohn G & Guder WG (1986). Renal substrate metabolism. *Physiol Rev* 66, 469-497.

Wright SH (2005). Role of organic cation transporters in the renal handling of therapeutic agents and xenobiotics. *Toxicol Appl Pharmacol* 204, 309-319.

Wright SJ, Centonze VE, Stricker SA, DeVries PJ, Paddock SP, & Schatten G (1993). In *Cell Biological Applications of confocal microscopy* Academic Press Inc.

Wrong OM, Norden AG, & Feest TG (1994). Dent's disease; a familial proximal renal tubular syndrome with low-molecular-weight proteinuria, hypercalciuria, nephrocalcinosis, metabolic bone disease, progressive renal failure and a marked male predominance. *QJM* 87, 473-493.

Wu LG (2004). Kinetic regulation of vesicle endocytosis at synapses. *Trends Neurosci* 27, 548-554.

Wu X, Zhao X, Baylor L, Kaushal S, Eisenberg E, & Greene LE (2001). Clathrin exchange during clathrin-mediated endocytosis. *J Cell Biol* 155, 291-300.

Wyatt CM & Klotman PE (2006). Antiretroviral therapy and the kidney: balancing benefit and risk in patients with HIV infection. *Expert Opin Drug Saf* 5, 275-287.

Yamada H, Seki G, Taniguchi S, Uwatoko S, Suzuki K, & Kurokawa K (1996). Mechanism of $[Ca^{2+}]_i$ increase by extracellular ATP in isolated rabbit renal proximal tubules. *Am J Physiol* 270, C1096-C1104.

Yaseen Z, Michoudet C, Baverel G, & Dubourg L (2008). Mechanisms of the ifosfamide-induced inhibition of endocytosis in the rat proximal kidney tubule. *Arch Toxicol* 82, 607-614.

Zhai XY, Nielsen R, Birn H, Drumm K, Mildenerberger S, Freudinger R, Moestrup SK, Verroust PJ, Christensen EI, & Gekle M (2000). Cubilin- and megalin-mediated uptake of albumin in cultured proximal tubule cells of opossum kidney. *Kidney Int* 58, 1523-1533.

Zhou G, Myers R, Li Y, Chen Y, Shen X, Fenyk-Melody J, Wu M, Ventre J, Doebber T, Fujii N, Musi N, Hirshman MF, Goodyear LJ, & Moller DE (2001). Role of AMP-activated protein kinase in mechanism of metformin action. *J Clin Invest* 108, 1167-1174.

Zong H, Ren JM, Young LH, Pypaert M, Mu J, Birnbaum MJ, & Shulman GI (2002). AMP kinase is required for mitochondrial biogenesis in skeletal muscle in response to chronic energy deprivation. *Proc Natl Acad Sci U S A* 99, 15983-15987.

Zou AP, Li N, & Cowley AW, Jr. (2001). Production and actions of superoxide in the renal medulla. *Hypertension* 37, 547-553.

Appendix

Mitochondrial study - patient information sheet

You are being invited to take part in a research study. Before you decide it is important for you to understand why the research is being done and what it will involve. Please take time to read the following information carefully. Please ask your consultant in clinic if there is anything that is not clear or if you would like more information. Take time to decide whether or not you wish to take part.

What is the purpose of the study?

All living cells in the body require energy to function properly. Mitochondria are the components of cells that are responsible for providing this energy. Abnormalities in mitochondria may therefore lead to cells not working properly. This study has been designed to investigate whether or not abnormalities in mitochondria may affect the function of cells in the kidney, and in particular their ability to reabsorb substances normally and stop them being lost in the urine (a medical condition called “The Renal Fanconi Syndrome”). This will be established by analysing samples of urine to look for these substances and evidence of mild kidney damage.

Why have I been chosen?

You have been asked to take part as you are known to have abnormalities in the function of your mitochondria, which has caused problems in other organs of your body (such as muscle) and has led to you being seen in this clinic. As part of the study we would like to analyse a sample of your urine to look for evidence of mild kidney damage which may be a result of abnormal mitochondrial function.

Do I have to take part?

No. It is up to you to decide whether or not to take part. If you do, you will be given this information sheet to keep and be asked to sign a consent form. You are still free to withdraw at any time and without giving a reason. A decision to withdraw at any time, or a decision not to take part, will not affect the standard of care you receive.

What will happen to me if I take part?

You will be asked to provide a urine specimen whilst attending the clinic. This sample will be sent away to a laboratory for analysis. In some cases, depending on the initial results, you may be asked for another sample of urine at a later date for more detailed analysis. Should any abnormalities be found the consultant looking

after you will notify you and you will be offered further tests and the opportunity to be seen by a kidney doctor should you wish.

What are the other possible benefits and disadvantages of taking part?

The possible disadvantage is that you may be diagnosed with having a kidney problem that you were unaware of. However, this is likely to only be mild and can be easily treated by taking certain supplements to replace those lost in the urine, which may have a beneficial effect on your health if you were previously deficient of these substances.

Will my taking part in the study be kept confidential?

Your participation will be strictly confidential and only your consultant will be aware. The researchers will not be aware of your identity and your GP will not be sent any results.

What will happen if I don't want to carry on with the study?

You may withdraw at any time and without giving any reason by contacting your consultant in clinic.

What will happen to any samples I give?

Samples will be destroyed after analysis.

What will happen to the results of the research study?

You will be informed by your consultant of any abnormalities in your urine specimen. It is intended that the results of the study when completed will be submitted to a scientific journal for publication. No-one will be able to identify you by reading the results as all results will be anonymous.

Who has reviewed the study?

The National Hospital for Neurology and Neurosurgery & Institute of Neurology Joint Regional Ethics Committee.

Who is organising the research?

The research has been organised by The Department of Physiology, University College London, in collaboration with University College London Hospitals NHS Trust and Camden Primary Care Trust. The lead investigators are Professor RJ Unwin and Prof MG Hanna.

Contact for further information

Prof Hanna can be contacted on the phone numbers at the top of this information sheet.

Thank you for taking the time to read this information sheet and for considering taking part in this study.

HIV study - patient information sheet

You are being invited to take part in a research study. Before you decide it is important for you to understand why the research is being done and what it will involve. Please take time to read the following information carefully. Please ask your consultant in clinic if there is anything that is not clear or if you would like more information. Take time to decide whether or not you wish to take part.

What is the purpose of the study?

All living cells in the body require energy to function properly. Mitochondria are the components of cells that are responsible for providing this energy. Abnormalities in mitochondria may therefore lead to cells not working properly. Recently it has been suggested that HIV infection and the drugs used to treat it may interfere with mitochondria in the kidney. This may affect the function of cells in the kidney, and in particular their ability to reabsorb substances normally and stop them being lost in the urine (a medical condition called “The Renal Fanconi Syndrome”). The study will investigate this possibility by analysing samples of urine to look for these substances and evidence of mild kidney damage.

Why have I been chosen?

You have been asked to take part as you are currently attending The Mortimer Market Clinic for monitoring or treatment of HIV infection. As part of the study we would like to analyse a sample of your urine to look for evidence of mild kidney damage which may be a result of abnormal mitochondrial function.

Do I have to take part?

No. It is up to you to decide whether or not to take part. If you do, you will be given this information sheet to keep and be asked to sign a consent form. You are still free to withdraw at any time and without giving a reason. A decision to withdraw at any time, or a decision not to take part, will not affect the standard of care you receive.

What will happen to me if I take part?

You will be asked to provide a urine specimen whilst attending the clinic. This sample will be sent away to a laboratory for analysis. In some cases, depending on the initial results, you may be asked for another sample of urine at a later date for more detailed analysis. Should any abnormalities be found the consultant looking after you will notify you and you will be offered further tests and the opportunity to be seen by a kidney doctor should you wish.

What are the other possible benefits and disadvantages of taking part?

A possible disadvantage is that you may be diagnosed with having a kidney problem that you were unaware of. However, this is likely to only be mild and can be treated by altering your anti-HIV medication and by taking certain supplements to replace those lost in the urine. This may have a beneficial effect on your health if you were previously deficient of these substances.

Will my taking part in the study be kept confidential?

Your participation will be strictly confidential and only your consultant will be aware. The researchers will not be aware of your identity and your GP will not be sent any results.

What will happen if I don't want to carry on with the study?

You may withdraw at any time and without giving any reason by contacting your consultant in clinic. This will not affect your usual medical care in any way.

What will happen to any samples I give?

Samples will be destroyed after analysis.

What will happen to the results of the research study?

You will be informed by your consultant of any abnormalities in your urine specimen. It is intended that the results of the study when completed will be submitted to a scientific journal for publication, and will also form part of a PhD project. No-one will be able to identify you by reading the results as all results will be anonymous.

Who has reviewed the study?

The National Hospital for Neurology and Neurosurgery & Institute of Neurology Joint Regional Ethics Committee.

Who is organising the research?

The research has been organised by The Department of Physiology, University College London, in collaboration with University College London Hospitals NHS Trust and Camden Primary Care Trust. The lead investigator is Professor RJ Unwin.

Contact for further information

The lead investigator, Prof RJ Unwin, can be contacted on the phone numbers at the top of this information sheet.

Thank you for taking the time to read this information sheet and for considering taking part in this study.

You will be given a copy of this form and the consent form to keep.

Ethics committee approval for clinical studies

Prof RJ Unwin
Professor of Nephrology
UCL
Centre for Nephrology, UCL medical
School, Hampstead Campus,
Rowland Hill St, London
NW3 2PF

Our Ref: 06L 286

Research & Development Department
1st Floor, Maple House
POSTAL ADDRESS:
Ground Floor, Rosenheim Wing
25 Grafton Way
London
WC1E 5DB
Tel: 020 7380 9579
Fax: 020 7380 9937
Email: sasha.vandayar@uclh.nhs.uk
Website: www.uclh.nhs.uk

30 August 2006

Dear Prof Unwin

Full title of study: **The role of mitochondria in the renal Fanconi Syndrome.**
REC reference number: **06/Q0512/62**

Thank you for your letter of 11 August 2006, responding to the Committee's request for further information on the above research and submitting revised documentation.

The further information was considered at the meeting of the Committee held on 22 August 2006. A list of the members who were present at the meeting is attached.

Confirmation of ethical opinion

On behalf of the Committee, I am pleased to confirm a favourable ethical opinion for the above research on the basis described in the application form, protocol and supporting documentation as revised.

06/Q0512/62 **Please quote this number on all correspondence**

With the Committee's best wishes for the success of this project

Yours sincerely

Mrs Katy Judd
Chair